The role of a glycosyltransferase, ST6Gal I in regulating viral specific T and B cell responses

A Thesis Presented for the
Doctor of Philosophy
Degree
The University of Tennessee, Knoxville

Junwei Zeng
December 2011

ACKNOWLEDGEMENTS

It is a wonderful long journey to the completion of this dissertation with many wonderful people along the way. First, my sincere appreciation goes to my advisor Dr.Onami for her support and guidance. Her helping me to think critically will benefit me for the rest of my academic life. I also would like to thank my committee members, Drs. Barry Rouse, Mark Sangster, Tim Sparer, and Chunlei Su for their support and encouragement. To my lab mates and friends in Walters Life Science building, Heather Dech, Pratima Suvas, Jenish Patel, Suneeta Archarya, Rajini Bheemreddy, John Harp, Whitney Connell, Joey Payant, Hye Mee Joo, Aarthi Sundarajan, Lifang Huan, Hung-Yi Wu, Bo-jhih Guan, Yuping, Shalini Sharma, Sachin Mulik, Amol Suryawanshi, Naveen Kumar, Pradeep, Mindy miller-kitrell for their help and inspirational discussions. To my parents, sisters, and my wife, for their unconditional love and support.

ABSTRACT

Glycosylation is one of the most abundant post-translational modifications of proteins. Glycoproteins participate in virtually all aspects of cellular functions. ST6Gal I is a glycosyltransferase highly expressed by B and T cells. Here, we interrogated the role of ST6Gal I in viral specific B and T cell immune responses, as well as examined how loss of this enzyme impacted viral pathogenesis.

First, to understand how loss of ST6Gal I expression impacted viral specific humoral responses, we infected ST6Gal $I^{-/-}$ mice with influenza virus. We discovered that loss of ST6Gal I expression results in both reduced influenza specific antibodies levels and decreased viral-specific antibody secreting cells numbers. Following influenza infection, mice that received ST6Gal $I^{-/-}$ B cells showed reduced influenza-specific IgM responses compared to mice that received wild-type B cells. These experiments demonstrated that the expression of ST6Gal I by B cells is required for optimal viral-specific humoral response.

We further examined how loss of ST6Gal I expression impacted the anti-influenza IgA response. We observed that immune ST6Gal $I^{-/-}$ mice displayed higher viral specific IgA levels and altered sialylation of IgG and IgA, which have been implicated in a human disease, IgA nephropathy. Moreover, ST6Gal $I^{-/-}$ mice exhibited increased immunoglobulin deposition in kidney glomeruli following influenza infection. These data suggest that ST6Gal I deficiency, together with influenza infection, may result in the initiation of a kidney disease.

Finally, we examined how ST6Gal I expression regulated CD8 T cell responses. We discovered that ST6Gal I is differentially expressed during CD8 T cell activation. To understand its relevance, we infected ST6Gal $I^{-/-}$ mice and demonstrated that the early expansion of effector T cells was impaired in a cell intrinsic manner. Moreover, in the absence of ST6Gal I, the differentiation of CD8

T cells skewed towards memory precursor cells, whereas terminal effector cell expansion was impaired. Mechanistically, we identified delayed surface expression of IL-2Ralpha on ST6Gal I$^{-/-}$ CD8 T cells due to impaired IL-2/IL-2R signaling. These studies implicate that ST6Gal I expression enhances early proliferation of terminal effector CD8 T cells by promoting the rapid surface expression of IL2Ralpha during acute viral infection.

TABLE OF CONTENTS

CHAPTER I 1
Introduction and overview 1
1. Adaptive immunity overview 2
1.1 B and T cells 3
1.2 Viral immunity 4
1.2.1 LCMV 4
1.2.2 Influenza 5
2. Glycomics and immunity 5
2.1 Glycosylation, glycomics, and glycosyltransferase 5
2.2 Glycosylation and disease 7
2.2.1 Glycosylation and cancer 7
2.2.2 Glycosylation and immune disorders 8
2.2.2.1 Hereditary aberrant glycosylation associated immune diseases 8
2.2.2.2 Acquired aberrant glycosylation associated immune diseases 9
2.2.2.3 IgA nephropathy 10
2.3 Sialyltransferase 11
2.3.1 α2,6-sialyltransferase family 12
2.3.2 ST6Gal I and immune regulation 13
2.3.3 ST6Gal I and disease 14
3. B cell activation and differentiation 15
3.1 B cell subsets and activation 15
3.2 B cell memory 16
4. CD8 T cell activation and differentiation 17
4.1 Effector and memory CD8 T cell subsets are heterogeneous 17
4.2 Regulation of CD8 T cell differentiation 18
5. Research focus 21
References 22

CHAPTER II The generation of influenza-specific humoral responses is impaired in ST6Gal I-deficient mice 34
Abstract 35
Introduction 36
Materials and methods 38
Mice and immunizations 38
Tissues harvest and flow cytometry 38
Immunofluorescence 39
Influenza viral titer determination 39
ELISPOT assay to detect influenza specific ASCs 39
Memory B cell assay 40
B cell transfer and ELISA 41
Results 42
SNA binding is high on naïve and in vivo activated B cells 42
Impaired generation of influenza specific humoral responses in ST6Gal I deficient mice 42
Germinal centers of ST6Gal $I^{-/-}$ mice do not bind GL7 44
Productive infection and replication of influenza in ST6Gal $I^{-/-}$ mice 44
Viral specific CD4 and CD8 T cells in the lungs and MedLN 45
Viral specific memory B cell responses 45
B cell expression of ST6Gal I is required to generate optimal levels of viral specific IgM 46
Discussion 46
References 50
Appendix 55
CHAPTER III ST6Gal I deficiency results in altered sialylation of IgG and IgA, and promotes IgA mesengial deposition following influenza infection 64
Abstract 65
Introduction 66
Materials and Methods 69

Mice and immunizations 69
Urinalysis 69
Histological Analysis 69
Immunohistochemistry 70
Immunoglobulin Measurement by ELISA 70
IgG and IgA purification 71
N-glycan release 71
Sialidase digestion and Permethylation 72
Mass spectrometry 72
Results 72
Increased IgA levels in influenza immune ST6Gal $I^{-/-}$ mice 72
ST6Gal $I^{-/-}$ mice show greater IgG deposition in glomeruli following influenza infection 73
ST6Gal I expression is required for sialylation of N-glycans on IgG 74
Loss of ST6Gal I expression leads to aberrant IgA glycosylation 75
Loss of ST6Gal I expression and influenza infection results in mesangial IgA deposition 77
Discussion 77
References 82
Appendix 87
CHAPTER IV ST6Gal I promotes rapid IL-2Rα surface expression, increasing early proliferation of terminal effector CD8 T cells 95
Abstract 96
Introduction 97
Materials and Methods 100
Mice and immunizations 100
Adoptive transfer 100
DNA Microarray Hybridization 102
In vivo CFSE proliferation assay 102
In vitro assays 103

Results 103
Dramatic changes in expression of the glycosyltransferase ST6Gal I during memory T cell differentiation 103
Impaired viral-specific responses in ST6Gal I-deficient mice 105
T-bet regulates St6gal1 expression 107
Impaired CD8 T cell expansion is cell intrinsic 108
Similar recruitment and T cell activation, but delayed IL-2Rα expression of ST6Gal $I^{-/-}$ CD8 T cells 109
IL-2/IL-2R signaling and surface expression is impaired in ST6Gal $I^{-/-}$ CD8 T cells 111
Discussion 113
References 116
Appendix 122
CHAPTER V CONCLUSIONS 134
The generation of Influenza-specific humoral responses is impaired in ST6Gal I-deficient mice 135
ST6Gal I deficiency results in altered sialylation of IgG and IgA, and promotes IgA mesengial deposition following influenza infection 136
ST6Gal I promotes rapid IL-2Rα surface expression, increasing early proliferation of terminal effector CD8 cells 137
References 139
VITA 140

LIST OF TABLES AND FIGURES

Chapter II

Figure 2.1. Binding of SNA on B cell populations. 56

Figure 2.2. Influenza-specific B cell responses in ST6Gal I$^{-/-}$ mice during acute infection..... 57

Figure 2.3. Germinal center B cells of ST6Gal I$^{-/-}$ mice do not bind GL7. 58

Figure 2.4. Influenza viral infection and clearance in lungs. 59

Figure 2.5. Influenza-specific T cell responses. 60

Figure 2.6. Immune influenza-specific IgG responses. 62

Figure 2.7. Loss of expression of ST6Gal I by B cells results in defective influenza specific IgM. 63

Chapter III

Figure 3. 1. Increased IgA levels in influenza immune ST6Gal I$^{-/-}$ mice. 88

Figure 3. 2. ST6Gal I$^{-/-}$ mice show greater IgG deposition in glomeruli following influenza infection. 91

Figure 3. 3. ST6Gal I expression is required for sialylation of N-glycans on IgG. 92

Figure 3. 4. Loss of ST6Gal I expression leads to aberrant IgA glycosylation.... 93

Figure 3. 5. Loss of ST6Gal I expression, concomitant with influenza viral infection, result in mesangial IgA deposition..... 94

Chapter IV

Figure 4. 1. Dramatic changes in expression of the glycosyltransferase ST6Gal I during memory T cell differentiation..... 123

Figure 4. 2. Impaired viral-specific responses in ST6Gal I-deficient mice. 126

Figure 4. 3. T-bet regulates *St6gal1* expression. 128

Figure 4. 4. Disrupted B cell follicle in ST6Gal I null mice following LCMV infection..... 129

Figure 4. 5. Impaired CD8 T cell expansion is cell intrinsic. 130

Figure 4. 6. Similar recruitment and T cell activation, but delayed IL-2Rα expression of ST6Gal I$^{-/-}$ CD8 T cells. 132
Figure 4. 7. IL-2/IL-2R signaling and surface expression is impaired in ST6Gal I$^{-/-}$ CD8 T cells. 133

Abbreviations

ST6Gal I	β-galactoside α2,6-sialyltransferase
ASC	Ab-secreting cell
LLPC	Long-lived plasma cell
MBC	Memory B cell
SNA	Sambucus nigra agglutinin
Siaα2-6Gal	α-2,6 sialic acid linked to galactose
ELISA	Enzyme-linked immunosorbent assay
ELISPOT	Enzyme-linked immunosorbent spot
i.v.	Intravenous
i.p.	Intraperitoneal
IgAN	Immunoglobulin A nephropathy
BCR	B cell receptor
LCMV	Lymphocytic choriomeningitis virus
SLEC	Short-lived effector cell
MPEC	Memory precursor effector cell
TCR	T cell receptor
STAT5	Signal transducer and activator of transcription 5

CHAPTER I
INTRODUCTION AND OVERVIEW

1. Adaptive immunity overview

The immune system is comprised of multiple cellular players. These cells express a variety of cell surface and intracellular molecules, which cooperate in an elaborate and dynamic network to recognize and eliminate pathogenic microorganisms. There are two arms of the immune system distinguished temporally, functionally, and in their antigen specificity. The innate immune system is distinguished by the use of pattern recognition receptors (PRRs)(Mogensen, 2009). Cells expressing PRRs recognize and destroy insulting pathogens expressing pathogen associated molecular patterns (PAMPs). The innate response consists of effector cells such as granulocytes, natural killer (NK) cells, and phagocytes and represents the first line of host defense against invading pathogens, launching the inflammatory response following infection. In addition, phagocytes engulf pathogens and cellular debris and subsequently present protein antigens to T lymphocytes to initiate adaptive immune responses(Bonilla and Oettgen, 2010). Importantly, the innate immune system differs functionally from the adaptive immune response in that it does not confer long-term immunity, or memory, to the host. The innate response behaves identically following re-infection with the same agent. The second arm of the immune system is the adaptive or acquired immune response. It provides the second line of defense, often taking days to respond following the onset of infection. The adaptive immune system is comprised of B and T lymphocytes, expressing a tremendous variety of antigen recognition receptors that recognize specific antigen--either unprocessed antigens in the case of B cells or processed antigen in complex with self-major histocompatibility complex (MHC), in the case of T cells(Bonilla and Oettgen, 2010; Cooper and Alder, 2006). The orchestration of B and T cells constitute a highly sophisticated biological response that enables the host to potentially recognize virtually any pathogenic agent. Following elimination of the pathogen, the adaptive immune system acquires

immunological memory, which can efficiently and quickly launch pathogen-specific responses to prevent re-infection with the same agents.

1.1 B and T cells

Instructed by environmental cues, pluripotent hematopoietic stem cells in the bone marrow differentiate into common myeloid progenitors and common lymphoid progenitors, and further develop into myeloid cells and lymphocytes, respectively(Cooper and Alder, 2006). In the bone marrow, the commitment to the B cell lineage is controlled by transcription factors, such as PU.1, IKAROS, and PAX5(Fuxa and Skok, 2007; LeBien and Tedder, 2008). B cell progenitors undergo several distinct developmental stages to achieve complete development to resting naïve B cells and then exit the bone marrow to circulate in the periphery. Following antigen stimulation, the majority of B cells will proliferate, differentiate into plasma cells, or enter germinal center reactions following contact with T-dependent antigens.

T lymphocytes also arise from common lymphoid progenitors in the bone marrow but must migrate to the thymus for further development, where they reach maturation under the control of Notch and other transcription factors(Jenkinson et al., 2006). Before T cells can exit the thymus to seed the periphery, they must pass strict quality control. After T cells express a functional T cell receptors (TCR) on their surface, they will go through a process called positive selection, during which only those T cells that recognize self-MHC receive signals enabling their survival. T cells also undergo negative selection, where those T cells that bind to self-MHC with high affinity will be eliminated to prevent autoimmunity.

During development in the thymus, T cells differentiate into two major subpopulations, distinguished by their surface expression of CD4 or CD8 molecules. CD4 T cells are the master regulators of adaptive immune

responses(Zhu and Paul, 2008). Upon contact with cognate antigen in the context of MHC class II expressed by antigen presenting cells (APCs), which are dendritic cells, activated macrophages, and activated B cells, naïve CD4 T cells differentiate into Th1, Th2, or other recently identified subsets. T helper subsets are characterized by the secretion of specific cytokines, such as IFNγ or IL-4. The diverse subsets of CD4 helper T cells orchestrate both B cell and T cell response against a plethora of pathogenic agents. CD8 T cells, also called cytotoxic lymphocytes (CTLs), can recognize processed peptide presented by MHC class I, expressed by all nucleated cells(Williams and Bevan, 2007). After a virus infects host cells, it usurps host protein synthesis machinery to produce viral protein, and viral peptides will be presented on the cell surface in the context of appropriate MHC class I. CD8 T cells can recognize MHC I/viral peptide complex, and kill virally-infected cells by either secreting a pore-forming protein (perforin), and a series of proteases (granzymes), or up-regulating a tumor necrosis factor (FasL) to induce apoptosis in the targeted cells. Thus, CD8 T cells are critical against intracellular pathogen infections and tumors.

1.2 Viral immunity

1.2.1 LCMV

Lymphocytic chriomeningitis virus (LCMV) is a member of the Arenaviridae family, causing acute or chronic infections of rodents(Buchmeier et al., 1980), the natural host. LCMV has a bisegmented, negative, enveloped, and single-stranded RNA genome, and the virus replicates systemically within the host(Fazakerley et al., 1991). It is a well-established virus model for investigating virus-specific T and B cell responses(Botten et al., 2010). During acute virus infection, a vigorous viral-specific CD8 T cells response is induced in lymphoid organs, and functional CD8 T cells are required for virus clearance (Asensio et al., 1999).

1.2.2 Influenza

Influenza virus belongs to Orthomyxoviridae family. It contains a segmented, negative, enveloped, and single-stranded RNA genome, causing an acute and contagious pulmonary disease(Cox et al., 2004; Nicholson, 1992). According to the antigenic differences of nucleoprotein and matrix protein, influenza viruses are categorized into three types: type A, B, C. Two major viral glycoproteins hemagglutinin (HA) and neuraminidase (NA) expressed on the virion surface mediate the binding and entry to target cells and the release of progeny virus from the infected cell, respectively(Cox et al., 2004). Influenza viruses are constantly undergoing antigenic mutations to escape from host adaptive immunity, especially humoral immunity, causing antigenic shift and antigenic drift. Influenza infection induces robust B cell responses, and vigorous viral-specific antibody production contributes to virus clearance(Gerhard et al., 1997). In addition, influenza virus also elicits strong CD4 and CD8 T cells responses in the lung(Doherty et al., 1997).

2. Glycomics and immunity

2.1 Glycosylation, glycomics, and glycosyltransferase

Glycosylation refers to the generation of different types of glycans or sugars that are attached to proteins and lipids(Varki., 2009). Glycan biosynthesis occurs along the protein secretory pathway, predominantly, within the Golgi apparatus. There are also some other forms of glycosylation that occur in the cytoplasm and nucleus. There are two types of glycans, and their classification depends on the nature of their linkage. N-glycans are glycosidically linked to the asparagine residues of polypeptides; in contrast, O-glycans are linked to serine or threonine residues of proteins.

Glycomics refers to the comprehensive study of total glycan structures of a given cell or organism，and is referred to as the glycome(Varki., 2009). In parallel with proteomics, glycomics is becoming a major research field. In fact, the glycome is far more complicated than either the genome or proteome. Studies have showed that most proteins and lipids on the surface of cellular membranes, as well as those of pathogens, are modified with a dense array of glycans, which undergo variable and dynamic changes in the course of development and pathogenesis(Cobb and Kasper, 2005; Varki, 2006). Indeed, glycans serve as linking bridges between cell-cell and cell-extracellular matrix (ECM) and glycans are recognized by carbohydrate-binding proteins, such as lectins and adhesion molecules(Alavi and Axford, 2008; Ohtsubo and Marth, 2006). These interactions allow glycans to participate in virtually all cellular processes that impact health or disease. Specifically, glycans have been found to regulate protein folding, cell adhesion, signal transduction, molecular homeostasis, endocytosis, receptor activation, molecular trafficking, and self/nonself recognition(Ohtsubo and Marth, 2006; Rudd et al., 2001; Varki., 2009).

Glycan biosynthesis occurs in a serially ordered pattern that is primarily catalyzed by glycosyltransferases(Varki., 2009). Molecular cloning and sequencing analysis showed that glycosyltransferases are a large enzyme group, composing up to 2% of the genome. Different from the nucleotide polymerases that require template to initiate replication, glycosyltransferases elongate glycan chains independently of template. Glycosyltransferases orchestrate with other enzymes to partially compete for and add monosaccharides from donor substrate to acceptor substrates, yielded by previous enzymes(Varki., 2009). This occurs rapidly and sequentially, extending the linear and/or diverged sugar chain. Moreover, glycosyltransferases are expressed and regulated in a cell- and/or stage-specific manner. As a consequence of this regulated expression, a given cell could readily and rapidly adopt a different glycan pattern on the cell surface in response to dynamic physiological or pathogenic stimuli. From this

perspective, abnormal changes in cellular processes caused by disease, are likely to generate a different glycan pattern on a given cell during disease processes(Ohtsubo and Marth, 2006; Varki., 2009).

2.2 Glycosylation and disease

2.2.1 Glycosylation and cancer

Cancer is a class of progressive diseases where clones of a cell show uncontrolled growth(Hanahan and Weinberg, 2011). These clones may invade and destroy surrounding tissues, and sometimes metastasize, where the clones move to other sites in the body through blood or lymph circulation. The development of cancer, or carcinogenesis, is a multiple-stage process that includes cancer initiation, promotion, and progression. A wide range of altered molecular events is found to cause cancer, such as the disruption of cell cycle, and the dysregulation of intracellular and/or intercellular signaling(Duffy et al., 2008; Hanahan and Weinberg, 2011).

It has been reported decades ago that the glycosylation pattern changes in an in vitro mouse transformed fibroblasts(Meezan et al., 1969). Since then, with the application of more tools and approaches, a deep insight of the crucial roles of glycans at various stages of carcinogenesis has been gained from intense experimental investigations. For example, the survival of melanoma and sarcoma cells *in vitro* was hampered when treated with N-glycosylation inhibitors (Dricu et al., 1999; Girnita et al., 2000). This is because inhibition of N-glycosylation leads to the down-regulation of cell surface insulin like growth factor-1 receptor (IRG-1R), which has been shown to be critical for tumor development(Dricu et al., 1999). As a consequence, there is a drastic reduction of IRG-1R autophosphorylation. This case illustrates how altered glycosylation in surface molecule affects tumor cell proliferation.

Glycosylation also regulate other aspects of tumor progression. When tumor cells are ready to invade adjacent tissues, they detach themselves from each other and from the extracellular matrix (ECM) and then move to neighboring sites(Duffy et al., 2008). This occurs through the changes of expression of cell-surface adhesion receptors and ligands, and the secretion of proteolytic enzymes and glycosidases that break ECM networks. Tumor cells have been shown to increase the expression of N-acetylglucosaminyltransferase V (GnT V), which would upregulate the surface expression of complex β1,6-branched N-linked glycans(Dennis et al., 2002; Yoshimura et al., 1996). Particularly, increased modification of β1,6-branched N-linked glycan structure on the E-cadherin molecule expressing on tumor cell surfaces mediates cell aggregation via homotypic interactions(Dennis et al., 2002). This results in decreased cell-cell adhesions, promoting cell detachment and invasiveness(Dennis et al., 2002).

2.2.2 Glycosylation and immune disorders

Abnormal glycomodifications, which can be inherited or acquired, are found to correlate with a wide spectrum of diseases such as cancer as discussed above. Altered glycosylation has also been described in several immune disorders, including Wiskott-Aldrich syndrome (WAS), rheumatoid arthritis (RA), systemic lupus erythematosus (SLE), congenital disorders of glycosylation (CDG), leukocyte adhesion deficiency (LAD), and IgA nephropathy (IgAN)(Alavi and Axford, 2008; Ohtsubo and Marth, 2006). Over the past decades, there is an increasing body of information regarding the mechanisms of glycan processing and their role in pathogenesis.

2.2.2.1 Hereditary aberrant glycosylation associated immune diseases

The numbers of diseases correlating with inherited aberrant glycosylation is relatively low due to either embryonic lethality mutations or limited tools to detect

mild syndromes(Alavi and Axford, 2008; Ohtsubo and Marth, 2006). Wiskott-Aldrich syndrome is an X-linked inherited immunodeficiency disorder, caused by mutations in the Wiskott-Aldrich syndrome protein (WASP) gene(Notarangelo et al., 2005). The symptoms of WAS include peripheral lymphopenia, thrombocytopenia, small platelet, eczama, and recurrent infections(Imai et al., 2004; Notarangelo et al., 2005). CD43 is a highly conserved transmembrane glycoprotein expressed on thymocytes and most hematopoietic cells(Notarangelo et al., 2005). CD43 has been shown to be involved in the regulation of T cell migration and immunity(Matsumoto et al., 2005; Onami et al., 2002). Aberrant glycomodifications of CD43 are present in WAS patients(Higgins et al., 1991; Piller et al., 1991). As altered glycoforms of CD43 have been shown to be important for T cell positive selection in the thymus, these changes might lead to abnormal thymic egress of self-reactive T cells, invoking autoimmune disease and progressive lymphopenia, which are commonly observed in WAS patients(Ellies et al., 1996; Khan et al., 2008).

2.2.2.2 Acquired aberrant glycosylation associated immune diseases

Extensive investigations have been carried out to illustrate the role of changes in the glycosylation of antibodies in autoimmune diseases(Opdenakker et al., 2006; Varki., 2009). A wealth of evidence suggested that the dysregulation of glycosylation in IgG contributes to the pathogenesis of the autoimmune disease rheumatoid arthritis (RA)(Alavi and Axford, 2008; Varki., 2009). IgGs have various glycomodifications in the constant domain of Fc region, which can be terminally decorated by galactose, sialic acid, bi-antennary N-acetylglucosamine, and fucose(Jefferis, 2005; Kaneko et al., 2006). One key feature of RA is a significant increase in agalactosylated IgG, which is a good indicator of the severity of RA symptoms(Gindzienska-Sieskiewicz et al., 2007; Troelsen et al., 2007). Without the galactosylation of IgG Fc region, it may alter immunogenic properties, resulting in auto-sensitization and the generation of anti IgG-G0

antibody, leading to the formation of immune complexes(Das et al., 2004; Varki., 2009). Loss of terminal galactose in IgG Fc also expose mannoses, which normally are not accessible for mannose binding lectin recognition, and may trigger an inappropriately complement response, generating inflammatory factors that disturb normal cellular activities(Arnold et al., 2006). The abnormal glycosylation in IgG Fc also may affect the timing and specificity of interaction with Fc receptor, thus activating unwanted inflammatory responses that contribute to RA disease(Kaneko et al., 2006).

2.2.2.3 IgA nephropathy

IgA nephropathy (IgAN) is a common worldwide immune complex-mediated glomerulonephritis, characterized by IgA deposition in glomerular mesangium(D'Amico, 1987; D'Amico, 2004). It is often associated with IgG deposition, hematuria, sometimes with proteinuria, and usually associated with elevated IgA level in serum(D'Amico, 2004). 20-40% of IgAN patients will develop renal failure(D'Amico, 2004). Despite the significant morbidity and mortality caused by IgAN, the root cause of this disease remains unknown. Linkage studies could not convincingly establish any genes that correlate to IgAN(Gharavi et al., 2000; Paterson et al., 2007). Studies have shown that IgA1 was abnormally O-glycosylated in IgAN(Hiki et al., 1995; Mestecky et al., 1993). Immune complexes containing the abnormally O-glycosylated IgA1 and IgG or IgA1 autoantibodies against the aberrant IgA1 were also reported in IgAN patients(Novak et al., 2008). The dysregulated O-glycosylation of IgA1 in IgAN is now well established. However, the molecular mechanisms causing this dysregulation and the initiation of the disease process in IgAN remains largely unknown.

Several groups have developed mouse models for human IgAN, including loss of uteroglobin, an anti-inflammatory protein, and a genetic knock-in mouse that

expresses human Fcα receptor on macrophages/monocytes(Launay et al., 2000; Zheng et al., 1999). Moreover, a recent study showed that β4GalT-1-deficient mice displayed most of the pathological and clinical traits of human IgAN, and therefore it may have utility as a novel animal model to study how aberrant glycosylation initiates an IgAN-lilke pathogenesis(Nishie et al., 2007).

2.3 Sialyltransferase

Sialic acids (SA) are a group of negatively charged 9-carbon monosaccharides derived from neuraminic acid. More than 50 naturally occurring SAs have been discovered(Varki and Varki, 2007). Numerous sialylated glycoconjugates have been identified, which exhibit remarkable diversity in both different linkages with other sugar molecules and structurally natural modifications in a cell type and developmentally modulated style(Varki., 2009). Typically, SAs are found abundantly attached to the outmost terminal positions of N-glycans, O-glycans and glycosphingolipids in all vertebrate cell types and throughout all tissues and body secretions. In addition, SA modifications often change in response to environmental signals. As a consequence of their tremendous diversity and terminal location on the cell membrane, SAs have been shown to play a wide variety of roles in many physiological or pathological processes, particularly in neural development, pathogen recognition, and immune function(Varki, 2008; Varki., 2009).

As a subset of glycosyltransferases, sialyltransferases catalyze the transfer of sialic acid residues from donor substrate CMP-NeuAc to the terminus of glycoproteins and glycolipids within the reticulum-Golgi biosynthesis factory. To date, 20 different sialyltransferases have been identified to generate three key types of sialic acid linkage in mouse and humans. The most abundant sialic acid linkage is α2,3 linkage and is produced at least by 6 α2,3-sialyltransferases (ST3Gal I-VI). α2,8 sialic acid linkages are generated by 6 α2,8-

sialyltransferases (ST8Gal I-VI). GalNAc α2,6-sialyltransferases (ST6Gal NAc-I-VI) and α2,6-sialyltransferases (ST6Gal I and II) catalyze the addition of α2,6 linked sialic acid to Galβ1,4GalNAc and Galβ1,4GlcNAc, respectively(Harduin-Lepers et al., 1995; Takashima, 2008).

2.3.1 α2,6-sialyltransferase family

The Galβ1,4GlcNAc (lactosamine) is a common component at the end of N-glycan chains of glycoproteins. It has been shown that ST6Gal I and II are the only two sialyltransferases to catalyze the addition of sialic acid to lactosamine to generate Siaα2-6Galβ1-4GlcNAc (Sia6LacNAc), a structure that is recognized by several lectins including a plant lectin *Sambucas nigra* agglutinin (SNA)(Hennet et al., 1998; Varki, 2008). ST6Gal II shows restricted acceptor substrate specificity toward oligosaccharides(Takashima, 2008). In addition, it is mainly expressed in brain and during embryonic development. In contrast, ST6Gal I exhibits broad substrate specificity toward glycoprotein, glycolipid, and oligosaccharides(Takashima, 2008). Moreover, ST6Gal I is expressed in many tissues at relatively low level except lymphoid organs(Takashima, 2008). Both ST6Gal genes have similar genomic structures. They use physically distinct promoters and the alternative splicing strategy to generate isoforms from primary RNA transcripts in different tissues(Wuensch et al., 2000). When P1, one of six promoters that drives murine ST6Gal I expression, is deleted, mice showed neutrophillia and eosinophillia, suggesting P1 region might be involved in the regulation of myelopoiesis(Nasirikenari et al., 2010; Nasirikenari et al., 2006). However, the functional relevance of these tissue-specific transcript variants is still not fully understood.

2.3.2 ST6Gal I and immune regulation

ST6Gal I RNA is highly expressed in hematopoietic cells such as T and B cells, implicating a physiological role of ST6Gal I in hematopoietic cells(Kitagawa and Paulson, 1994; Wen et al., 1992). Indeed, ST6Gal I generates the Sia6LacNAc which serves as the ligand for the mammalian lectin CD22 molecule, which is exclusively expressed on B cells. CD22 is a transmembrane glycoprotein, which negatively regulates B cell signaling by recruiting phosphatase SHP-1 to the B cell receptor to dampen B cell signaling(Nitschke, 2005). When ST6Gal I knockout mice were generated, these mice displayed impaired B cell responses, including reduced serum IgM levels, hampered B cell proliferation in response to IgM and CD40 ligation, and impaired antibodies generation when immunized with T-independent (DNP-Ficoll) and T-dependent antigens (DNP-KLH)(Hennet et al., 1998). These studies clearly showed that ST6Gal I played a critical role in B cell immune responses.

Early studies reported that ST6Gal I-deficient T cells proliferated normally when stimulated with anti-CD3 antibody *in vitro*(Hennet et al., 1998). However, a global gene profiling analysis showed a significant decrease of *Stgal1* mRNA after T cell activation(Comelli et al., 2006; Kaech et al., 2002), suggesting a role of ST6Gal I in T cell activation. Another study demonstrated that, compared to Th1 and Th17 cells, Th2 CD4 T cells expressed significantly more ST6Gal I, which might account for reduced galectin-1 binding and subsequent apoptosis, implicating that ST6Gal I regulated CD4 T cell differentiation(Toscano et al., 2007). Nonetheless, the in vivo role of ST6Gal I in T lymphocyte immune responses remains largely unexplored.

On the other hand, ST6Gal I is involved in inflammation regulation. It has been shown that knockout mice demonstrated significantly enhanced neutrophil and eosinophil infiltration into peritoneal cavity after intraperitoneally challenge with thioglycollate(Nasirikenari et al., 2010; Nasirikenari et al., 2006), suggesting a

regulatory role of ST6Gal I in inflammatory responses. Surprisingly, ST6Gal I also can contribute to modulating inflammation via differential α2,6-sialylation of IgG Fc fragment, which may determine the pro- or anti-inflammatory effects of IgG by regulating its binding to corresponding Fcγ receptors(Kaneko et al., 2006).

2.3.3 ST6Gal I and disease

It has long been appreciated that ST6Gal I expression correlated with inflammation(Dall'Olio, 2000). It seems that the expression of ST6Gal I, similar to acute phase proteins, is enhanced upon induced inflammation(Kaplan et al., 1983). Furthermore, it has been suggested that IL-6 may regulate ST6Gal I expression, at least the induction of hepatic ST6Gal I (Dalziel et al., 1999). The increased expression of ST6Gal I during inflammation would generate higher levels of sialyl α2,6-lactosaminyl terminals, which might serve as decoy biding sites to prevent incoming pathogens from interacting with host cells that express surface α 2,6-linked sialic acid for important endogenous recognition. Another potential function of increased ST6Gal I is that the increased levels of α2,6 sialylation would decrease the numbers of α2,3 sialylated epitopes, which are preferentially recognized by incoming pathogens(Gagneux and Varki, 1999). Thus, manipulating the expression of ST6Gal I might serve to combat pathogen.

The increased expression of ST6Gal I has been implicated in diseases such as colon and breast carcinoma, acute myeloid leukemia, and in some brain tumors (Dall'Olio and Chiricolo, 2001). Moreover, increased Siaα2,6 Gal levels have been shown to enhance transformed cell motility and invasiveness *in vitro*(Chiricolo et al., 2006; Seales et al., 2005). A recent *in vivo* study demonstrated that loss of ST6Gal I affect the integrin signaling pathway, and consequently favor mammary tumor progression(Hedlund et al., 2008).

3. B cell activation and differentiation

3.1 B cell subsets and activation

B cells undergo antigen-independent development first in bone marrow and then in spleen. After complete maturation, some B cells migrate to the marginal zone and remain there as naïve resident marginal zone (MZ) B cells(Steiniger et al., 2006). The majority of B cells will go on to circulate to the splenic follicles, and to other sites, such as the lymph nodes and bone marrow(LeBien and Tedder, 2008). After exposure to cognate antigen, B cells increase in size and start to proliferate to become B-cell blasts. Those B-cell blasts that synthesize and secrete antibody are named plasmablasts, and can terminally differentiate into plasma cells, which secret measurable amounts of immunoglobulin without proliferation. MZ B cells are unique in their inborn ability to rapidly (within hours) develop into short-lived plasma cells that secrete immunoglobulin, responding to antigenic stimuli in the absence of T-cell help(Oliver et al., 1997; Snapper et al., 1993). In contrast, circulating naïve B cells require two signals to become fully activated and undergo further differentiation(Bonilla and Oettgen, 2010; Oracki et al., 2010). The first signal is the antigen-mediated cross-linking of the immunoglobulin receptor, which activates the intracellular signaling pathway. As a consequence of this activation, B cells internalize the antigen-BCR complex and process the antigen to peptides that subsequently conjugates to appropriate MHC II molecules. These peptide-MHC II complexes then are delivered to the cell surface. When B cells interact with previously activated CD4 T cells specific for this peptide-MHC II complex, the CD4 T cells provide direct cell-cell contact (signal 2) to fully activate B cells. Consequently, the activated B cells can undergo proliferation and differentiation to plasma cells to elicit extra-follicular responses. Alternatively, fully activated B cells enter germinal centers. Germinal centers are special sites within the follicle, where B cells change from the generation of IgM and IgD to other isotypes, such as IgA, IgG, and IgE through

rearrangement of gene segments that encode the constant region of immunoglobulin heavy chain(Stavnezer et al., 2008). Meanwhile, B cells also undergo rounds of proliferation to accumulate point mutations in the variable chains of the immunoglobulin heavy and light chain, a process called somatic hypermutation, which results in the production of antigen-specific immunoglobulins with high affinity(Peled et al., 2008). B cells eventually develop into long-lived plasma cells (LLPCs), or memory B cells (MBCs) expressing high-affinity, and class-switched surface immunoglobulin receptors. These cells exit the germinal center approximately two weeks after immunization(Bonilla and Oettgen, 2010; Shapiro-Shelef and Calame, 2005).

3.2 B cell memory

B cell memory consists of two cellular components, including MBCs and LLPCs(Kurosaki et al., 2010; LeBien and Tedder, 2008). Both cell types provide long-term immunity. Generated in the germinal center, MBCs retain high affinity surface BCR and co-express the mature B cell markers B220 and CD19(Kurosaki et al., 2010). After exit from the germinal center, MBCs distribute throughout the body. MBCs can persist in the absence of antigenic stimulation and do not secrete immunoglobulin(Kurosaki et al., 2010). However, MBCs can more rapidly differentiate into plasma cells and produce antigen-specific antibody to contain an infection compared to naïve B cells when re-encounter the pathogenic agent and in the presence of CD4 T cell help. In contrast, LLPCs are terminally differentiated B cells with a long lifespan that constantly secrete high affinity antibodies and persist in the absence of antigen or additional proliferation(Bonilla and Oettgen, 2010). Once developed from intrafollicular B cells in the germinal center, LLPCs express the homing chemokine receptors CXCR3, CXCR6, and integrin $\alpha 4\beta 1$, enabling LLPCs to migrate to bone marrow, where they reside for the rest of their life(Kunkel and Butcher, 2003).

4. CD8 T cell activation and differentiation

4.1 Effector and memory CD8 T cell subsets are heterogeneous

Antigen-inexperienced, naïve CD8 T cells egress from thymus and populate secondary lymphoid organs. During an infection, naïve CD8 T cells that interact with specific peptide-MHC I complex, costimulatory signals, and cytokines, become activated and undergo proliferation and differentiation into effector CD8 T cells(Lefrancois and Obar, 2010; Smith-Garvin et al., 2009). During differentiation, they acquire effector cytotoxic activities, changes in adhesion molecules and chemokine receptor expression, which allows them to migrate to sites of infection. About one week following acute infection, antigen-specific CD8 T cell numbers peak, then undergo a significant attrition or contraction, where only 5-10% of the cells survive and become long-lasting memory cells. Memory CD8 T cells are long-lived, maintaining stable numbers via homeostatic turnover that is IL-15 dependent. Memory CD8 T cells remain in a resting state with low cytotoxicity, however, they are able to rapidly expand and regain effector functions following re-exposure to the same pathogen(Cui and Kaech, 2010; Lefrancois and Obar, 2010; Rutishauser and Kaech, 2010).

Only a small number of effector cells survive to become memory cells. However, the phenotypic and transcriptional traits embedded in the effector cells, which direct them to differentiate either into end-stage effector cells, or into memory cells, are largely unknown. Recent work to compare the global gene expression profiles of naïve, effector, and memory cells identified a few genes that are distinctly expressed at different stages of CD8 T cells development(Kaech et al., 2002; Schluns et al., 2000). First, IL-7Rα expression was identified as being differently expressed in effector subsets(Kaech et al., 2002). Together with the identification of surface marker killer cell lectin-like receptor G1 (KLRG1), which also distinguished effector populations, a new classification emerged where

effector subsets could be identified and used to study heterogeneity within effector CD8 T cells(Joshi et al., 2007; Sarkar et al., 2008). It is now established in several mouse infection models that during a primary infection, naïve CD8 T cells expand and differentiate into two subsets of effector cells, one termed short-lived effector cells or SLECs (KLRG1^{hi} IL-7Rα^{lo}), also known as terminal effectors, and these cells account for the majority of effector cells. SLECs have a shortened lifespan, proliferate earlier and more extensively, and fade after pathogen clearance. The other subset is called memory precursor effector cells or MPECs (KLRG1^{lo} IL-7Rα^{hi}), and have higher capacity to give rise to memory cells(Joshi et al., 2007; Kaech et al., 2003).

The memory CD8 T cell population is also heterogeneous. Memory CD8 T cells that show high expression of CD62L and CCR7 are defined as central memory cells (Tcm)(Cui and Kaech, 2010). These cells are preferentially localized in lymphoid organs, display low cytotoxic activity ex vivo, and have a higher capacity to proliferate and generate IL-2(Cui and Kaech, 2010; Rutishauser and Kaech, 2010). The other memory CD8 T cell subpopulation is termed effector memory CD8 T cells (Tem). These Tem, preferentially reside in non-lymphoid organs, maintain ex vivo lytic activity, undergo less homeostatic renewal, have a more limited lifespan, and lack expression of lymph node homing molecules such as CD62L and CCR7 (Hikono et al., 2007; Wherry et al., 2003).

4.2 Regulation of CD8 T cell differentiation

How do different populations of effector and memory CD8 T cells arise during a pathogen infection? A recent study demonstrated that the fate of naïve CD8 T cells is not predetermined: an individual naïve precursor CD8 T cell can develop into heterogeneous effector and memory CD8 T cell populations. In this study, single cell transfer of an antigen-specific naïve CD8 T cell into a recipient mouse, followed by challenge with *Listeria monocytogenes*, showed that different effector

and memory cell subsets could develop from a single precursor CD8 T cell. This study suggested the concept of “one naïve cell, multiple fate” regarding CD8 T cell development(Stemberger et al., 2007). But when and how the cell fate decision was made still remain controversial. Several models have been proposed to explain the developmental relationship of the effector and memory T cell, which differentially highlight the role of extrinsic factors, such as quality, duration, or quantity of antigenic stimulation, or the intrinsic factors in CD8 T cells themselves, such as the differentiation status(Chang et al., 2007; Kaech and Ahmed, 2001; Sarkar et al., 2008; Williams and Bevan, 2007).

What determines the effector versus memory differentiation decision? It has been shown that many factors influence the establishment of heterogeneity of effector and memory CD8 T cell, such as the duration of infection, time of recruitment of naïve CD8 T cells during infection, sufficiency of inflammatory signals, and tissue-specific microenvironment(D'Souza and Hedrick, 2006; Hikono et al., 2007; Joshi et al., 2007; Rutishauser and Kaech, 2010). These different signals may synergize with each other to drive T cell activation, proliferation, and differentiation(Harty and Badovinac, 2008; Mescher et al., 2006). It seems that activated CD8 T cells will automatically undergo an effector cell program, as both SLEC and MPEC possess lytic activity(Joshi et al., 2007). In particular, recently it has been reported that the strength of IL2-IL-2R signaling is strongly correlated with the cell fate of effector cells(Kalia et al., 2010; Obar et al., 2010; Pipkin et al., 2010). In the presence of strong IL-2 signals or with a higher, early expression of IL-2 receptor α chain, cells rapidly acquire effector functions such as perforin and granzyme B expression, but show a reduced capacity to gain MPEC marker expression. On the other hand, with weak IL-2 inputs or low early expression of IL-2Rα, cells tend to undergo incomplete effector differentiation and obtain more features of memory cells(Kalia et al., 2010; Pipkin et al., 2010). These studies suggested that the dose of IL-2 signaling, or the ability to receive IL-2 input (surface expression level of IL-2Rα), might push early activated CD8 cells to

favorably differentiate towards terminal effector cell or memory cells. Other inflammatory cytokines, such as IL-12 and IFNα, also seem to augment SLEC development during pathogen infection(Joshi et al., 2007).

As activated CD8 T cells are exposed to numerous signals during infection, how these exogenous signals are transmitted to cells and converted into transcriptional regulators that initiate and promote effector versus memory cell fate differentiation is a critical question. The gene expression levels of a range of transcription factors, such as Id2, Gfi-1, Blimp-1, and two highly homologous T-box proteins T-bet and Eomesdermin, changes as the naïve CD8 T cell differentiates into effector cells. This suggests that transcriptional regulation plays an important role in CD8 T cell differentiation(Kaech et al., 2002; Rutishauser and Kaech, 2010). In particular, the expression of T-bet or Blimp-1 was found to be elevated in short-lived effector CD8 T cells relative to memory precursor cells(Joshi et al., 2007; Kallies et al., 2009; Rutishauser et al., 2009). In addition, T-bet or Blimp-1-deficient CD8 T cells preferentially developed into memory precursor cells, demonstrating their importance in the early steps of CD8 T cell differentiation.

Within the cell, how exactly the downstream regulators of different exogenous signals cooperate to determine early CD8 T cells differentiation remains unclear. Different signals might take charge at different stages of development. The TCR signal is absolutely needed for the initiation of T cell activation and differentiation, although not necessarily memory differentiation as has been shown in several studies of lymphopenia induced memory(Cho et al., 2000; Hamilton et al., 2006; Lee et al., 2011). The extent of the activated CD8 T cell response is presumably enhanced by costimulatory signals(Smith-Garvin et al., 2009). To some extent, it seems that the combination of inflammatory cytokines, which probably represent certain cellular- or tissue- and/or stage- specific environment signals, tip the T cell developmental direction according to environmental cues. Downstream

transcriptional regulators that become activated following TCR signals might first open up and expose critical gene loci, which are targets for other downstream regulators of additional signals. Consequently, the expression level of specific transcription factors such as T-bet and other effector molecules might be altered(Letimier et al., 2007; Placek et al., 2009). Therefore, the activated CD8 T cells adopt either the terminal effector or SLEC differentiation or the MPEC program.

5. Research focus

The goal of my dissertation study was to extensively investigate the role of α2,6 sialylation, catalyzed by the glycosyltransferase ST6Gal I in viral T and B cell immunity. I addressed several questions. What role does ST6Gal I expression play in antiviral humoral responses? How does ST6Gal I deficiency affect the generation of viral-specific antibody secreting plasma cells, long-lived plasma cells, and memory B cells? What role does ST6Gal I expression by B cells play in the antiviral homoral response?

Additionally, we examined how loss of α2,6 sialylation affected the generation of viral-specific IgA. How does sialylation of IgG and IgA change in the absence of ST6Gal I expression? Additionally, we examined the pathogenic outcome in ST6Gal I-deficient mice of IgA and IgG deposition in the kidney.

Finally, we probed the role of ST6Gal I in virus-specific CD8 T cell responses. What is the relevance of the differential expression of ST6Gal I in CD8 T cell subpopulations following viral infection? How does loss of ST6Gal I affect the differentiation of effector CD8 T cells during acute viral infection? We determined the mechanisms underlaying differences in CD8 T cell differentiation in the absence of ST6Gal I. our studies revealed a role for ST6Gal I expression in regulating IL-2 receptor signaling during effector CD8 T cell differentiation.

References

Alavi, A., and J.S. Axford. 2008. Sweet and sour: the impact of sugars on disease. *Rheumatology (Oxford)* 47:760-70.

Arnold, J.N., R.A. Dwek, P.M. Rudd, and R.B. Sim. 2006. Mannan binding lectin and its interaction with immunoglobulins in health and in disease. *Immunol Lett* 106:103-10.

Asensio, V.C., C. Kincaid, and I.L. Campbell. 1999. Chemokines and the inflammatory response to viral infection in the central nervous system with a focus on lymphocytic choriomeningitis virus. *J Neurovirol* 5:65-75.

Bonilla, F.A., and H.C. Oettgen. 2010. Adaptive immunity. *J Allergy Clin Immunol* 125:S33-40.

Botten, J., J. Sidney, B.R. Mothe, B. Peters, A. Sette, and M.F. Kotturi. 2010. Coverage of related pathogenic species by multivalent and cross-protective vaccine design: arenaviruses as a model system. *Microbiol Mol Biol Rev* 74:157-70.

Buchmeier, M.J., R.M. Welsh, F.J. Dutko, and M.B. Oldstone. 1980. The virology and immunobiology of lymphocytic choriomeningitis virus infection. *Adv Immunol* 30:275-331.

Chang, J.T., V.R. Palanivel, I. Kinjyo, F. Schambach, A.M. Intlekofer, A. Banerjee, S.A. Longworth, K.E. Vinup, P. Mrass, J. Oliaro, N. Killeen, J.S. Orange, S.M. Russell, W. Weninger, and S.L. Reiner. 2007. Asymmetric T lymphocyte division in the initiation of adaptive immune responses. *Science* 315:1687-91.

Chiricolo, M., N. Malagolini, S. Bonfiglioli, and F. Dall'Olio. 2006. Phenotypic changes induced by expression of beta-galactoside alpha2,6 sialyltransferase I in the human colon cancer cell line SW948. *Glycobiology* 16:146-54.

Cho, B.K., V.P. Rao, Q. Ge, H.N. Eisen, and J. Chen. 2000. Homeostasis-stimulated proliferation drives naive T cells to differentiate directly into memory T cells. *J Exp Med* 192:549-56.

Cobb, B.A., and D.L. Kasper. 2005. Coming of age: carbohydrates and immunity. *Eur J Immunol* 35:352-6.

Comelli, E.M., M. Sutton-Smith, Q. Yan, M. Amado, M. Panico, T. Gilmartin, T. Whisenant, C.M. Lanigan, S.R. Head, D. Goldberg, H.R. Morris, A. Dell, and J.C. Paulson. 2006. Activation of murine CD4+ and CD8+ T lymphocytes leads to dramatic remodeling of N-linked glycans. *J Immunol* 177:2431-40.

Cooper, M.D., and M.N. Alder. 2006. The evolution of adaptive immune systems. *Cell* 124:815-22.

Cox, R.J., K.A. Brokstad, and P. Ogra. 2004. Influenza virus: immunity and vaccination strategies. Comparison of the immune response to inactivated and live, attenuated influenza vaccines. *Scand J Immunol* 59:1-15.

Cui, W., and S.M. Kaech. 2010. Generation of effector CD8+ T cells and their conversion to memory T cells. *Immunol Rev* 236:151-66.

D'Amico, G. 1987. The commonest glomerulonephritis in the world: IgA nephropathy. *Q J Med* 64:709-27.

D'Amico, G. 2004. Natural history of idiopathic IgA nephropathy and factors predictive of disease outcome. *Semin Nephrol* 24:179-96.

D'Souza, W.N., and S.M. Hedrick. 2006. Cutting edge: latecomer CD8 T cells are imprinted with a unique differentiation program. *J Immunol* 177:777-81.

Dall'Olio, F. 2000. The sialyl-alpha2,6-lactosaminyl-structure: biosynthesis and functional role. *Glycoconj J* 17:669-76.

Dall'Olio, F., and M. Chiricolo. 2001. Sialyltransferases in cancer. *Glycoconj J* 18:841-50.

Dalziel, M., S. Lemaire, J. Ewing, L. Kobayashi, and J.T. Lau. 1999. Hepatic acute phase induction of murine beta-galactoside alpha 2,6

sialyltransferase (ST6Gal I) is IL-6 dependent and mediated by elevation of exon H-containing class of transcripts. *Glycobiology* 9:1003-8.

Das, H., T. Atsumi, Y. Fukushima, H. Shibuya, K. Ito, Y. Yamada, Y. Amasaki, K. Ichikawa, O. Amengual, and T. Koike. 2004. Diagnostic value of antiagalactosyl IgG antibodies in rheumatoid arthritis. *Clin Rheumatol* 23:218-22.

Dennis, J.W., J. Pawling, P. Cheung, E. Partridge, and M. Demetriou. 2002. UDP-N-acetylglucosamine:alpha-6-D-mannoside beta1,6 N-acetylglucosaminyltransferase V (Mgat5) deficient mice. *Biochim Biophys Acta* 1573:414-22.

Doherty, P.C., D.J. Topham, R.A. Tripp, R.D. Cardin, J.W. Brooks, and P.G. Stevenson. 1997. Effector CD4+ and CD8+ T-cell mechanisms in the control of respiratory virus infections. *Immunol Rev* 159:105-17.

Dricu, A., L. Kanter, M. Wang, G. Nilsson, M. Hjertman, J. Wejde, and O. Larsson. 1999. Expression of the insulin-like growth factor 1 receptor (IGF-1R) in breast cancer cells: evidence for a regulatory role of dolichyl phosphate in the transition from an intracellular to an extracellular IGF-1 pathway. *Glycobiology* 9:571-9.

Duffy, M.J., P.M. McGowan, and W.M. Gallagher. 2008. Cancer invasion and metastasis: changing views. *J Pathol* 214:283-93.

Ellies, L.G., W. Tao, W. Fellinger, H.S. Teh, and H.J. Ziltener. 1996. The CD43 130-kD peripheral T-cell activation antigen is downregulated in thymic positive selection. *Blood* 88:1725-32.

Fazakerley, J.K., P. Southern, F. Bloom, and M.J. Buchmeier. 1991. High resolution in situ hybridization to determine the cellular distribution of lymphocytic choriomeningitis virus RNA in the tissues of persistently infected mice: relevance to arenavirus disease and mechanisms of viral persistence. *J Gen Virol* 72 (Pt 7):1611-25.

Fuxa, M., and J.A. Skok. 2007. Transcriptional regulation in early B cell development. *Curr Opin Immunol* 19:129-36.

Gagneux, P., and A. Varki. 1999. Evolutionary considerations in relating oligosaccharide diversity to biological function. *Glycobiology* 9:747-55.

Gerhard, W., K. Mozdzanowska, M. Furchner, G. Washko, and K. Maiese. 1997. Role of the B-cell response in recovery of mice from primary influenza virus infection. *Immunol Rev* 159:95-103.

Gharavi, A.G., Y. Yan, F. Scolari, F.P. Schena, G.M. Frasca, G.M. Ghiggeri, K. Cooper, A. Amoroso, B.F. Viola, G. Battini, G. Caridi, C. Canova, A. Farhi, V. Subramanian, C. Nelson-Williams, S. Woodford, B.A. Julian, R.J. Wyatt, and R.P. Lifton. 2000. IgA nephropathy, the most common cause of glomerulonephritis, is linked to 6q22-23. *Nat Genet* 26:354-7.

Gindzienska-Sieskiewicz, E., P.A. Klimiuk, D.G. Kisiel, A. Gindzienski, and S. Sierakowski. 2007. The changes in monosaccharide composition of immunoglobulin G in the course of rheumatoid arthritis. *Clin Rheumatol* 26:685-90.

Girnita, L., M. Wang, Y. Xie, G. Nilsson, A. Dricu, J. Wejde, and O. Larsson. 2000. Inhibition of N-linked glycosylation down-regulates insulin-like growth factor-1 receptor at the cell surface and kills Ewing's sarcoma cells: therapeutic implications. *Anticancer Drug Des* 15:67-72.

Hamilton, S.E., M.C. Wolkers, S.P. Schoenberger, and S.C. Jameson. 2006. The generation of protective memory-like CD8+ T cells during homeostatic proliferation requires CD4+ T cells. *Nat Immunol* 7:475-81.

Hanahan, D., and R.A. Weinberg. 2011. Hallmarks of cancer: the next generation. *Cell* 144:646-74.

Harduin-Lepers, A., M.A. Recchi, and P. Delannoy. 1995. 1994, the year of sialyltransferases. *Glycobiology* 5:741-58.

Harty, J.T., and V.P. Badovinac. 2008. Shaping and reshaping CD8+ T-cell memory. *Nat Rev Immunol* 8:107-19.

Hedlund, M., E. Ng, A. Varki, and N.M. Varki. 2008. alpha 2-6-Linked sialic acids on N-glycans modulate carcinoma differentiation in vivo. *Cancer Res* 68:388-94.

Hennet, T., D. Chui, J.C. Paulson, and J.D. Marth. 1998. Immune regulation by the ST6Gal sialyltransferase. *Proc Natl Acad Sci U S A* 95:4504-9.

Higgins, E.A., K.A. Siminovitch, D.L. Zhuang, I. Brockhausen, and J.W. Dennis. 1991. Aberrant O-linked oligosaccharide biosynthesis in lymphocytes and platelets from patients with the Wiskott-Aldrich syndrome. *J Biol Chem* 266:6280-90.

Hiki, Y., A. Horii, H. Iwase, A. Tanaka, Y. Toda, K. Hotta, and Y. Kobayashi. 1995. O-linked oligosaccharide on IgA1 hinge region in IgA nephropathy. Fundamental study for precise structure and possible role. *Contrib Nephrol* 111:73-84.

Hikono, H., J.E. Kohlmeier, S. Takamura, S.T. Wittmer, A.D. Roberts, and D.L. Woodland. 2007. Activation phenotype, rather than central- or effector-memory phenotype, predicts the recall efficacy of memory CD8+ T cells. *J Exp Med* 204:1625-36.

Imai, K., T. Morio, Y. Zhu, Y. Jin, S. Itoh, M. Kajiwara, J. Yata, S. Mizutani, H.D. Ochs, and S. Nonoyama. 2004. Clinical course of patients with WASP gene mutations. *Blood* 103:456-64.

Jefferis, R. 2005. Glycosylation of recombinant antibody therapeutics. *Biotechnol Prog* 21:11-6.

Jenkinson, E.J., W.E. Jenkinson, S.W. Rossi, and G. Anderson. 2006. The thymus and T-cell commitment: the right niche for Notch? *Nat Rev Immunol* 6:551-5.

Joshi, N.S., W. Cui, A. Chandele, H.K. Lee, D.R. Urso, J. Hagman, L. Gapin, and S.M. Kaech. 2007. Inflammation directs memory precursor and short-lived effector CD8(+) T cell fates via the graded expression of T-bet transcription factor. *Immunity* 27:281-95.

Kaech, S.M., and R. Ahmed. 2001. Memory CD8+ T cell differentiation: initial antigen encounter triggers a developmental program in naive cells. *Nat Immunol* 2:415-22.

Kaech, S.M., S. Hemby, E. Kersh, and R. Ahmed. 2002. Molecular and functional profiling of memory CD8 T cell differentiation. *Cell* 111:837-51.

Kaech, S.M., J.T. Tan, E.J. Wherry, B.T. Konieczny, C.D. Surh, and R. Ahmed. 2003. Selective expression of the interleukin 7 receptor identifies effector CD8 T cells that give rise to long-lived memory cells. *Nat Immunol* 4:1191-8.

Kalia, V., S. Sarkar, S. Subramaniam, W.N. Haining, K.A. Smith, and R. Ahmed. 2010. Prolonged interleukin-2Ralpha expression on virus-specific CD8+ T cells favors terminal-effector differentiation in vivo. *Immunity* 32:91-103.

Kallies, A., A. Xin, G.T. Belz, and S.L. Nutt. 2009. Blimp-1 transcription factor is required for the differentiation of effector CD8(+) T cells and memory responses. *Immunity* 31:283-95.

Kaneko, Y., F. Nimmerjahn, and J.V. Ravetch. 2006. Anti-inflammatory activity of immunoglobulin G resulting from Fc sialylation. *Science* 313:670-3.

Kaplan, H.A., B.M. Woloski, M. Hellman, and J.C. Jamieson. 1983. Studies on the effect of inflammation on rat liver and serum sialyltransferase. Evidence that inflammation causes release of Gal beta 1 leads to 4GlcNAc alpha 2 leads to 6 sialyltransferase from liver. *J Biol Chem* 258:11505-9.

Khan, S., S. Holding, P.C. Dore, and W.A. Sewell. 2008. Abnormal O-glycosylation of CD43 may account for some features of Wiskott-Aldrich syndrome. *Med Hypotheses* 70:269-72.

Kitagawa, H., and J.C. Paulson. 1994. Differential expression of five sialyltransferase genes in human tissues. *J Biol Chem* 269:17872-8.

Kunkel, E.J., and E.C. Butcher. 2003. Plasma-cell homing. *Nat Rev Immunol* 3:822-9.

Kurosaki, T., Y. Aiba, K. Kometani, S. Moriyama, and Y. Takahashi. 2010. Unique properties of memory B cells of different isotypes. *Immunol Rev* 237:104-16.

Launay, P., B. Grossetete, M. Arcos-Fajardo, E. Gaudin, S.P. Torres, L. Beaudoin, N. Patey-Mariaud de Serre, A. Lehuen, and R.C. Monteiro. 2000. Fcalpha receptor (CD89) mediates the development of immunoglobulin A (IgA) nephropathy (Berger's disease). Evidence for pathogenic soluble receptor-Iga complexes in patients and CD89 transgenic mice. *J Exp Med* 191:1999-2009.

LeBien, T.W., and T.F. Tedder. 2008. B lymphocytes: how they develop and function. *Blood* 112:1570-80.

Lee, Y.J., S.C. Jameson, and K.A. Hogquist. 2011. Alternative memory in the CD8 T cell lineage. *Trends Immunol* 32:50-6.

Lefrancois, L., and J.J. Obar. 2010. Once a killer, always a killer: from cytotoxic T cell to memory cell. *Immunol Rev* 235:206-18.

Letimier, F.A., N. Passini, S. Gasparian, E. Bianchi, and L. Rogge. 2007. Chromatin remodeling by the SWI/SNF-like BAF complex and STAT4 activation synergistically induce IL-12Rbeta2 expression during human Th1 cell differentiation. *Embo J* 26:1292-302.

Matsumoto, M., K. Atarashi, E. Umemoto, Y. Furukawa, A. Shigeta, M. Miyasaka, and T. Hirata. 2005. CD43 functions as a ligand for E-Selectin on activated T cells. *J Immunol* 175:8042-50.

Meezan, E., H.C. Wu, P.H. Black, and P.W. Robbins. 1969. Comparative studies on the carbohydrate-containing membrane components of normal and virus-transformed mouse fibroblasts. II. Separation of glycoproteins and glycopeptides by sephadex chromatography. *Biochemistry* 8:2518-24.

Mescher, M.F., J.M. Curtsinger, P. Agarwal, K.A. Casey, M. Gerner, C.D. Hammerbeck, F. Popescu, and Z. Xiao. 2006. Signals required for programming effector and memory development by CD8+ T cells. *Immunol Rev* 211:81-92.

Mestecky, J., M. Tomana, P.A. Crowley-Nowick, Z. Moldoveanu, B.A. Julian, and S. Jackson. 1993. Defective galactosylation and clearance of IgA1

molecules as a possible etiopathogenic factor in IgA nephropathy. *Contrib Nephrol* 104:172-82.

Mogensen, T.H. 2009. Pathogen recognition and inflammatory signaling in innate immune defenses. *Clin Microbiol Rev* 22:240-73, Table of Contents.

Nasirikenari, M., E.V. Chandrasekaran, K.L. Matta, B.H. Segal, P.N. Bogner, A.A. Lugade, Y. Thanavala, J.J. Lee, and J.T. Lau. 2010. Altered eosinophil profile in mice with ST6Gal-1 deficiency: an additional role for ST6Gal-1 generated by the P1 promoter in regulating allergic inflammation. *J Leukoc Biol* 87:457-66.

Nasirikenari, M., B.H. Segal, J.R. Ostberg, A. Urbasic, and J.T. Lau. 2006. Altered granulopoietic profile and exaggerated acute neutrophilic inflammation in mice with targeted deficiency in the sialyltransferase ST6Gal I. *Blood* 108:3397-405.

Nicholson, K.G. 1992. Clinical features of influenza. *Semin Respir Infect* 7:26-37.

Nishie, T., O. Miyaishi, H. Azuma, A. Kameyama, C. Naruse, N. Hashimoto, H. Yokoyama, H. Narimatsu, T. Wada, and M. Asano. 2007. Development of immunoglobulin A nephropathy- like disease in beta-1,4-galactosyltransferase-I-deficient mice. *Am J Pathol* 170:447-56.

Nitschke, L. 2005. The role of CD22 and other inhibitory co-receptors in B-cell activation. *Curr Opin Immunol* 17:290-7.

Notarangelo, L.D., L.D. Notarangelo, and H.D. Ochs. 2005. WASP and the phenotypic range associated with deficiency. *Curr Opin Allergy Clin Immunol* 5:485-90.

Novak, J., B.A. Julian, M. Tomana, and J. Mestecky. 2008. IgA glycosylation and IgA immune complexes in the pathogenesis of IgA nephropathy. *Semin Nephrol* 28:78-87.

Obar, J.J., M.J. Molloy, E.R. Jellison, T.A. Stoklasek, W. Zhang, E.J. Usherwood, and L. Lefrancois. 2010. CD4+ T cell regulation of CD25 expression controls development of short-lived effector CD8+ T cells in primary and secondary responses. *Proc Natl Acad Sci U S A* 107:193-8.

Ohtsubo, K., and J.D. Marth. 2006. Glycosylation in cellular mechanisms of health and disease. *Cell* 126:855-67.

Oliver, A.M., F. Martin, G.L. Gartland, R.H. Carter, and J.F. Kearney. 1997. Marginal zone B cells exhibit unique activation, proliferative and immunoglobulin secretory responses. *Eur J Immunol* 27:2366-74.

Onami, T.M., L.E. Harrington, M.A. Williams, M. Galvan, C.P. Larsen, T.C. Pearson, N. Manjunath, L.G. Baum, B.D. Pearce, and R. Ahmed. 2002. Dynamic regulation of T cell immunity by CD43. *J Immunol* 168:6022-31.

Opdenakker, G., C. Dillen, P. Fiten, E. Martens, I. Van Aelst, P.E. Van den Steen, I. Nelissen, S. Starckx, F.J. Descamps, J. Hu, H. Piccard, J. Van Damme, M.R. Wormald, P.M. Rudd, and R.A. Dwek. 2006. Remnant epitopes, autoimmunity and glycosylation. *Biochim Biophys Acta* 1760:610-5.

Oracki, S.A., J.A. Walker, M.L. Hibbs, L.M. Corcoran, and D.M. Tarlinton. 2010. Plasma cell development and survival. *Immunol Rev* 237:140-59.

Paterson, A.D., X.Q. Liu, K. Wang, R. Magistroni, X. Song, J. Kappel, J. Klassen, D. Cattran, P. St George-Hyslop, and Y. Pei. 2007. Genome-wide linkage scan of a large family with IgA nephropathy localizes a novel susceptibility locus to chromosome 2q36. *J Am Soc Nephrol* 18:2408-15.

Peled, J.U., F.L. Kuang, M.D. Iglesias-Ussel, S. Roa, S.L. Kalis, M.F. Goodman, and M.D. Scharff. 2008. The biochemistry of somatic hypermutation. *Annu Rev Immunol* 26:481-511.

Piller, F., F. Le Deist, K.I. Weinberg, R. Parkman, and M. Fukuda. 1991. Altered O-glycan synthesis in lymphocytes from patients with Wiskott-Aldrich syndrome. *J Exp Med* 173:1501-10.

Pipkin, M.E., J.A. Sacks, F. Cruz-Guilloty, M.G. Lichtenheld, M.J. Bevan, and A. Rao. 2010. Interleukin-2 and inflammation induce distinct transcriptional programs that promote the differentiation of effector cytolytic T cells. *Immunity* 32:79-90.

Placek, K., M. Coffre, S. Maiella, E. Bianchi, and L. Rogge. 2009. Genetic and epigenetic networks controlling T helper 1 cell differentiation. *Immunology* 127:155-62.

Rudd, P.M., T. Elliott, P. Cresswell, I.A. Wilson, and R.A. Dwek. 2001. Glycosylation and the immune system. *Science* 291:2370-6.

Rutishauser, R.L., and S.M. Kaech. 2010. Generating diversity: transcriptional regulation of effector and memory CD8 T-cell differentiation. *Immunol Rev* 235:219-33.

Rutishauser, R.L., G.A. Martins, S. Kalachikov, A. Chandele, I.A. Parish, E. Meffre, J. Jacob, K. Calame, and S.M. Kaech. 2009. Transcriptional repressor Blimp-1 promotes CD8(+) T cell terminal differentiation and represses the acquisition of central memory T cell properties. *Immunity* 31:296-308.

Sarkar, S., V. Kalia, W.N. Haining, B.T. Konieczny, S. Subramaniam, and R. Ahmed. 2008. Functional and genomic profiling of effector CD8 T cell subsets with distinct memory fates. *J Exp Med* 205:625-40.

Schluns, K.S., W.C. Kieper, S.C. Jameson, and L. Lefrancois. 2000. Interleukin-7 mediates the homeostasis of naive and memory CD8 T cells in vivo. *Nat Immunol* 1:426-32.

Seales, E.C., G.A. Jurado, B.A. Brunson, J.K. Wakefield, A.R. Frost, and S.L. Bellis. 2005. Hypersialylation of beta1 integrins, observed in colon adenocarcinoma, may contribute to cancer progression by up-regulating cell motility. *Cancer Res* 65:4645-52.

Shapiro-Shelef, M., and K. Calame. 2005. Regulation of plasma-cell development. *Nat Rev Immunol* 5:230-42.

Smith-Garvin, J.E., G.A. Koretzky, and M.S. Jordan. 2009. T cell activation. *Annu Rev Immunol* 27:591-619.

Snapper, C.M., H. Yamada, D. Smoot, R. Sneed, A. Lees, and J.J. Mond. 1993. Comparative in vitro analysis of proliferation, Ig secretion, and Ig class

switching by murine marginal zone and follicular B cells. *J Immunol* 150:2737-45.

Stavnezer, J., J.E. Guikema, and C.E. Schrader. 2008. Mechanism and regulation of class switch recombination. *Annu Rev Immunol* 26:261-92.

Steiniger, B., E.M. Timphus, and P.J. Barth. 2006. The splenic marginal zone in humans and rodents: an enigmatic compartment and its inhabitants. *Histochem Cell Biol* 126:641-8.

Stemberger, C., K.M. Huster, M. Koffler, F. Anderl, M. Schiemann, H. Wagner, and D.H. Busch. 2007. A single naive CD8+ T cell precursor can develop into diverse effector and memory subsets. *Immunity* 27:985-97.

Takashima, S. 2008. Characterization of mouse sialyltransferase genes: their evolution and diversity. *Biosci Biotechnol Biochem* 72:1155-67.

Toscano, M.A., G.A. Bianco, J.M. Ilarregui, D.O. Croci, J. Correale, J.D. Hernandez, N.W. Zwirner, F. Poirier, E.M. Riley, L.G. Baum, and G.A. Rabinovich. 2007. Differential glycosylation of TH1, TH2 and TH-17 effector cells selectively regulates susceptibility to cell death. *Nat Immunol* 8:825-34.

Troelsen, L.N., P. Garred, H.O. Madsen, and S. Jacobsen. 2007. Genetically determined high serum levels of mannose-binding lectin and agalactosyl IgG are associated with ischemic heart disease in rheumatoid arthritis. *Arthritis Rheum* 56:21-9.

Varki, A. 2006. Nothing in glycobiology makes sense, except in the light of evolution. *Cell* 126:841-5.

Varki, A. 2008. Sialic acids in human health and disease. *Trends Mol Med* 14:351-60.

Varki, N.M., and A. Varki. 2007. Diversity in cell surface sialic acid presentations: implications for biology and disease. *Lab Invest* 87:851-7.

Varki., A. 2009. Essentials of Glycobiology, 2nd edition.

Wen, D.X., E.C. Svensson, and J.C. Paulson. 1992. Tissue-specific alternative splicing of the beta-galactoside alpha 2,6-sialyltransferase gene. *J Biol Chem* 267:2512-8.

Wherry, E.J., V. Teichgraber, T.C. Becker, D. Masopust, S.M. Kaech, R. Antia, U.H. von Andrian, and R. Ahmed. 2003. Lineage relationship and protective immunity of memory CD8 T cell subsets. *Nat Immunol* 4:225-34.

Williams, M.A., and M.J. Bevan. 2007. Effector and memory CTL differentiation. *Annu Rev Immunol* 25:171-92.

Wuensch, S.A., R.Y. Huang, J. Ewing, X. Liang, and J.T. Lau. 2000. Murine B cell differentiation is accompanied by programmed expression of multiple novel beta-galactoside alpha2, 6-sialyltransferase mRNA forms. *Glycobiology* 10:67-75.

Yoshimura, M., Y. Ihara, Y. Matsuzawa, and N. Taniguchi. 1996. Aberrant glycosylation of E-cadherin enhances cell-cell binding to suppress metastasis. *J Biol Chem* 271:13811-5.

Zheng, F., G.C. Kundu, Z. Zhang, J. Ward, F. DeMayo, and A.B. Mukherjee. 1999. Uteroglobin is essential in preventing immunoglobulin A nephropathy in mice. *Nat Med* 5:1018-25.

Zhu, J., and W.E. Paul. 2008. CD4 T cells: fates, functions, and faults. *Blood* 112:1557-69.

CHAPTER II
THE GENERATION OF INFLUENZA-SPECIFIC HUMORAL RESPONSES IS IMPAIRED IN ST6GAL I-DEFICIENT MICE

A version of this chapter was originally published by Junwei Zeng., Hye-Mee Joo, Bheemreddy Rajini, Jens P. Wrammert, Mark Y. Sangster, and Thandi M. Onami.

Junwei Zeng, Hye-Mee Joo, Bheemreddy Rajini, Jens P. Wrammert, Mark Y. Sangster, and Thandi M. Onami."The generation of influenza-specific humoral responses is impaired in ST6Gal I-deficient mice" J Immunol. 2009 Apr 15; 182 (8): 4721-7.

In this chapter, "our" and "we" refer to me and co-authors. My contribution to this paper includes: 1) planning and performing experiments, 2) analyzing data, 3) preparing figures, and 4) editing.

Abstract

Post-translational modification of proteins, such as glycosylation, can impact cell signaling and function. ST6Gal I, a glycosyltransferase expressed by B cells, catalyzes the addition of α-2, 6 sialic acid to galactose (Siaα2-6Gal), a modification found on N-linked glycoproteins such as CD22, a negative regulator of B cell activation. We show that SNA lectin, which binds Siaα2-6Gal, shows high binding on plasma blasts and germinal center B cells following viral infection, suggesting ST6Gal I expression remains high on activated B cells *in vivo*. To understand the relevance of this modification on the antiviral B cell immune response, we infected ST6Gal $I^{-/-}$ mice with influenza A/HKx31. We demonstrate that the loss of ST6Gal I expression results in similar influenza infectivity in the lung, but significantly reduced early influenza-specific IgM and IgG levels in the serum, as well as significantly reduced numbers of early viral specific antibody-secreting cells (ASCs). At later memory time points, ST6Gal $I^{-/-}$

mice show comparable numbers of IgG influenza-specific memory B cells and long-lived plasma cells, with similarly high antiviral IgG titers, with the exception of IgG2c. Finally, we adoptively transfer purified B cells from WT or ST6Gal $I^{-/-}$ mice into B cell deficient ($\mu MT^{-/-}$) mice. Recipient mice that received ST6Gal $I^{-/-}$ B cells demonstrated reduced influenza-specific IgM levels, but similar levels of influenza-specific IgG, compared to mice that received WT B cells. These data suggest that a B cell intrinsic defect partially contributes to the impaired antiviral humoral response.

Introduction

Humoral immunity is characterized by prolonged antibody production, even after resolution of infection, in stark contrast to the T cell response, where effector T cell function is relatively short-lived. Antibodies, by neutralizing or opsonizing free extracellular pathogens, serve as a critical first-line defense against infection. Humoral immunity is comprised of pre-existing antibody produced by antibody secreting cells (ASCs) termed long-lived plasma cells (LLPCs), as well as a population of memory B cells (MBCs) that can differentiate following antigenic stimulation into plasma cells (Kalia et al., 2006; Slifka and Ahmed, 1996; Slifka and Ahmed, 1998; Slifka et al., 1998).

The enzyme ST6Gal I is a glycosyltransferase highly expressed by B and T cells that synthesizes the glycan sequence α2,6 sialic acid linked to galactose (Siaα2-6Gal) (Hennet et al., 1998). This structure is typically found on N-linked glycans of glycoproteins, such as the mammalian lectin CD22, a transmembrane glycoprotein expressed by B cells that has high specificity for (Siaα2-6Gal). CD22 has been shown to be a negative regulator of B cell signaling by recruiting SHP-1 to the BCR, thus attenuating signals via the BCR (Collins et al., 2006; Hennet et al., 1998; Nitschke, 2005). The plant lectin *Sambucas nigra agglutinin*

(SNA) binds the product of ST6Gal I, Siaα2-6Gal, so SNA lectin binding can be used as an indicator of ST6Gal I expression and/or activity (Hennet et al., 1998).

ST6Gal I null mice were initially described several years ago (Hennet et al., 1998). These mice demonstrate normal T cell activation to anti-CD3 cross-linking *in vitro*, but defective BCR signaling *in vitro*, and reduced antibody production following immunization with T-independent and T-dependent antigens (DNP-Ficoll or DNP-KLH) *in vivo* (Hennet et al., 1998). However, despite indications that B cell immune function may be compromised in these mice, as well as evidence that addition of cytokines could abrogate *in vitro* B cell proliferation differences, no studies have documented whether or not protective antibody and memory B cell responses are compromised in these mice when exposed to pathogenic microorganisms such as live viral infection.

In this study, we have compared the outcome of influenza viral infection of wild type or ST6Gal I deficient mice. The haemagglutinin (HA) glycoprotein plays a key role in influenza pathogenicity and is involved in host-cell recognition (Horimoto and Kawaoka, 2005). First, we show that effective replication of influenza A/HKx31 (Orthomyxoviridae, Influenza A) does occur in the lungs of ST6Gal $I^{-/-}$ mice, however these mice demonstrate defective early influenza-specific B cell responses. Next, we determine that expansion of CD4 and CD8 influenza-specific T cell numbers in the lung and lymph nodes is normal in ST6Gal $I^{-/-}$ mice. Further, we demonstrate similar overall numbers of influenza specific IgG MBCs and LLPCs, though we note both a reduction in serum levels of influenza specific IgG2c and IgG2c producing LLPCs in the bone marrow. Finally, we demonstrate an impaired influenza specific IgM response in B cell deficient mice that receive ST6Gal $I^{-/-}$ B cells, suggesting that a B cell intrinsic defect partially contributes to the impaired humoral response. Overall, our findings suggest that lack of ST6Gal I expression appears to prominently impair

the generation of a viral specific humoral response, but plays a lesser role in influenza-specific memory.

Materials and methods

Mice and immunizations

ST6Gal I deficient mice were generated by J. Marth and obtained from the Consortium for Functional Glycomics and bred in-house (Hennet et al., 1998). C57BL/6 female mice and B6.129S2-Igh-6^{tm1Cgn}/J (μMT-/- mice) were purchased from The Jackson Laboratory (Bar Harbor, ME). Mice were maintained under specific pathogen-free conditions at the University of Tennessee in accordance with university IACUC guidelines and used at 6-12 weeks of age. Anesthetized mice were intra-nasally infected with $10^{6.8}$ EID_{50} influenza A/HKx31 in 30 μl PBS as previously described (Li et al., 2006; Sangster et al., 2003). mMT$^{-/-}$ mice were primed with $10^{7.4}$ EID_{50} influenza A/HKx31 i.p.

Tissues harvest and flow cytometry

At specified time points (day 7, 10, > 40 post-infection), animals were sacrificed and tissues harvested for viral titer (lungs only), immunofluorescence, or isolation of lymphocytes. For isolation of lymphocytes from lungs, lungs were perfused with 5 ml cold PBS before removal and processed as previously described (Masopust et al., 2006). Single cell suspensions were stained with mAbs purchased from BD Pharmingen (CD4, CD8, CD44, B220, CD138, FAS, GL7, IFNg and TNFa), Vector Labs (SNA and PNA lectins), or Southern Biotech (IgD). Intracellular cytokine staining was assayed on cells from spleen, lung, and MedLN. All samples were run on a FACSCalibur (BD Biosciences). All data were analyzed with FlowJo software (Tree Star). Unpaired student t tests were

performed to determine statistical significance with *denoting p<.05 ** denoting P<0.01, and *** denoting P<0.001.

Immunofluorescence

MedLNs were removed from mice on day 7 p.i. and frozen in OCT at –80°C. The frozen tissues were cut at 8-μm thickness, thaw-mounted onto slides, air dried and fixed in cold acetone for 10 minutes. The sections were then blocked with 3% BSA and stained for germinal centers with PNA-FITC (Vector Laboratories), anti-B220-PE, and/or GL7-FITC (BD Pharmingen) as indicated. After staining, sections were washed with PBS, mounted using Vectashield mounting medium (Vector Laboratories), and analyzed using a laser scanning confocal microscope (Leica SP2).

Influenza viral titer determination

Lungs were collected on indicated days post-infection and homogenized in Hanks media with 0.1% BSA (GIBCO). Eight replicates of the homogenized lung were serially diluted tenfold across 96-well U-bottom plates in 1xMEM with 0.3% BSA, 1μg/ml Trypsin TPCK-treated (Worthington), penicillin (100IU/ml), streptomycin (100 μg/ml), and 5% FBS. The titrated lung samples were added to serum-free MEM MDCK cell monolayer prepared in 96-well tissue culture plates and incubated for 48h at 37°C and 5% CO_2. Wells that were positive for viral growth were identified by testing supernatants for hemagglutinating activity using 0.5% chicken red blood cells.

ELISPOT assay to detect influenza specific ASCs

A preparation of concentrated viral particles was disrupted for 10 min at room temperature in a 1:10 dilution of disruption buffer (0.5% Triton X-100, 0.6 M KCl,

and 0.05 M Tris-HCl, pH 7.5) in PBS, further diluted in PBS, and plated at 1 μg/well in nitrocellulose-bottomed 96-well Multiscreen HA filtration plates (Millipore, Bedford, MA). After overnight incubation at 4°C, plates were washed with PBS, and blocked with BCM containing 10% FBS. Plates were emptied by flicking, and cell suspensions (including resuspended cells from 96-well MBC assay plates) were added in volumes of approximately 100 μl/well. After incubation for 3-4 h at 37°C in a humidified atmosphere containing 5% CO_2, plates were thoroughly washed with PBS alone and PBS containing 0.1% Tween 20. Alkaline phosphatase-conjugated goat anti-mouse IgG, IgM, or IgA (Southern Biotechnology, Birmingham, AL) diluted to 2 μg/ml in PBS containing 5% bovine serum albumin was added (100 μl/well), and the plates were incubated overnight at 4°C. The plates were then washed extensively with PBS alone and PBS containing 0.1% Tween 20, including washing the underside of the nitrocellulose filters. Spots were developed at room temperature by the addition of 1 mg/ml of 5-bromo-4-chloro-3-indolyl phosphate (Sigma, St. Louis, MO) in diethanolamine buffer (10% diethanolamine, 0.1 M NaCl, 5 mM $MgCl_2$, and 0.1 M Tris-HCl, pH 9.5), 100 μl/well. After spot development, plates were washed with PBS and dried, and spots representing individual ASCs were counted using an Olympus SZX9 stereozoom microscope.

Memory B cell assay

Influenza-specific MBC frequencies were determined by a previously described LDA based on *in vitro* stimulation of MBC to differentiate into ASCs (Joo et al., 2008; Li et al., 2006). Briefly, two-fold dilutions of cells were incubated in 96-well tissue culture plates (routinely 12 wells per dilution), together with 10^6 irradiated (3000 rad) syngeneic naïve spleen cell feeders plus b-propiolactone-inactivated HKx31 (Charles River, Wilmington, MA). After incubation, cells in each well were transferred to ELISPOT plates for the enumeration of influenza-specific IgG

ASCs. Pre-existing virus-specific ASC numbers at the time of sampling were determined by direct *ex vivo* ELISPOT assay. After *in vitro* MBC activation and ELISPOT analysis, individual wells were scored positive for virus-specific MBC if progeny ASC numbers were greater than twice the mean pre-existing ASC. The virus-specific MBC frequency was calculated from the number of negative wells per cell dilution by extrapolation to the dilution that gave 37% negative wells (Joo et al., 2008). Linearity between the proportion of negative cultures and the input cell dose indicated direct measurement of MBC. No influenza-specific IgG ASCs were detected after *in vitro* stimulation of lymphocytes from naïve mice or from mice infected i.n 8 wk previously with an unrelated virus.

B cell transfer and ELISA

MACS B220 beads (Miltenyi Biotech) were used for purification of B cells according to the manufacturer's instructions. Purity of $B220^+$ B cells was 95% determined by FACS. $2x10^7$ $B220^+$ spleen cells were adoptively transferred into individual primed μMT deficient mice i.v. followed by infection with influenza i.n. 24 hrs later. For serum antibody determination by ELISA, plates were coated with purified, detergent disrupted influenza A/HKx31 virus (0.5μg/well) and incubated at 4°C overnight. Plates were washed with PBS-Tween20 (0.05%), blocked with PBS/FBS (3%), and washed again. Serial three-fold serum dilutions were prepared in PBS-Tween20 (0.05%)-BSA (0.5%). The plates were incubated at RT 4 h or overnight at 4°C, then washed thoroughly. Plate-bound secreted Abs were detected using alkaline phosphatase-conjugated goat anti-mouse Abs with specificity for IgM, IgG, IgG1, IgG2b, IgG2c or IgG3 (Southern Biotechnology, Birmingham, AL) diluted in PBS-BSA (1%). After 4 h incubation at RT, plates were washed extensively, and color development with *p*-nitrophenyl phosphate (Sigma) in diethanolamine buffer was read at 405 nm using a Synergy2 Multi-Detection Microplate Reader (BioTek Instruments, Inc.). The virus-specific serum Ab titer is expressed as the reciprocal of the highest dilution giving an

absorbance value more than twice that for simultaneously titrated samples from naïve mice.

Results

SNA binding is high on naïve and in vivo activated B cells

The plant lectin SNA preferentially binds a2-6-linked sialic acids and previous reports have demonstrated high SNA binding on naïve lymphocytes that is abrogated in lymphocytes lacking ST6Gal I expression (Hennet et al., 1998). Gene expression studies comparing naïve B cells to *in vitro* activated B cells revealed that ST6Gal I expression remains high on activated B cells (Comelli et al., 2006).

We examined SNA lectin binding by flow cytometry on B cells following *in vivo* B cell activation (Figure 2.1). We observed that on day 8 following viral infection, $B220^{+}$ $CD138^{+}$ plasma blasts remain SNA high similar to $B220^{+}$ IgD^{+} naïve B cells in uninfected mice. Additionally, on day 15 post-infection, $B220^{+}$, Fas^{+}, IgD^{lo} germinal center B cells also show high SNA lectin binding (Figure 2.1).

Impaired generation of influenza specific humoral responses in ST6Gal I deficient mice

To examine the functional relevance of this modification for antiviral humoral responses, we obtained ST6Gal I null mice. ST6Gal $I^{-/-}$ mice develop normally and show a normal lymphoid compartment and architecture (Hennet et al., 1998; Martin et al., 2002). However, B cells from ST6Gal $I^{-/-}$ mice show impaired proliferation *in vitro* to anti-IgM, anti-CD40, and LPS stimulation that can be rescued by the addition of IL-4, or gene ablation of CD22 (Collins et al., 2006;

Grewal et al., 2006; Hennet et al., 1998). These mice also show defective T-dependent and T-independent humoral responses to hapten-protein immunization. Previous studies examining antibody responses following viral infection have sometimes contrasted with results using hapten-protein immunizations (Kawabe et al., 1994; Whitmire et al., 1999). We infected ST6Gal I$^{-/-}$ mice with influenza A/HKx31 and serially bled them to determine influenza-specific IgM and IgG by serum ELISA (Figure 2.2A). We observed ~10-fold reductions and ~5-fold reductions in the levels of influenza-specific IgM and IgG, respectively on day 7 p.i. (Figure 2.2A). Analysis of IgG isotypes on day 7 p.i. revealed that all isotypes were significantly reduced compared to wild type mice, with IgG3 and IgG2c showing the most impairment of the IgG isotypes (3- and 7-fold, respectively) (Figure 2.2B). By day 14 p.i., influenza-specific IgG was similar comparing wild-type and ST6Gal I$^{-/-}$ mice, while influenza-specific IgM still remained impaired.

One possible explanation for the differences observed could be aberrantly glycosylated antibodies are preferentially scavenged *in vivo* by lectin bearing macrophages (Onami et al., 2002). We determined whether ST6Gal I$^{-/-}$ mice are defective in the generation of viral specific plasma cells (Figure 2.2C). Examination of influenza-specific ASCs by ELISPOT in the CLN, MedLN, and spleen show significantly reduced numbers at day 7. Influenza-specific IgM producing ASCs showed the most impairment, especially in the spleen. Influenza-specific IgA producing ASCs were reduced, but the reduction was not statistically significant (Figure 2.2C). These results show that the reduced serum levels of antiviral antibodies are likely not the effect of preferential scavenging by macrophages, but rather a defect in the generation of the humoral immune response.

Germinal centers of ST6Gal I$^{-/-}$ mice do not bind GL7

To determine if any differences in germinal center formation are present in ST6Gal I$^{-/-}$ mice, we performed immuno-staining in the lymph nodes. Our analysis of the MedLN by immuno-fluorescence on day 7 p.i. revealed that germinal center B cells in ST6Gal I$^{-/-}$ mice show no expression of the germinal center marker GL7, but show high binding by the PNA lectin (Figure 2.3A). These data are consistent with results demonstrating that the monoclonal antibody GL7 shows specificity for a sialylated glycan epitope expressed on germinal center B cells (Naito et al., 2007). FACS analysis of lymphocytes from the CLN of these mice gating on IgD^{lo}B220^{+} cells showed similar percentages and numbers of GC cells as measured by expression of germinal center markers Fas and PNA, and confirmed loss of GL7 binding (Figure 2.3B,D). We also noted that the MFI of PNA binding was significantly higher in ST6Gal I$^{-/-}$ GC cells compared to WT (MFI = 1178 vs 549). The frequencies of total plasma cells (CD138^{+}B220^{+}) were reduced in ST6Gal I$^{-/-}$ mice, consistent with the reduction in viral specific ASCs and as expected, showed no binding of the SNA lectin (Figure 2.2C and 2.3C).

Productive infection and replication of influenza in ST6Gal I$^{-/-}$ mice

Entry of influenza virus, as well as the productive infection and replication in lung epithelial cells is dependent on sialic acid modification of glycoproteins. Productive influenza infection in humans depends specifically on sialyloligosaccharides containing terminal N-acetyl sialic acid linked to galactose by an α2,6-linkage, while in mice the data suggests α2,3-linked sialic acids are important (Hatakeyama et al., 2005; Ibricevic et al., 2006). Influenza viral titers were determined in the lungs of mice infected with A/HKx31 (Figure 2.4). We confirm that similar to wild-type mice, lungs from ST6Gal I$^{-/-}$ mice become productively infected with influenza A/HKx31 and show comparable viral titers at day 3 and 5 p.i. By day 7 p.i., we see a trend towards higher viral titers in the lungs of ST6Gal I$^{-/-}$ mice, which coincides with the early impairment of viral

specific antibody responses observed in these mice. However, this difference is not statistically significant (p=.07) and by day 10 virus was cleared by both wild-type and ST6Gal I$^{-/-}$ mice. These results extend the findings in a recently published report showing several human influenza A viruses are able to productively infect the respiratory tract of mice lacking ST6Gal I expression (Glaser et al., 2007).

Viral specific CD4 and CD8 T cells in the lungs and MedLN

Since T cells also express ST6Gal I, we enumerated influenza-specific T cells isolated from the lungs or draining nodes (MedLN) of wild-type or ST6Gal I$^{-/-}$ mice on day 10 using CD4 specific (NP311-325) or CD8 specific (NP366-374) peptides performing intracellular cytokine staining to detect IFNg (Crowe et al., 2006). ST6Gal I$^{-/-}$ mice generate similar numbers of viral specific CD4 and CD8 T cells in the lung and MedLN, show similar co-production of TNFa and IL-2, and show similar numbers of CD44^{high} CD4 and CD8 T cells in these tissues (Figure 2.5 and data not shown). However, we did note reduced numbers of viral specific CD8 T cells in the spleen on day 10 consistent with our observations of reduced viral specific T cells following LCMV infection in these mice.

Viral specific memory B cell responses

ST6Gal I$^{-/-}$ mice control influenza infection by day 10, despite impaired influenza specific humoral responses (Figure 2.4). The strong antiviral T cell responses in the lungs of these mice likely contribute to this effective viral clearance. Immune ST6Gal I$^{-/-}$ mice show high levels of class switched IgG antibody; however, a significant reduction in serum levels of IgG2c was observed, supported by a significant reduction in frequencies of influenza-specific IgG2c producing LLPCs in the bone marrow (Figure 2.6A,B). Examination of MBCs in the spleen and MedLN reveal comparable frequencies of total influenza-specific IgG MBCs

(Figure 2.6C). These results clearly indicate that with the exception of the reduced IgG2c levels, immune ST6Gal $I^{-/-}$ mice generated similar high titers of antiviral specific antibody.

B cell expression of ST6Gal I is required to generate optimal levels of viral specific IgM

Our data indicate that ST6Gal $I^{-/-}$ mice are able to generate strong antiviral humoral memory despite early impairments in the generation of the viral specific humoral response (Figures 2.2 and 2.6). To determine whether it is the expression of ST6Gal I by B cells alone that results in impairment of the early antiviral IgM and IgG response, we transferred purified naïve B cells from either wild-type or ST6Gal $I^{-/-}$ mice into primed B cell deficient $\mu MT^{-/-}$ mice. Recipient mice were intra-nasally infected with influenza, and serially bled to determine influenza specific antibody levels. Mice that received ST6Gal $I^{-/-}$ B cells show impaired influenza specific IgM levels, but similar viral specific IgG (Figure 2.7). These data argue that the observed impairment in production of viral specific IgM in ST6Gal $I^{-/-}$ mice is likely B cell intrinsic, however the impairment in early production of viral specific IgG is not B cell intrinsic. Thus, expression of ST6Gal I by B cells, at least in part, is required for normal antiviral humoral immunity.

Discussion

In this report, we have evaluated the influence of post-translational modification of glycoproteins on the immune response to influenza virus infection. Changes in the post-translational modification of glycoproteins during immune responses have been reported for decades, but their functional importance remains obscure (Baum et al., 1996; Galvan et al., 1998b; Harrington et al., 2000; Kosco et al., 1988; London et al., 1978; London and Horton, 1980; Onami et al., 2002; Schrader et al., 1982). We demonstrate that in contrast to observations with PNA

lectin binding which changes during activation/differentiation B cells, naïve and activated B cells *in vivo* show similar high binding of SNA (Figure 2.1). This supports recently published data showing that ST6Gal I gene expression does not change following B cell activation *in vitro* (Comelli et al., 2006). Using ST6Gal $I^{-/-}$ mice, which lack the ability to catalyze the addition of α2,6 sialic acids to N-linked glycoproteins, we investigated the role of this modification on the generation of an influenza-specific humoral response. Serum levels of influenza-specific antibodies in these mice are reduced early in the immune response, with influenza-specific IgM responses showing the greatest impairment (Figure 2.2A). These data are supported by reductions in the frequencies of viral specific plasma cells, suggesting that the impaired viral specific antibody levels are likely a result of altered generation of short-lived viral specific plasma cells, and not a result of preferential scavenging of antibodies lacking α2,6 sialic acids. (Figure 2.2C and 2.3C). Additionally, ST6Gal $I^{-/-}$ mice show no differences in influenza viral replication in the lungs, so the reduced antibody levels are not due to reduced viral load or antigen availability in these mice (Figure 2.4). We did observe comparable influenza-specific CD4 and CD8 T cell responses in the lung and draining lymph nodes of these mice, and this most likely explains why ST6Gal $I^{-/-}$ mice are able to control and clear influenza viral infection in the lungs by day 10, similar to wild-type mice (Figure 2.5). Despite significant impairments in the generation of an early antiviral humoral response, ST6Gal $I^{-/-}$ mice are able to generate potent antiviral humoral immunity, with high levels of class switched IgG antibodies by day 14 and memory time-points (Figure 2.2A, and Figure 2.6). This is the first reported analysis of antiviral immune responses in ST6Gal $I^{-/-}$ mice.

To determine whether the observed impairment of antiviral humoral responses were B cell intrinsic, we adoptively transferred ST6Gal $I^{+/+}$ or $^{-/-}$ B cells into primed B cell deficient $\mu MT^{-/-}$ mice (Figure 2.7). Primed mice were used to ensure adequate CD4 T help in these mice. The antiviral IgM response to infection was

substantially impaired in mice that received ST6Gal I$^{-/-}$ B cells. However, the antiviral IgG response was similar compared to mice that received wild-type B cells. These results suggest that the defective antiviral IgM response observed in ST6Gal I$^{-/-}$ mice is likely B cell intrinsic. While we must be cautious with our interpretations of antiviral responses in B cell deficient mice due to known alterations in lymphoid architecture, the results raise the possibility that subtle defects in an additional cell compartment in ST6Gal I$^{-/-}$ mice may contribute to the delayed antiviral IgG response. Future studies will investigate how ST6Gal I deficiency affects other lymphoid cells, and how this loss contributes to the defective anti-viral response.

Recent reports have demonstrated that loss of expression of ST6Gal I by B cells results in preferential co-localization of the BCR with CD22, a negative regulator of BCR signaling, in clathrin-rich membrane microdomains (Collins et al., 2006; Grewal et al., 2006). Aged CD22 deficient mice have been reported to develop IgM autoantibodies (Walker and Smith, 2008). Ablation of CD22 expression in ST6Gal I$^{-/-}$ mice rescues BCR signaling defects (Collins et al., 2006). In naïve B cells, modification of CD22 by ST6Gal I normally results in segregation of CD22 molecules, due to homotypic interactions with the α2, 6 sialic acid *cis*-ligands of other CD22 molecules (Collins et al., 2006). Following antigen receptor engagement, CD22 is tyrosine phosphorylated, and phosphorylated CD22 recruits SHP-1 (Src homology domain2-containing tyrosine phosphatase), mediating signal inhibition via the BCR (Horikawa et al., 2007; Walker and Smith, 2008). Due to the absence of these *cis*-CD22 ligands in ST6Gal I$^{-/-}$ mice, there is increased association of sIgM with the inhibitory receptor CD22 on naïve B cells; following antigen receptor engagement *in vivo,* this could result in immediate attenuated BCR signaling. We speculate that a possible *in vivo* outcome of this could be significantly impaired differentiation of naïve B cells into extra-follicular short-lived plasma cells following viral infection of ST6Gal I$^{-/-}$ mice (Benson et al., 2007; Fujimoto and Sato, 2007; Junt et al., 2007; Paus et al., 2006; Walker and

Smith, 2008). Viral-specific B cells in the ST6Gal I$^{-/-}$ mice, with “weak or moderate BCR” signaling could enter germinal centers and undergo affinity maturation and differentiation into plasma cells. This could explain why we observe that after day 14 p.i, influenza-specific IgG responses are quite comparable to wild-type mice. Thus in a normal immune response, ST6Gal I modification of glycoproteins on naïve B cells may influence the signaling threshold required following antigen receptor signaling, and the biological outcome *in vivo* would favor differentiation of a greater proportion of Ag-specific B cells into extra-follicular short-lived plasma cells, important in the early control of pathogens. Alternatively, the repertoire of B cells available in ST6Gal I$^{-/-}$ mice could be different from wild-type mice due to differences in signaling strength during development (Ghosh et al., 2006; Santos et al., 2008).

In conclusion, our data demonstrate that despite early defects in the generation of an antiviral humoral response, ST6Gal I$^{-/-}$ mice are able to clear virus and generate potent humoral memory. Further, our data suggests that loss of ST6Gal I expression by B cells may be responsible for the impaired antiviral IgM response. Finally, loss of expression of ST6Gal I in non-B cells likely contributes to the impaired IgG humoral response. Future experiments will elucidate how the expression of this enzyme by different lymphocyte populations, influences the generation of an antiviral immune response.

References

Baum, L.G., K. Derbin, N.L. Perillo, T. Wu, M. Pang, and C. Uittenbogaart. 1996. Characterization of terminal sialic acid linkages on human thymocytes. Correlation between lectin-binding phenotype and sialyltransferase expression. *J Biol Chem* 271:10793-9.

Benson, M.J., L.D. Erickson, M.W. Gleeson, and R.J. Noelle. 2007. Affinity of antigen encounter and other early B-cell signals determine B-cell fate. *Curr Opin Immunol* 19:275-80.

Collins, B.E., B.A. Smith, P. Bengtson, and J.C. Paulson. 2006. Ablation of CD22 in ligand-deficient mice restores B cell receptor signaling. *Nat Immunol* 7:199-206.

Comelli, E.M., M. Sutton-Smith, Q. Yan, M. Amado, M. Panico, T. Gilmartin, T. Whisenant, C.M. Lanigan, S.R. Head, D. Goldberg, H.R. Morris, A. Dell, and J.C. Paulson. 2006. Activation of murine CD4+ and CD8+ T lymphocytes leads to dramatic remodeling of N-linked glycans. *J Immunol* 177:2431-40.

Crowe, S.R., S.C. Miller, D.M. Brown, P.S. Adams, R.W. Dutton, A.G. Harmsen, F.E. Lund, T.D. Randall, S.L. Swain, and D.L. Woodland. 2006. Uneven distribution of MHC class II epitopes within the influenza virus. *Vaccine* 24:457-67.

Fujimoto, M., and S. Sato. 2007. B cell signaling and autoimmune diseases: CD19/CD22 loop as a B cell signaling device to regulate the balance of autoimmunity. *J Dermatol Sci* 46:1-9.

Galvan, M., K. Murali-Krishna, L.L. Ming, L. Baum, and R. Ahmed. 1998. Alterations in cell surface carbohydrates on T cells from virally infected mice can distinguish effector/memory CD8+ T cells from naive cells. *J Immunol* 161:641-8.

Galvan, M., S. Tsuboi, M. Fukuda, and L.G. Baum. 2000. Expression of a specific glycosyltransferase enzyme regulates T cell death mediated by galectin-1. *J Biol Chem* 275:16730-7.

Ghosh, S., C. Bandulet, and L. Nitschke. 2006. Regulation of B cell development and B cell signalling by CD22 and its ligands alpha2,6-linked sialic acids. *Int Immunol* 18:603-11.

Glaser, L., G. Conenello, J. Paulson, and P. Palese. 2007. Effective replication of human influenza viruses in mice lacking a major alpha2,6 sialyltransferase. *Virus Res* 126:9-18.

Grewal, P.K., M. Boton, K. Ramirez, B.E. Collins, A. Saito, R.S. Green, K. Ohtsubo, D. Chui, and J.D. Marth. 2006. ST6Gal-I restrains CD22-dependent antigen receptor endocytosis and Shp-1 recruitment in normal and pathogenic immune signaling. *Mol Cell Biol* 26:4970-81.

Harrington, L.E., M. Galvan, L.G. Baum, J.D. Altman, and R. Ahmed. 2000. Differentiating between memory and effector CD8 T cells by altered expression of cell surface O-glycans. *J Exp Med* 191:1241-6.

Hatakeyama, S., Y. Sakai-Tagawa, M. Kiso, H. Goto, C. Kawakami, K. Mitamura, N. Sugaya, Y. Suzuki, and Y. Kawaoka. 2005. Enhanced expression of an alpha2,6-linked sialic acid on MDCK cells improves isolation of human influenza viruses and evaluation of their sensitivity to a neuraminidase inhibitor. *J Clin Microbiol* 43:4139-46.

Hennet, T., D. Chui, J.C. Paulson, and J.D. Marth. 1998. Immune regulation by the ST6Gal sialyltransferase. *Proc Natl Acad Sci U S A* 95:4504-9.

Horikawa, K., S.W. Martin, S.L. Pogue, K. Silver, K. Peng, K. Takatsu, and C.C. Goodnow. 2007. Enhancement and suppression of signaling by the conserved tail of IgG memory-type B cell antigen receptors. *J Exp Med* 204:759-69.

Horimoto, T., and Y. Kawaoka. 2005. Influenza: lessons from past pandemics, warnings from current incidents. *Nat Rev Microbiol* 3:591-600.

Ibricevic, A., A. Pekosz, M.J. Walter, C. Newby, J.T. Battaile, E.G. Brown, M.J. Holtzman, and S.L. Brody. 2006. Influenza virus receptor specificity and cell tropism in mouse and human airway epithelial cells. *J Virol* 80:7469-80.

Joo, H.M., Y. He, and M.Y. Sangster. 2008. Broad dispersion and lung localization of virus-specific memory B cells induced by influenza pneumonia. *Proc Natl Acad Sci U S A*

Junt, T., E.A. Moseman, M. Iannacone, S. Massberg, P.A. Lang, M. Boes, K. Fink, S.E. Henrickson, D.M. Shayakhmetov, N.C. Di Paolo, N. van Rooijen, T.R. Mempel, S.P. Whelan, and U.H. von Andrian. 2007. Subcapsular sinus macrophages in lymph nodes clear lymph-borne viruses and present them to antiviral B cells. *Nature* 450:110-4.

Kalia, V., S. Sarkar, T.S. Gourley, B.T. Rouse, and R. Ahmed. 2006. Differentiation of memory B and T cells. *Curr Opin Immunol* 18:255-64.

Kawabe, T., T. Naka, K. Yoshida, T. Tanaka, H. Fujiwara, S. Suematsu, N. Yoshida, T. Kishimoto, and H. Kikutani. 1994. The immune responses in CD40-deficient mice: impaired immunoglobulin class switching and germinal center formation. *Immunity* 1:167-78.

Kosco, M.H., A.K. Szakal, and J.G. Tew. 1988. In vivo obtained antigen presented by germinal center B cells to T cells in vitro. *J Immunol* 140:354-60.

Li, X., D.J. Vanitha, H.M. Joo, Y. He, B.T. Rouse, and M.Y. Sangster. 2006. A strategy for selective, CD4+ T cell-independent activation of virus-specific memory B cells for limiting dilution analysis. *J Immunol Methods* 313:110-8.

London, J., S. Berrih, and J.F. Bach. 1978. Peanut agglutinin. I. A new tool for studying T lymphocyte subpopulations. *J Immunol* 121:438-43.

London, J., and M.A. Horton. 1980. Peanut agglutinin. V. Thymocyte subpopulations in the mouse studied with peanut agglutinin and Ly-6.2 antiserum. *J Immunol* 124:1803-7.

Martin, L.T., J.D. Marth, A. Varki, and N.M. Varki. 2002. Genetically altered mice with different sialyltransferase deficiencies show tissue-specific alterations in sialylation and sialic acid 9-O-acetylation. *J Biol Chem* 277:32930-8.

Masopust, D., V. Vezys, E.J. Wherry, D.L. Barber, and R. Ahmed. 2006. Cutting edge: gut microenvironment promotes differentiation of a unique memory CD8 T cell population. *J Immunol* 176:2079-83.

Naito, Y., H. Takematsu, S. Koyama, S. Miyake, H. Yamamoto, R. Fujinawa, M. Sugai, Y. Okuno, G. Tsujimoto, T. Yamaji, Y. Hashimoto, S. Itohara, T. Kawasaki, A. Suzuki, and Y. Kozutsumi. 2007. Germinal center marker GL7 probes activation-dependent repression of N-glycolylneuraminic acid, a sialic acid species involved in the negative modulation of B-cell activation. *Mol Cell Biol* 27:3008-22.

Nitschke, L. 2005. The role of CD22 and other inhibitory co-receptors in B-cell activation. *Curr Opin Immunol* 17:290-7.

Onami, T.M., L.E. Harrington, M.A. Williams, M. Galvan, C.P. Larsen, T.C. Pearson, N. Manjunath, L.G. Baum, B.D. Pearce, and R. Ahmed. 2002. Dynamic regulation of T cell immunity by CD43. *J Immunol* 168:6022-31.

Onami, T.M., M.Y. Lin, D.M. Page, S.A. Reynolds, C.D. Katayama, J.D. Marth, T. Irimura, A. Varki, N. Varki, and S.M. Hedrick. 2002. Generation of mice deficient for macrophage galactose- and N-acetylgalactosamine-specific lectin: limited role in lymphoid and erythroid homeostasis and evidence for multiple lectins. *Mol Cell Biol* 22:5173-81.

Paus, D., T.G. Phan, T.D. Chan, S. Gardam, A. Basten, and R. Brink. 2006. Antigen recognition strength regulates the choice between extrafollicular plasma cell and germinal center B cell differentiation. *J Exp Med* 203:1081-91.

Sangster, M.Y., J.M. Riberdy, M. Gonzalez, D.J. Topham, N. Baumgarth, and P.C. Doherty. 2003. An early CD4+ T cell-dependent immunoglobulin A response to influenza infection in the absence of key cognate T-B interactions. *J Exp Med* 198:1011-21.

Santos, L., K.E. Draves, M. Boton, P.K. Grewal, J.D. Marth, and E.A. Clark. 2008. Dendritic cell-dependent inhibition of B cell proliferation requires CD22. *J Immunol* 180:4561-9.

Schrader, J.W., W.F. Chen, and R. Scollay. 1982. The acquisition of receptors for peanut agglutinin by peanut agglutinin-negative thymocytes and peripheral T cells. *J Immunol* 129:545-9.

Slifka, M.K., and R. Ahmed. 1996. Limiting dilution analysis of virus-specific memory B cells by an ELISPOT assay. *J Immunol Methods* 199:37-46.

Slifka, M.K., and R. Ahmed. 1998. Long-lived plasma cells: a mechanism for maintaining persistent antibody production. *Curr Opin Immunol* 10:252-8.

Slifka, M.K., R. Antia, J.K. Whitmire, and R. Ahmed. 1998. Humoral immunity due to long-lived plasma cells. *Immunity* 8:363-72.

Walker, J.A., and K.G. Smith. 2008. CD22: an inhibitory enigma. *Immunology* 123:314-25.

Whitmire, J.K., R.A. Flavell, I.S. Grewal, C.P. Larsen, T.C. Pearson, and R. Ahmed. 1999. CD40-CD40 ligand costimulation is required for generating antiviral CD4 T cell responses but is dispensable for CD8 T cell responses. *J Immunol* 163:3194-201.

Appendix

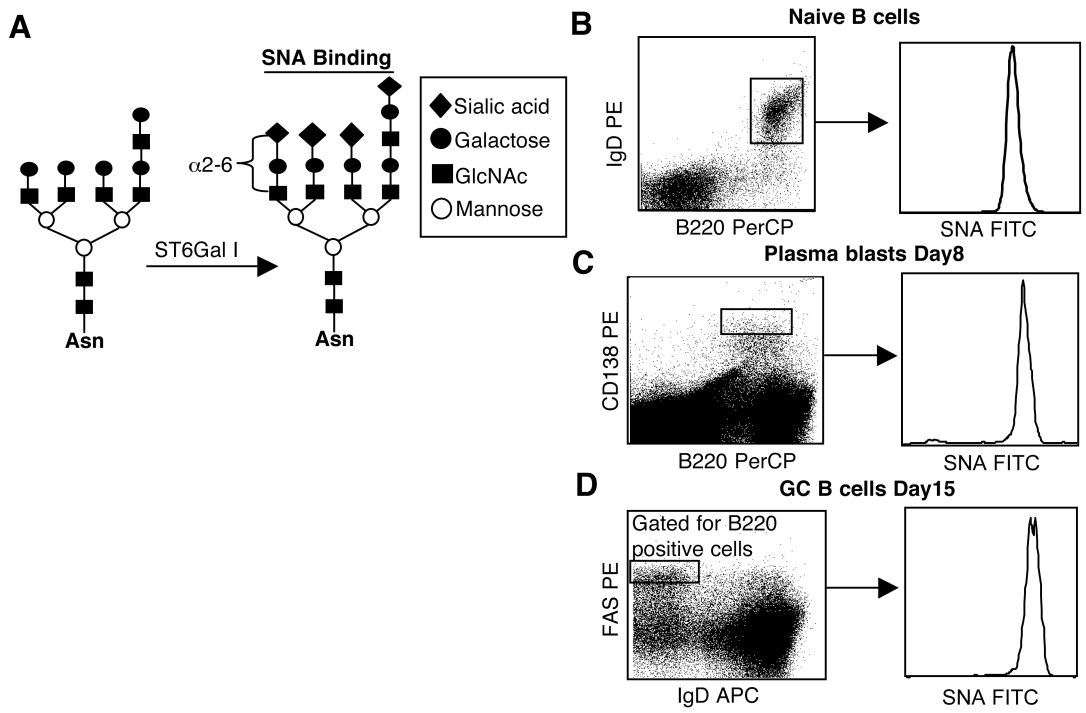

Figure 2.1. Binding of SNA on B cell populations.

Splenocytes from uninfected C57BL/6 mice, or mice infected with $2x10^5$ pfu LCMV Armstrong i.p. either 8 or 15 days earlier were used for the analysis. The left panel in B-D shows the gating, and the right panel SNA binding as histograms of the gated population. *A*, Cartoon depicting the glycosyltransferase ST6Gal I which catalyzes addition of terminal α2,6 sialic acids to galactose. SNA lectin binds Sia α 2-6Galβ1-4GlcNac. *B*, Naive B cells from uninfected mice gated on $B220^+/IgD^+$ cells *C*, CD138+/B220lo plasma blasts on day 8 and *D*, $B220^+FAS^+/IgD^-$ germinal center cells all show high SNA binding.

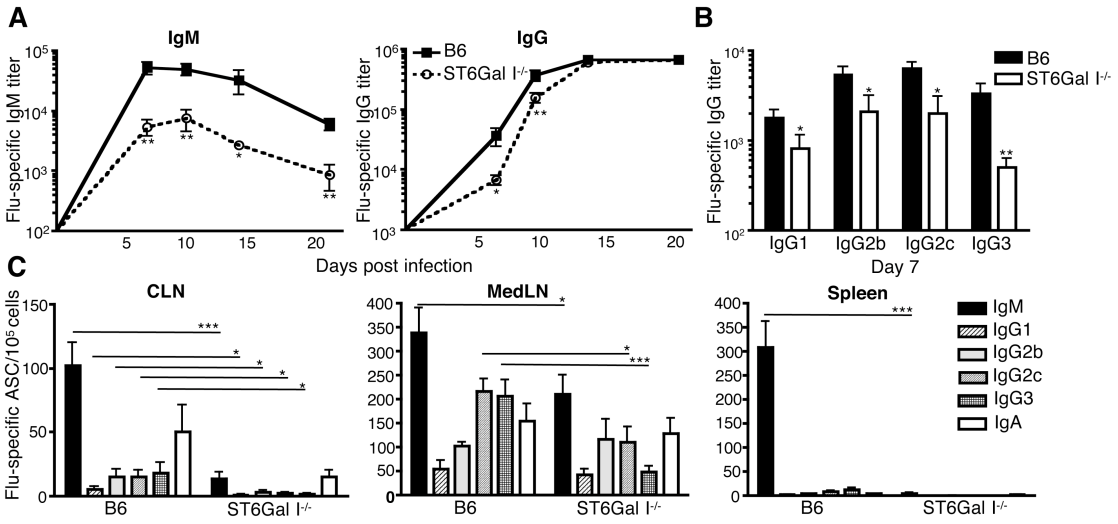

Figure 2.2. Influenza-specific B cell responses in ST6Gal I$^{-/-}$ mice during acute infection.

B6 or ST6Gal I$^{-/-}$ mice were infected with influenza A/HKx31 i.n. and bled on indicated days. *A*, Serum virus-specific IgM (left), IgG (right) and *B*, IgG isotypes on day 7 were measured by ELISA. Data is expressed as the reciprocal endpoint antibody titer on serial titration of influenza antibody. *C*, Cell suspensions of CLN, MedLN and spleen were prepared from individual mice on day 7 p.i., and the ELISPOT assay was used to measure the number of cells producing virus-specific IgM, IgG1, IgG2b, IgG2c, IgG3 or IgA as indicated, with N =6-8 mice per group. Results are expressed as the number of ASC/10^5 nucleated cells. (∗, indicate $p < 0.05$, ∗∗ indicate $p < 0.01$, ∗∗∗ indicate $p < 0.001$)

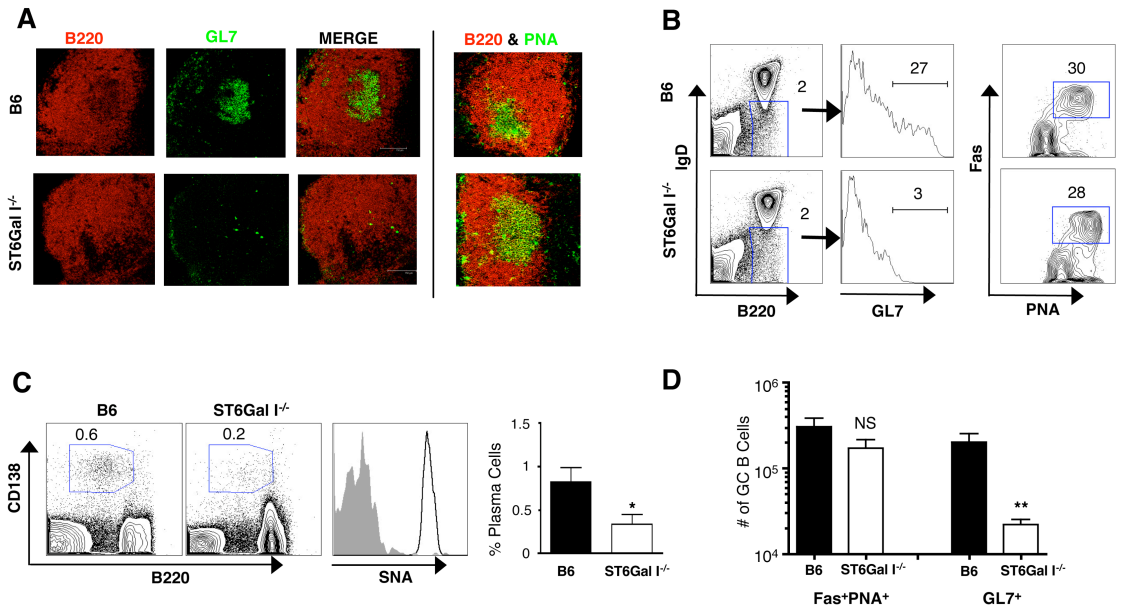

Figure 2.3. Germinal center B cells of ST6Gal $I^{-/-}$ mice do not bind GL7.

Mice were infected with influenza x31 i.n. and on day 7 p.i. lymph nodes were isolated and either frozen for immunofluorescence, or stained for FACS analysis using germinal center or plasma cell markers. Numbers show percentages of gated population. *A*, Immunofluorescence staining of MedLN using B220 and GL7 or B220 and PNA as indicated. B220 in red and GL7 or PNA staining in green. *B*, FACS analysis of germinal center B cells in CLN of same mice, gating on $IgD^{lo}B220^{+}$ cells. Histogram shows GL7 binding on gated $IgD^{lo}B220^{+}$ cells. Dot plot shows $PNA^{high}Fas^{+}$ cell population of gated $IgD^{low}B220^{+}$ cells. *C*, FACS analysis of plasma cells in CLN gating on $CD138^{+}B220^{+}$ cells. Histogram overlay of SNA binding of gated population. Filled histogram shows ST6Gal $I^{-/-}$, and open histogram shows B6. Bar graph shows frequencies of total plasma cells in indicated mice. *D*, Total number of germinal center B cells in CLN gating on $IgD^{low}B220^{+}$ $PNA^{high}Fas^{+}$ or $IgD^{low}B220^{+}$ $GL7^{+}$ cells. Bar graphs show data from n=5 mice. (∗, $p < 0.05$ and ∗∗, $p < 0.01$.)

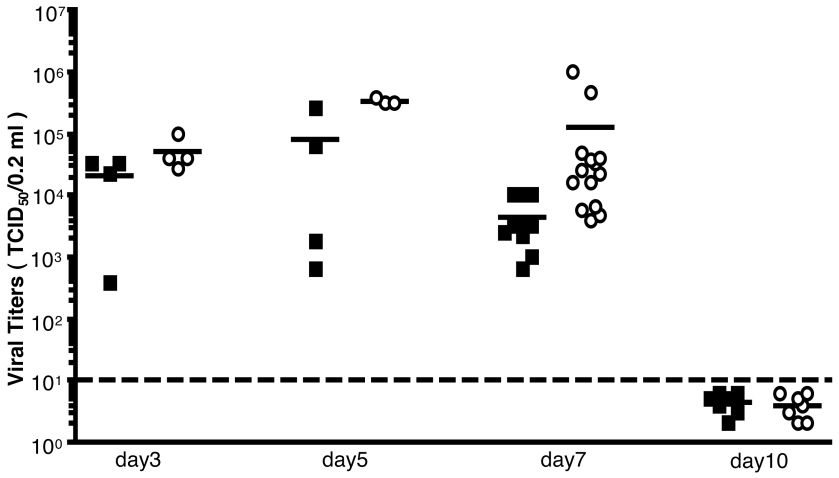

Figure 2.4. Influenza viral infection and clearance in lungs.

B6 and ST6Gal I$^{-/-}$ mice were infected i.n. and on indicated days post infection, lungs were collected and assayed for influenza viral titer. Black/filled symbols are B6 mice and white/open symbols are ST6Gal I$^{-/-}$ mice. Each symbol represents one mouse tested. The limit of detection is shown by the dotted line.

Figure 2.5. Influenza-specific T cell responses.

At day 10 p.i., lymphocytes from MedLN and lung were stimulated with indicated peptides for 5 hrs, and stained for intracellular cytokine production of IFNγ. *A*, Representative staining for each tissue gating on CD4 or CD8 T cells. Numbers indicate the percentage of CD4 or CD8 T cells specific for each peptide. *B*, Total NP311-325 specific CD4 or NP366-374 CD8 T cells were enumerated in MedLN and lung at day 10, n = 4 mice in each group.

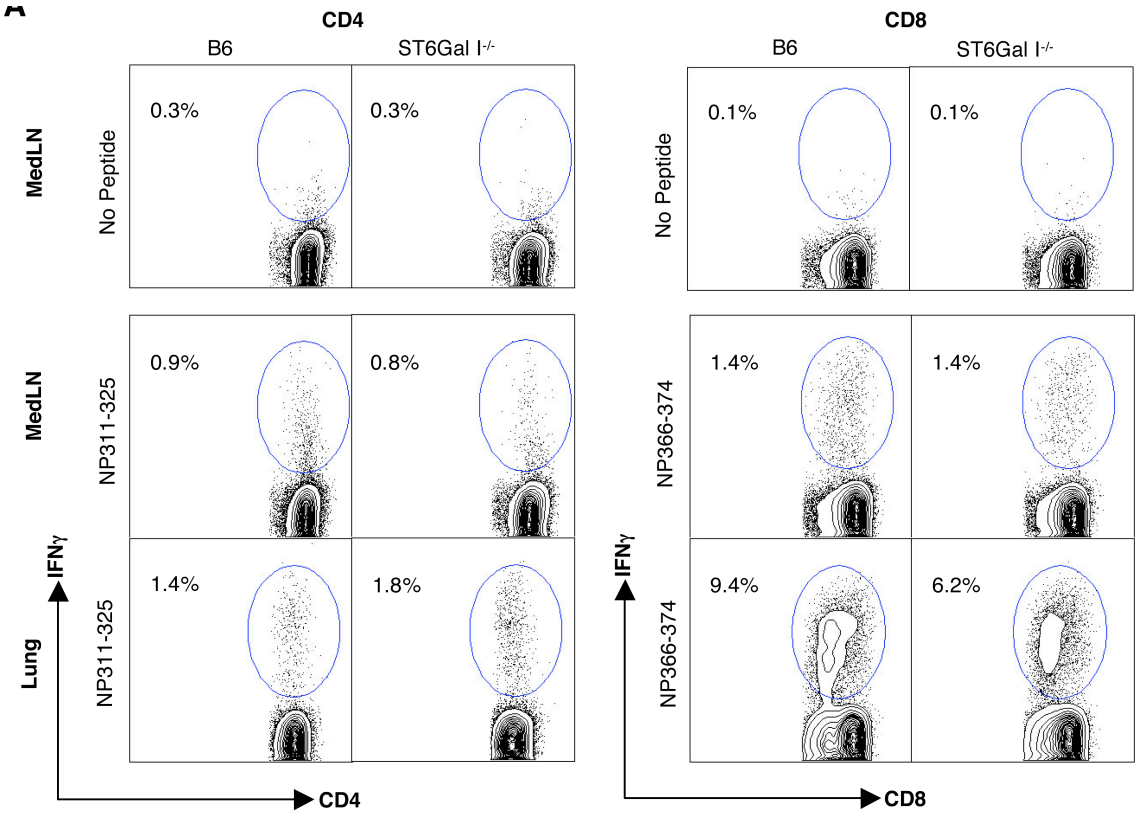
A
CD4
B6
ST6Gal I-/-
CD8
B6
ST6Gal I-/-
MedLN
No Peptide
0.3%
0.3%
0.1%
0.1%
MedLN
NP311-325
0.9%
0.8%
NP366-374
1.4%
1.4%
Lung
NP311-325
1.4%
1.8%
NP366-374
9.4%
6.2%
IFNγ
CD4
IFNγ
CD8

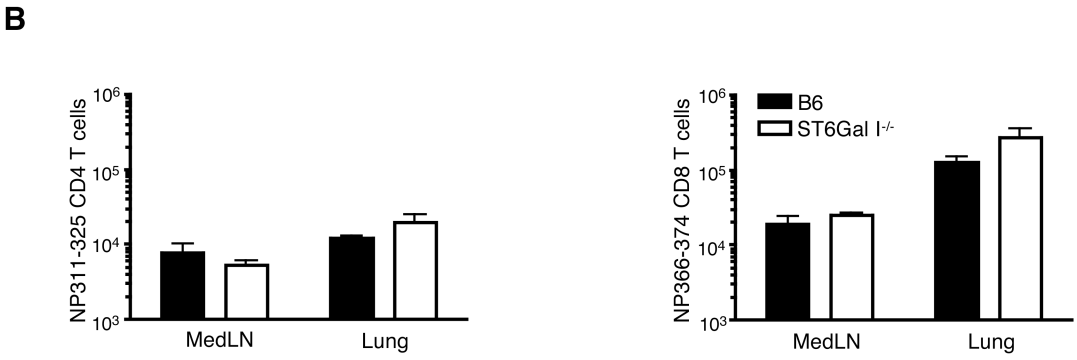
B
NP311-325 CD4 T cells
10^6
10^5
10^4
10^3
MedLN
Lung
NP366-374 CD8 T cells
B6
ST6Gal I-/-
MedLN
Lung

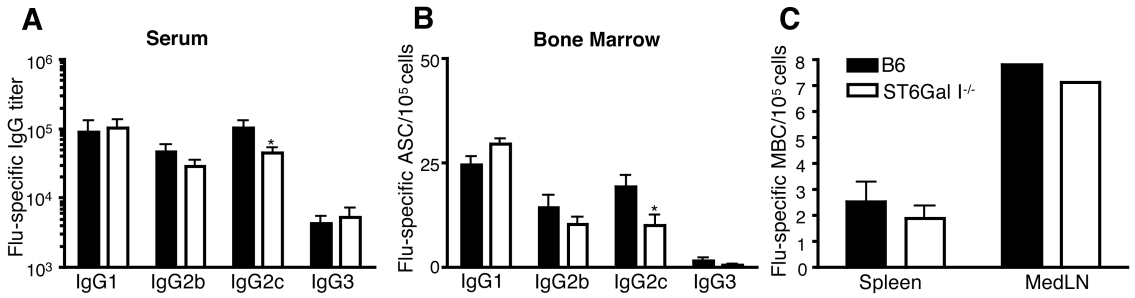

Figure 2.6. Immune influenza-specific IgG responses.

A, Influenza specific IgG isotypes from day 180 sera samples of B6 or ST6Gal I$^{-/-}$ mice. *B*, ELISPOT assay was used to determine the virus-specific IgG1, IgG2b, IgG2c and IgG3 antibody secreting cells in bone marrow of mice (LLPCs). *C*, Memory B cell numbers from spleen and MedLN; cells are pooled from 4 mice for MedLN, n = 4-8 mice per group.

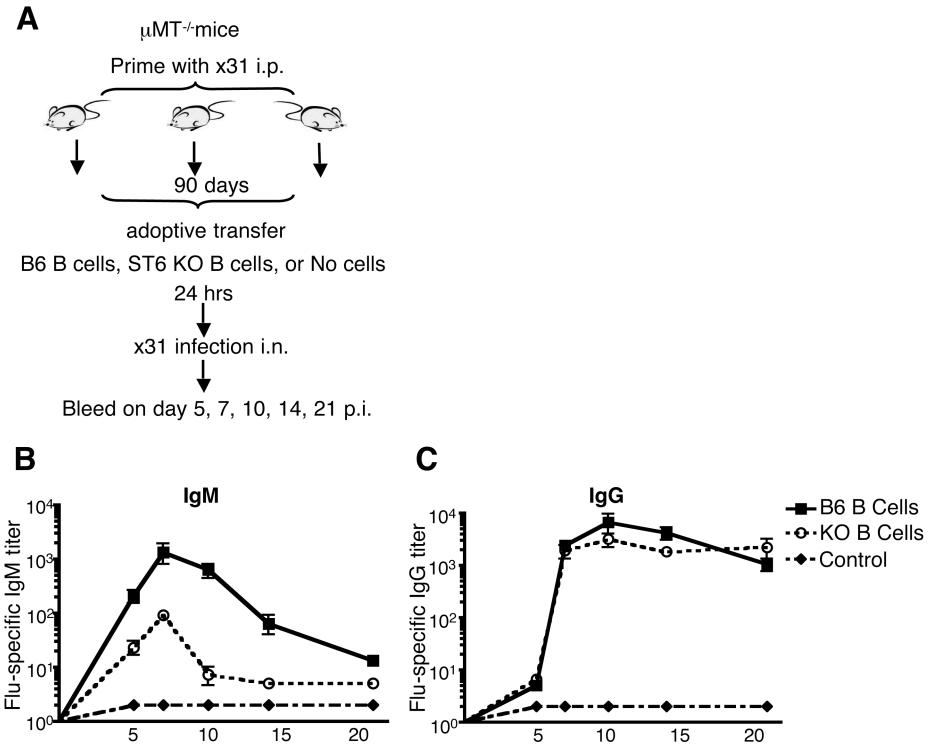

Figure 2.7. Loss of expression of ST6Gal I by B cells results in defective influenza specific IgM.

A, Cartoon depicting experimental protocol where $\mu MT^{-/-}$ recipient mice were primed with $10^{7.4}$ EID_{50} i.p; 90 days later, $2x10^7$ purified naïve $B220^+$ B cells from B6 or ST6Gal $I^{-/-}$ mice were adoptively transferred i.v. into mice. Control mice received no transferred cells. Mice were infected with $10^{6.8}$ EID_{50} influenza A/HKx31 i.n. one day later and bled on indicated days. *B*, Serum virus-specific antibodies for IgM or *C*, IgG levels were detected by ELISA, n = 3 mice in each group.

CHAPTER III

ST6GAL I DEFICIENCY RESULTS IN ALTERED SIALYLATION OF IGG AND IGA, AND PROMOTES IGA MESENGIAL DEPOSITION FOLLOWING INFLUENZA INFECTION

Abstract

ST6Gal I, a glycosyltransferase highly expressed by B cells, catalyzes the addition of α-2, 6 sialic acid to galactose (Siaα2-6Gal), a modification found on N-linked glycoproteins. Aberrant glycosylation has been associated with the pathogenesis of IgA nephropathy (IgAN), a disease characterized by immune complex deposits in the glomerular mesangium, which can lead to end-stage renal failure in 20-40% of diagnosed patients. We have previously shown that ST6Gal $I^{-/-}$ mice infected with influenza A/HKx31 demonstrated profound impairment in the generation of viral-specific humoral responses, although memory viral-specific IgG levels were normal.

We have further analyzed influenza-specific humoral responses in ST6Gal $I^{-/-}$ mice. Here we report the paradoxical finding that at memory, influenza infected ST6Gal $I^{-/-}$ mice show higher influenza-specific IgA, as well as total IgA, compared to WT mice, despite impaired early responses. Using MALDI-TOF MS analysis and immuno-histology, we demonstrate that immune ST6Gal $I^{-/-}$ mice show significant deficiencies in N-glycan sialylation of IgG and IgA, as well as increased immunoglobulin deposition in the kidney glomeruli.

These data show that loss of expression of an α-2,6 sialyltransferase, together with influenza viral infection, results in both aberrant glycosylation of IgG and IgA, and leads to increased immunoglobulin deposition in kidney glomeruli. These data raise the possibility that a common form of glomerulonephritis, IgAN, may be similarly initiated by altered sialyltransferase gene expression in concert with influenza infection.

Introduction

The enzyme ST6Gal I is a glycosyltransferase highly expressed by B and T cells that synthesizes the glycan sequence α2,6 sialic acid linked to galactose (Siaα2-6Gal) (Hennet et al., 1998). This structure is typically found on N-linked glycans on glycoproteins such as the mammalian lectin CD22, a transmembrane glycoprotein expressed by B cells with high specificity for (Siaα2-6Gal). CD22 is a negative regulator of B cell signaling that recruits SHP-1 to the BCR, thus attenuating signals via the BCR (Collins et al., 2006; Hennet et al., 1998; Nitschke, 2005). Several studies of ST6Gal I null mice demonstrated that these mice show profound impairment in the generation of humoral responses to viral, protein, and hapten antigens (Hennet et al., 1998; Zeng et al., 2009). These defective humoral responses observed in ST6Gal $I^{-/-}$ mice are at least partially B cell intrinsic, and are likely due to impaired B cell responses due to altered co-localization of the BCR with the negative regulator CD22 (Collins et al., 2006; Grewal et al., 2006; Zeng et al., 2009). Despite defects in the early generation of humoral responses, ST6Gal $I^{-/-}$ mice control influenza viral infection and generate potent humoral memory (Zeng et al., 2009).

Humoral immunity is characterized by prolonged antibody production, even after resolution of infection, in stark contrast to the T cell response, where effector T cell function is relatively short-lived. Antibodies, by neutralizing or opsonizing free extracellular pathogens, serve as a critical first-line defense against re-infection. Humoral immunity is provided by pre-existing antibody produced by a population of antibody secreting cells (ASCs) termed long-lived plasma cells (LLPCs), as well as a population of memory B cells (MBCs) that can rapidly differentiate following antigenic stimulation into plasma cells (Kalia et al., 2006; Slifka and Ahmed, 1996; Slifka and Ahmed, 1998; Slifka et al., 1998).

Recently, work from several groups has demonstrated an important role for IgG terminal glycosylation. Terminal glycans influence binding to Fc receptors and C1q of complement, and sialylation has specifically been shown to have important effects on antibody function (Nimmerjahn and Ravetch, 2007; Raju, 2008). Therapeutically, intravenous immune globulin (IVIG), which is used for the treatment of diverse autoimmune and systemic inflammatory diseases, has been shown in animal models to mediate enhanced anti-inflammatory effects when enriched for sialic acid containing IgG (Anthony et al., 2008; Kaneko et al., 2006; Kaveri et al., 2008). Thus alterations in sialylation of IgG may critically influence its function and clearance.

In addition to a role for glycosylation in IgG function and human disease, aberrant glycosylation of IgA has also been implicated in human disease, specifically in the pathogenesis of IgA nephropathy (IgAN), one of the most common forms of glomerulonephritis globally (Allen and Feehally, 2000; Nishie et al., 2007; Raska et al., 2007; Suzuki et al., 2008; Tomana et al., 1999; Xu et al., 2005). Recent examination of IgAN patients suggested that expression of an α2,6 sialyltransferase (ST6GALNAcII) is significantly reduced in peripheral B cells from patients suffering from IgAN, and IgAN patients show reduced IgA1 α2,6 sialic acid content (Khan et al., 2008). IgA1 is the dominant circulating subclass of IgA in humans and primates, but not other species, and is characterized by a hinge region containing as many as 5 O-linked glycans (Glassock, 2009; Novak et al., 2008). Although murine IgA does not have the O-glycans characteristic of human IgA1, a recent study of mice lacking the β-1,4 galactosyltransferase I (β4GalT-I) reported the spontaneous development of a human IgAN-like disease, characterized by glomerular lesions, increased IgA levels, and IgA deposition in kidneys (Nishie et al., 2007). However, only a single infant patient has ever been diagnosed with a congenital mutation in β4GalT-I, so the relevance of this enzyme to IgAN disease development in humans remains obscure (Hansske et al., 2002). Recently, a study found an association between mutations in core 1

β1,3-galactosyltransferase I (C1β3GalTI) and genetic susceptibility to IgAN, suggesting that galactose-deficiency may play a role in disease development (Li et al., 2007a; Novak et al., 2008). This work fits with data suggesting that many IgAN patients exhibit under-galactosylation of O-glycans in the IgA1 hinge region, and that abnormal IgA1 glycosylation is a heritable trait (Gharavi et al., 2008). However, since many family members with abnormal IgA1 glycoforms remain asymptomatic, additional factors other than aberrant glycosylation appear to be required for IgAN disease development and pathogenesis (Gharavi et al., 2008).

In the following report, we investigated the nature of alterations in terminal glycans in serum immunoglobulins from ST6Gal $I^{-/-}$ mice to determine whether ST6Gal $I^{-/-}$ mice developed any evidence of glomerulonephritis. We show that despite impaired generation of influenza-specific humoral responses, ST6Gal $I^{-/-}$ mice paradoxically showed higher levels of influenza-specific IgA and total IgA by day 60 p.i. We also show that although levels of influenza-specific IgG and total IgG were comparable in immune ST6Gal $I^{-/-}$ and WT mice, IgG N-glycans were characterized by a complete deficiency of terminal sialylation in ST6Gal $I^{-/-}$ mice. Moreover, while gross pathology of the mesangial matrix and kidney function remained normal, influenza immune ST6Gal $I^{-/-}$ mice show significant IgA and IgG deposition in the glomeruli. Examination of glycosylation differences for IgA also revealed that ST6Gal $I^{-/-}$ IgA showed aberrant terminal sialylation. Our data raise the possibility that a combination of influenza infection history, as well as genetic remodeling of protein glycosylation, such as loss of expression of an α2,6 sialyltransferase, may be key factors in the pathogenesis of a common form of glomerulonephritis.

Materials and Methods

Mice and immunizations

ST6Gal I-deficient mice were originally generated by J. Marth (University of California, San Diego) and obtained from the Consortium for Functional Glycomics and bred in-house, backcrossed to C57BL/6 x10 generations (Hennet et al., 1998). C57BL/6 female mice were purchased from The Jackson Laboratory (Bar Harbor, ME). Mice were maintained under specific pathogen-free conditions at the University of Tennessee in accordance with university IACUC guidelines. Anesthetized mice were intra-nasally infected with $10^{6.8}$ EID_{50} influenza A/HKx31 in 30 μl of PBS, as previously described (Zeng et al., 2009).

Urinalysis

Urine samples from C57BL/6 or ST6Gal $I^{-/-}$ mice were obtained at day 0 (uninfected) or day 380 post-infection (p.i). Chemstrip 5 OB urinalysis strips (Roche Diagnostics, Indianapolis, IN) were used to test urine samples for hematuria and proteinuria. Urine samples were also tested for albumin content via a double-sandwich ELISA kit using affinity-purified goat anti-mouse albumin antibody and HRP-conjugated goat anti-mouse albumin antibody, as per the manufacturer's instructions (Bethyl Laboratories, Montgomery, TX).

Histological Analysis

Kidneys were harvested from influenza immune mice, fixed in 10% formalin, embedded in paraffin and thin sections cut on a microtome. Sections were stained with H&E, PAS, and Masson's Trichrome.

Immunohistochemistry

Kidneys were harvested from mice at day 0 and day 400 p.i. and frozen in O.C.T. compound at -80°C. Kidneys were sectioned at 7 μm, and frozen sections were blocked with 3% BSA in PBS, stained with IgG-biotin or IgA-biotin, followed by streptavidin-AlexaFluor 488. Sections were examined using an epi-fluorescent microscope (Nikon Eclipse E600). The mean fluorescence was measured on the same samples using a Nikon NIS-Elements BR 2.30, measuring the MFI of three randomly selected glomeruli per sample. Unpaired student t tests were performed to determine statistical significance with *denoting $p<.05$ ** denoting $P<0.01$.

Immunoglobulin Measurement by ELISA

Total IgA or total IgG was measured in serum or vaginal washes of individual mice at day 0, day 7, day 14 or day 60-175 p.i. with influenza. Plates were coated with goat anti-mouse IgA or goat anti-mouse IgG (Southern Biotech, Birmingham, AL) and incubated at 4°C overnight. Plates were washed with PBS-Tween 20 (0.05%), blocked with PBS-BSA (3%), and washed again. Serial 3-fold sample dilutions were prepared in PBS-Tween 20 (0.05%) and BSA (0.5%). The plates were incubated at room temperature for 4 h or overnight at 4°C then washed thoroughly. Plate-bound secreted Abs were detected using alkaline phosphatase-conjugated goat anti-mouse Abs with specificity for IgA or IgG (Southern Biotech) diluted in PBS-BSA (1%) and incubated for 4 h at room temperature or overnight at 4°C. Plates were then washed thoroughly, and color development with *p*-nitrophenyl phosphate (Sigma-Aldrich, St. Louis, MO) in diethanolamine buffer was read at 405 nm using a Synergy II Multi-Detection Microplate Reader (Bio-Tek Instruments, Winooski, VT). The Ab titer is expressed as the reciprocal of the highest dilution giving an absorbance value more than twice that for simultaneously titrated samples from naïve mice.

Influenza-specific titers were measured as previously described (Sangster et al., 2003; Zeng et al., 2009).

IgG and IgA purification

IgGs were purified from serum samples on a FPLC system by affinity chromatography at a flow rate of 1ml/min. Mouse serum (1 ml) was loaded on a 1 ml protein A/G affinity column that had previously been equilibrated with 100 mM $NaPO_4$, 150 mM NaCl, pH 7.2 (buffer A). The column was subsequently washed with 10 column volumes of buffer A. Bound IgGs were eluted with 0.1 M glycin pH 2.3. Fractions of 500 µL were collected in tubes containing 50-µL neutralization buffer (1M Tris, pH 8.8). Finally, all the fractions containing antibodies were pooled and concentrated using 30-kDa cut-off filter system. For IgA, mouse serum (400 µL) was applied to 600µL Jacalin-sepharose slurry previously equilibrated with buffer A. The mixture was incubated for 30 min at room temperature then the beads were washed extensively as follows: first 400 µL, then 1500 µL buffer A, each with 15 min. incubation under rotation. IgAs were eluted from the slurry in 1.5 ml buffer A supplemented with 0.1 M α-D-galactose.

N-glycan release

IgG (50 µg) were digested with trypsin for 16 h at 37°C. The reaction was terminated by heating the sample for 5 min at 95°C. Antibodies were further digested with 100 mU PNGase F (EC 3.5.1.52; Roche Applied Science, IN) for 18 h at 37°C. Released N-glycans were isolated and desalted on reverse-phase Sep-Pak C18 cartridges (Alltech, Deerfield, IL) followed by carbograph extract-clean columns (Alltech, Deerfield, IL) (von Horsten et al., 2010).

Sialidase digestion and Permethylation

IgA samples, dissolved in 50mM phosphate buffer pH 6.0, were digested overnight at 37°C with 5 U/ml *Streptococcus pneumoniae* neuraminidase (sialidase S) (GKX-80020, Prozyme, San Leandro, CA). Permethylation was carried out using methyl iodide as described previously (von Horsten et al., 2010; Wedepohl et al., 2010). After the reaction, chloroform was added and the chloroform phase was washed with water until the pH of the water phase was neutral. The chloroform phase was finally evaporated under reduced atmosphere and the sample was dissolved in 75% aqueous acetonitrile for MALDI-TOF measurements.

Mass spectrometry

MALDI-TOF mass spectra were recorded on a Ultraflex III mass spectrometer (Bruker Daltonics) equipped with a Smartbeam laser and a LIFT-MS/MS facility. Spectra were recorded in reflector positive ionization mode. 0.5 μl desialylated or permethylated N-glycans were mixed on the ground steel target in a ratio 1:1 with the matrix consisting of D-arabinosazone (5 mg/ml) dissolved in 70% aqueous ethanol (Wedepohl et al., 2010). Calibration was performed on a glucose ladder.

Results

Increased IgA levels in influenza immune ST6Gal I$^{-/-}$ mice

We have previously examined influenza-specific antibody responses in ST6Gal I$^{-/-}$ mice and showed significant impairment in the generation of influenza-specific IgM and IgG responses (Zeng et al., 2009). However, memory B cell (MBC) and long-lived plasma cell (LLPC) responses were robust in immune ST6Gal I$^{-/-}$ mice (Zeng et al., 2009). In this study, we analyzed influenza-specific IgA responses. In naïve mice, there were no significant differences in total IgG or total IgA

comparing WT and ST6Gal I$^{-/-}$ mice (Figure 3.1A). However, we discovered that levels of total IgA, as well as influenza-specific IgA, were significantly higher in immune ST6Gal I$^{-/-}$ mice at day 175 (Figure 3.1A). To examine this difference in more detail, mice were infected with influenza A/HKx31 i.n. and mice were serially bled to obtain longitudinal samples from individual mice. While both influenza-specific IgG and influenza-specific IgA were significantly reduced at day 7 in ST6Gal I$^{-/-}$ mice, by day 15 IgG and IgA levels were similar, and by day 60 (memory), influenza-specific IgA levels had surpassed levels in WT mice, in contrast to influenza-specific IgG, which remained comparable (Figure 3.1B). We also observed increased influenza-specific IgA levels in mucosal secretions of ST6Gal I$^{-/-}$ mice (data not shown).

Since circulating IgA levels were higher in ST6Gal I-deficient mice, we examined whether these mice exhibited any defects in kidney function since high levels of serum IgA is a hallmark of IgAN. Urine samples were collected from immune mice and examined for the presence of blood (hematuria) or proteins (proteinuria) using urinalysis test strips (Table 3.1). We also measured urine albumin levels by ELISA (Figure 3.1C). ST6Gal I$^{-/-}$ mice were similar in all measures of kidney function to WT mice (Figure 3.1C and Table 3.1). Histological analysis of kidney sections from immune mice by H&E (Figure 3.1D) or PAS staining (not shown) revealed similarly normal gross pathology, with no evidence of mesangial proliferation in the glomeruli.

ST6Gal I$^{-/-}$ mice show greater IgG deposition in glomeruli following influenza infection

The first description of IgAN disease established that immunoglobulin deposition preceded development of pathological abnormalities in kidney (Berger and Hinglais, 1968). Since ST6Gal I$^{-/-}$ mice exhibited normal gross pathology of the

kidneys, we examined kidney glomeruli to determine whether there was evidence of immunoglobulin deposition. Frozen kidney sections from uninfected (naïve) WT and ST6Gal $I^{-/-}$ mice were first examined for IgG deposition in the glomeruli by immuno-fluorescence. No significant deposition was observed in either naïve WT or naïve ST6Gal $I^{-/-}$ mice (Figure 3.2A, upper panels). However, both WT and ST6Gal $I^{-/-}$ influenza immune mice showed significant IgG deposition in the glomeruli compared to naïve mice (Figure 3.2A, lower panels), consistent with several studies that have previously established that immunization or infection results in increased immune complex deposition in the kidney that is easily detected by immuno-fluorescence (Dixon et al., 1961; Semkow and Wilczynski, 1979a; Semkow and Wilczynski, 1979b). To ascertain if there were any differences in IgG deposition comparing immune WT versus immune ST6Gal $I^{-/-}$ mice, we measured mean fluorescence intensity (MFI) of IgG in the kidney glomeruli (Figure 3.2B). This additional analysis revealed that ST6Gal $I^{-/-}$ immune mice showed a consistent trend of greater IgG deposition (~30%) compared to WT immune mice ($p<0.05$). Taken together, these data show that following influenza infection, WT and ST6Gal $I^{-/-}$ mice show significant IgG deposition in the kidney glomeruli, however ST6Gal I deficiency leads to higher IgG deposition.

ST6Gal I expression is required for sialylation of N-glycans on IgG

Since IgG levels were similar in all groups of mice, but IgG deposition varied (Figure 3.1A, 3.2B), we hypothesized that changes in the quality of IgG were contributing to differences in IgG deposition in the kidney glomeruli. Following influenza infection of mice, there is a significant increase in influenza specific-IgG titers (Figure 3.1B), resulting in the formation of antigen-antibody immune complexes that deposit in kidneys (Figure 3.2 and (Semkow and Wilczynski, 1979b)). However, it has also been known for many years that significant changes occur in glycosylation during an immune response, with substantial

changes in lectin binding such as peanut agglutinin (PNA) binding by B and T cell glycoproteins and glycolipids (Galvan et al., 1998b; Kersh et al., 2003; London et al., 1978; Onami et al., 2002; Schrader et al., 1982). Aberrant immunogobulin glycosylation has been proposed to influence the pathogenesis of glomerulonephritis by influencing clearance mechanisms of immune complexes from the circulation (Novak et al., 2008).

We examined alterations in IgG N-glycans by performing MALDI-TOF analysis of purified IgG from sera samples from naïve and immune WT, as well as naïve and immune ST6Gal I$^{-/-}$ mice. N-glycans were released and isolated from IgG samples, and they were subsequently permethylated for mass spectrometric analyses by MALDI-TOF-MS. When we compared N-glycans of IgG for naïve versus influenza immune WT mice, we observed no significant changes (Figure 3). Similarly, no differences were observed comparing naïve and immune ST6Gal I$^{-/-}$ IgG (Figure 3.3). These data confirm that overall, composition of IgG N-glycans remains similar before and after influenza infection. Importantly, our analysis revealed that sialylated N-glycans of IgG, which were present in WT mice, were completely absent in ST6Gal I$^{-/-}$ IgG (Figure 3.3, *right panels*). This deficiency of sialylated N-glycans was seen with IgG purified from both naïve and immune ST6Gal I$^{-/-}$ mice (Figure 3.3). In the IgG fraction from WT mice, mono- and di-sialylated N-glycans could be found in both naive and influenza immune samples at *m/z* 2431.2, 2635.4 and 3026.6. This observation suggests that Neu5Gc in IgG N-glycans are exclusively (α-2,6)-linked. These results provide evidence that ST6Gal I expression is required for the synthesis of sialylated N-glycans on mouse IgG.

Loss of ST6Gal I expression leads to aberrant IgA glycosylation

Since our analysis of IgG N-glycans revealed significant changes in sialylation, we asked whether similar changes occurred in IgA. We therefore performed

MALDI-TOF analysis of N-glycan structures from purified IgA obtained from serum samples from WT and ST6Gal I$^{-/-}$ mice to examine changes in N-glycan sialylation of IgA. Previous reports have established that N-glycans of IgA are sialylated bi-and tri-antennary complex-type glycans (Lipniunas et al., 1993). These sialylated N-glycans are acidic and generally give poor MALDI mass spectra (Harvey, 1999; Nishie et al., 2007). We therefore examined mass spectra of IgA N-glycans before and after digestion with an α2,3 sialidase.

N-glycans were released and isolated from IgA and were subsequently permethylated for mass spectrometric analyses by MALDI-TOF-MS. A fraction of the IgA samples was digested with sialidase S before being permethylated. As shown in Figure 3.4A, before treatment with sialidase, IgA samples contained sialylated N-glycans and no differences were noted comparing WT and ST6Gal I$^{-/-}$ IgA. However, following sialidase treatment clear differences were noted between WT and ST6Gal I$^{-/-}$ IgA (Figure 3.4B). Comparing purified IgA from WT versus ST6Gal I$^{-/-}$ mice, we discovered that α2,3 sialidase abolished virtually all sialylated N-glycans in ST6Gal I$^{-/-}$ IgA (Figure 3.4B). In contrast, sialylated N-glycans remained prominently visible on IgA from WT samples treated with α2,3 sialidase (Figure 3.4B). Similar results were obtained using IgA from naïve WT mice compared to naïve ST6Gal I$^{-/-}$ mice (data not shown). These data demonstrate that mouse IgA contains both α2,3- and α2,6-linked sialic acids on N-glycans, in contrast to mouse IgG where loss of expression of ST6Gal I revealed that sialic acids on N-glycans were exclusively α2,6-linked (Figure 3.3). Moreover, these data illustrate that loss of expression of ST6Gal I results in significant alterations in sialylation of N-glycans of IgG and IgA.

Loss of ST6Gal I expression and influenza infection results in mesangial IgA deposition

Finally, since our data indicated immune ST6Gal $I^{-/-}$ mice had high circulating levels of aberrantly glycosylated IgA, we examined kidney glomeruli of WT and ST6Gal $I^{-/-}$ mice by immuno-fluorescence to determine whether they showed IgA deposition. Naive WT mice show little evidence of IgA deposition in the glomeruli, and this was also true for naïve ST6Gal $I^{-/-}$ mice (Figure 3.5A, upper panels). Immune WT mice also showed little evidence of IgA deposition. In contrast, immune ST6Gal $I^{-/-}$ mice showed significant mesangial IgA deposition (Figure 3.5A, lower panels). Measurement of IgA mean fluorescence confirmed our observation of significantly higher deposition (Figure 3.5B). In contrast to IgG deposition, where we observed that influenza infection of both WT and ST6Gal $I^{-/-}$ mice resulted in IgG deposits in the kidney glomeruli, IgA deposition was only evident in immune ST6Gal $I^{-/-}$ mice (Figure 3.2 and 3.5). Thus, IgA deposition appeared to be influenced both by 1) immune history and 2) genetic remodeling of protein glycosylation. Perhaps, altered sialylation of N-glycans causes a conversion to occur, transforming normal IgA into pathogenic IgA, resulting in IgA mesangial deposition in ST6Gal $I^{-/-}$ influenza immune mice.

Discussion

Glycosylation is an important post-translational modification that influences several aspects of protein function, including conformation, stability, activation, and clearance from the circulation. Aberrant glycosylation has been implicated in several human diseases including cancer and metastasis, leukocyte adhesion deficiency diseases (LAD/CDG-IIc), and muscular dystrophy (Freeze and Schachter, 2009; Varki., 2009). Understanding how changes in glycosylation contribute to disease pathogenesis may provide clues for advances in clinical treatment.

We have previously reported that mice deficient in ST6Gal $I^{-/-}$ show altered immune responses, including significant impairments in the generation of humoral responses (Hennet et al., 1998; Zeng et al., 2009). In this report, we make the paradoxical observation that although generation of influenza-specific IgA responses are also impaired in ST6Gal $I^{-/-}$ mice, by memory time-points immune ST6Gal $I^{-/-}$ mice display increased levels of circulating viral-specific and total IgA (Figure 3.1). Our observation of increased IgA levels in immune ST6Gal $I^{-/-}$ mice led us to examine whether these mice developed evidence of glomerulonephritis.

Analysis of immune ST6Gal $I^{-/-}$ mice revealed that although these mice show evidence of normal kidney function (Figure 3.1 and Table 3.1), they also show increased IgG and IgA deposition in kidney glomeruli (Figure 3.2 and Figure 3.5). Glycan analysis of IgG and IgA by MALDI-TOF revealed that N-glycans of both IgG and IgA from ST6Gal $I^{-/-}$ mice show aberrant glycosylation (Figure 3.3 and Figure 3.4). These alterations in glycosylation were characterized by significant losses in sialylation as evidenced by a complete deficiency of terminally sialylated N-glycan structures in IgG, and reductions in sialylated N-glycans in IgA (Figure 3.3 and 3.4). Together, these data suggest that expression of this α2,6 sialyltransferase is critical for the synthesis of terminal sialic acids on IgG and IgA, and may influence circulating antibody levels and immunoglobulin deposition in the kidney glomeruli.

The sialic acid content of antibodies has been proposed to play a key role in the anti-inflammatory therapeutic effect of IVIG via Fc interactions with activating and inhibitory FcγRs (Nimmerjahn and Ravetch, 2007). Although it plays a primary role in protective humoral immunity, IgG also plays a pathogenic role in autoimmune diseases via the generation of auto-antibodies such as occurs in systemic lupus erythematosus (SLE), immune thrombocytopenia (ITP), rheumatoid arthritis (RA), and multiple sclerosis (MS). Pooled polyclonal IgG

from the sera of thousands of donors is used to make IVIG that is in turn used both for replacement therapy for patients lacking immunoglobulins, and in high doses as an anti-inflammatory agent for the treatment of autoimmune diseases such as ITP, SLE, MS, and scleroderma (Nimmerjahn and Ravetch, 2007). Several models have been proposed to account for the anti-inflammatory activity of Fc fragments in IVIG, and one model proposes that sialic acid rich IgG facilitates the induction of inhibitory FcγRIIB on effector macrophages, increasing the threshold for cell activation, thus reducing inflammation (Nimmerjahn and Ravetch, 2007). Enrichment of sialic acid containing IgG significantly lowers the amount of IVIG needed for its anti-inflammatory activity (Kaneko et al., 2006). The deficiency of sialylated N-glycans on IgG from ST6Gal I deficient mice would presumably alter this proposed interaction of Fc-bearing sialic acids with sialic acid binding receptors on regulatory macrophages. This in turn may lead to reduced ability for IgG derived from ST6Gal $I^{-/-}$ mice to upregulate FcγRIIB on effector macrophages.

In addition to changes in the sialylation of IgG, our data also revealed significant alterations in the sialylation of IgA (Figure 3.4). In humans, abnormalities in galactosylation and sialylation of IgA1 have been reported to play a key role in pathogenesis of IgAN. IgA1, which is not produced in mice, is modified by ST6GalNAcII, an α2,6 sialyltransferase that modifies O-glycans of the IgA1 hinge region (Li et al., 2007b). Reduced expression of ST6GalNAcII has previously been reported in peripheral B cells from IgAN patients (Khan et al., 2008). However, another report using immortalized B cell lines from IgAN patients reached a different conclusion suggesting that ST6GalNAcII was increased in expression, while two other glycosyltransferases (C1GalT1 and Cosmc) were reduced in expression (Suzuki et al., 2008). The discrepancies in the conclusions of the two studies may be due to the different patient groups, and/or differences in the cells used in the two studies (peripheral B cells versus immortalized B cells) to examine ST6GalNAcII expression. However, it should also be

considered that transcriptional regulation of α2,6 sialyltransferases is known to be influenced by cell type, differentiation, and transformation status (Hedlund et al., 2008; Li et al., 2007b).

Our results using influenza infection of mice deficient in ST6Gal I, the α2,6 sialyltransferase involved in N-glycan sialylation, demonstrated not only aberrant terminal sialylation of N-glycans from ST6Gal $I^{-/-}$ IgA, but also increased circulating IgA, and increased IgA deposition in kidney glomeruli. These observations would be consistent with early development of an IgAN-like disease in ST6Gal $I^{-/-}$ mice. Our findings are reminiscent of the initial study by Berger and Hinglais characterizing IgAN (aka Berger's disease) where they first proposed using immuno-fluorescence techniques to diagnose this disease (Berger and Hinglais, 1968). In their study, increased glomerular IgA deposition preceded disease development, as well as evidence of pathological abnormalities in the kidney (Berger and Hinglais, 1968). A recent study proposed that carbohydrates of serum IgA may be involved in the development of IgAN-like diseases, regardless of whether they are O-or N-glycans, and our data would support this conclusion, although the mechanism of pathogenesis remains unclear (Nishie et al., 2007). Importantly, while changes in terminal N-glycan sialylation were evident in IgG and IgA before influenza infection of ST6Gal $I^{-/-}$ mice, no significant differences in immunoglobulin deposition were observed in non-immunized mice compared to WT mice. Our observations of increased deposition were limited to mice with a history of influenza infection. We observed no evidence of spontaneous IgAN-like disease development as reported in the study of β4GalT $I^{-/-}$ mice (Nishie et al., 2007).

Interestingly, our data is consistent with several familial studies of IgAN that have suggested that additional co-factors besides altered glycosylation may be required for IgAN disease development, such as respiratory infections (Gharavi et al., 2008; Woodroffe et al., 1980). One clinical study showed that patients with

IgAN are high responders for IgA production following administration of influenza vaccine (Endoh et al., 1984). We also observed higher memory influenza-specific IgA responses in ST6Gal I$^{-/-}$ mice compared to WT mice (Figure 3.1). However, it remains unclear what mechanisms mediate the increased flu-specific IgA levels in ST6Gal I$^{-/-}$ mice. One possibility is that more IgA-specific plasmablasts are generated in ST6Gal I$^{-/-}$ mice, and this accounts for the increased circulating levels of IgA. However, our data analyzing the generation of influenza-specific IgA plasmablasts showed modest defects in ST6Gal I$^{-/-}$ mice, and influenza-specific IgA LLPC and MBC numbers were similar comparing WT and ST6Gal I$^{-/-}$ immune mice ((Zeng et al., 2009) and data not shown). If so, this would suggest that higher IgA levels in influenza immune ST6Gal I$^{-/-}$ mice was more likely due to defective IgA clearance, or higher per cell production of IgA. While further studies are needed to examine this in more detail, we favor the former explanation since it has been proposed that immune complexes of aberrantly glycosylated IgA1 escape normal clearance mechanisms, and deposit in the renal mesangium where they induce glomerular injury in humans (Novak et al., 2008). A similar phenomenon may occur with aberrantly glycosylated IgA in ST6Gal I deficient mice. Possibly, these mice may provide a useful model by which influenza infection, and the generation of under-sialylated IgA (and IgG), can be evaluated to determine how genetic remodeling of protein glycosylation and immune history together contribute to immunoglobulin deposition and development of glomerulonephritis.

REFERENCES

Allen, A.C., and J. Feehally. 2000. IgA1 glycosylation and the pathogenesis of IgA nephropathy. *Am J Kidney Dis* 35:551-6.

Anthony, R.M., F. Nimmerjahn, D.J. Ashline, V.N. Reinhold, J.C. Paulson, and J.V. Ravetch. 2008. Recapitulation of IVIG anti-inflammatory activity with a recombinant IgG Fc. *Science* 320:373-6.

Berger, J., and N. Hinglais. 1968. [Intercapillary deposits of IgA-IgG]. *J Urol Nephrol (Paris)* 74:694-5.

Collins, B.E., B.A. Smith, P. Bengtson, and J.C. Paulson. 2006. Ablation of CD22 in ligand-deficient mice restores B cell receptor signaling. *Nat Immunol* 7:199-206.

Ding, J.X., L.X. Xu, L. Zhu, J.C. Lv, M.H. Zhao, H. Zhang, and H.Y. Wang. 2009. Activity of alpha2,6-sialyltransferase and its gene expression in peripheral B lymphocytes in patients with IgA nephropathy. *Scand J Immunol* 69:174-80.

Dixon, F.J., J.D. Feldman, and J.J. Vazquez. 1961. Experimental glomerulonephritis. The pathogenesis of a laboratory model resembling the spectrum of human glomerulonephritis. *J Exp Med* 113:899-920.

Endoh, M., T. Suga, M. Miura, Y. Tomino, Y. Nomoto, and H. Sakai. 1984. In vivo alteration of antibody production in patients with IgA nephropathy. *Clin Exp Immunol* 57:564-70.

Freeze, H.H., and H. Schachter. 2009. Genetic Disorders of Glycosylation. In Essentials of Glycobiology. C.R. Varki A, Esko JD, editor Cold Spring Harbor Laboratory Press, Cold Spring Harbor (NY).

Galvan, M., K. Murali-Krishna, L.L. Ming, L. Baum, and R. Ahmed. 1998. Alterations in cell surface carbohydrates on T cells from virally infected mice can distinguish effector/memory CD8+ T cells from naive cells. *J Immunol* 161:641-8.

Gharavi, A.G., Z. Moldoveanu, R.J. Wyatt, C.V. Barker, S.Y. Woodford, R.P. Lifton, J. Mestecky, J. Novak, and B.A. Julian. 2008. Aberrant IgA1

glycosylation is inherited in familial and sporadic IgA nephropathy. *J Am Soc Nephrol* 19:1008-14.

Glassock, R.J. 2009. Analyzing antibody activity in IgA nephropathy. *J Clin Invest* 119:1450-2.

Grewal, P.K., M. Boton, K. Ramirez, B.E. Collins, A. Saito, R.S. Green, K. Ohtsubo, D. Chui, and J.D. Marth. 2006. ST6Gal-I restrains CD22-dependent antigen receptor endocytosis and Shp-1 recruitment in normal and pathogenic immune signaling. *Mol Cell Biol* 26:4970-81.

Hansske, B., C. Thiel, T. Lubke, M. Hasilik, S. Honing, V. Peters, P.H. Heidemann, G.F. Hoffmann, E.G. Berger, K. von Figura, and C. Korner. 2002. Deficiency of UDP-galactose:N-acetylglucosamine beta-1,4-galactosyltransferase I causes the congenital disorder of glycosylation type IId. *J Clin Invest* 109:725-33.

Harvey, D.J. 1999. Matrix-assisted laser desorption/ionization mass spectrometry of carbohydrates. *Mass Spectrom Rev* 18:349-450.

Hedlund, M., E. Ng, A. Varki, and N.M. Varki. 2008. alpha 2-6-Linked sialic acids on N-glycans modulate carcinoma differentiation in vivo. *Cancer Res* 68:388-94.

Hennet, T., D. Chui, J.C. Paulson, and J.D. Marth. 1998. Immune regulation by the ST6Gal sialyltransferase. *Proc Natl Acad Sci U S A* 95:4504-9.

Kalia, V., S. Sarkar, T.S. Gourley, B.T. Rouse, and R. Ahmed. 2006. Differentiation of memory B and T cells. *Curr Opin Immunol* 18:255-64.

Kaneko, Y., F. Nimmerjahn, and J.V. Ravetch. 2006. Anti-inflammatory activity of immunoglobulin G resulting from Fc sialylation. *Science* 313:670-3.

Kaveri, S.V., S. Lacroix-Desmazes, and J. Bayry. 2008. The antiinflammatory IgG. *N Engl J Med* 359:307-9.

Kersh, E.N., S.M. Kaech, T.M. Onami, M. Moran, E.J. Wherry, M.C. Miceli, and R. Ahmed. 2003. TCR signal transduction in antigen-specific memory CD8 T cells. *J Immunol* 170:5455-63.

Li, G.S., H. Zhang, J.C. Lv, Y. Shen, and H.Y. Wang. 2007. Variants of C1GALT1 gene are associated with the genetic susceptibility to IgA nephropathy. *Kidney Int* 71:448-53.

Li, G.S., L. Zhu, H. Zhang, J.C. Lv, J.X. Ding, M.H. Zhao, Y. Shen, and H.Y. Wang. 2007. Variants of the ST6GALNAC2 promoter influence transcriptional activity and contribute to genetic susceptibility to IgA nephropathy. *Hum Mutat* 28:950-7.

Lipniunas, P., G. Gronberg, H. Krotkiewski, A.S. Angel, and B. Nilsson. 1993. Investigation of the structural heterogeneity in the carbohydrate portion of a mouse monoclonal immunoglobulin A antibody. *Arch Biochem Biophys* 300:335-45.

London, J., S. Berrih, and J.F. Bach. 1978. Peanut agglutinin. I. A new tool for studying T lymphocyte subpopulations. *J Immunol* 121:438-43.

Nimmerjahn, F., and J.V. Ravetch. 2007. The antiinflammatory activity of IgG: the intravenous IgG paradox. *J Exp Med* 204:11-5.

Nishie, T., O. Miyaishi, H. Azuma, A. Kameyama, C. Naruse, N. Hashimoto, H. Yokoyama, H. Narimatsu, T. Wada, and M. Asano. 2007. Development of immunoglobulin A nephropathy- like disease in beta-1,4-galactosyltransferase-I-deficient mice. *Am J Pathol* 170:447-56.

Nitschke, L. 2005. The role of CD22 and other inhibitory co-receptors in B-cell activation. *Curr Opin Immunol* 17:290-7.

Novak, J., B.A. Julian, M. Tomana, and J. Mestecky. 2008. IgA glycosylation and IgA immune complexes in the pathogenesis of IgA nephropathy. *Semin Nephrol* 28:78-87.

Onami, T.M., L.E. Harrington, M.A. Williams, M. Galvan, C.P. Larsen, T.C. Pearson, N. Manjunath, L.G. Baum, B.D. Pearce, and R. Ahmed. 2002. Dynamic regulation of T cell immunity by CD43. *J Immunol* 168:6022-31.

Onami, T.M., M.Y. Lin, D.M. Page, S.A. Reynolds, C.D. Katayama, J.D. Marth, T. Irimura, A. Varki, N. Varki, and S.M. Hedrick. 2002. Generation of mice deficient for macrophage galactose- and N-acetylgalactosamine-specific

lectin: limited role in lymphoid and erythroid homeostasis and evidence for multiple lectins. *Mol Cell Biol* 22:5173-81.

Raju, T.S. 2008. Terminal sugars of Fc glycans influence antibody effector functions of IgGs. *Curr Opin Immunol* 20:471-8.

Raska, M., Z. Moldoveanu, H. Suzuki, R. Brown, R. Kulhavy, J. Andrasi, S. Hall, H.L. Vu, F. Carlsson, G. Lindahl, M. Tomana, B.A. Julian, R.J. Wyatt, J. Mestecky, and J. Novak. 2007. Identification and characterization of CMP-NeuAc:GalNAc-IgA1 alpha2,6-sialyltransferase in IgA1-producing cells. *J Mol Biol* 369:69-78.

Sangster, M.Y., J.M. Riberdy, M. Gonzalez, D.J. Topham, N. Baumgarth, and P.C. Doherty. 2003. An early CD4+ T cell-dependent immunoglobulin A response to influenza infection in the absence of key cognate T-B interactions. *J Exp Med* 198:1011-21.

Schrader, J.W., W.F. Chen, and R. Scollay. 1982. The acquisition of receptors for peanut agglutinin by peanut agglutinin-negative thymocytes and peripheral T cells. *J Immunol* 129:545-9.

Semkow, R., and J. Wilczynski. 1979. Clearance of antibody and complement in serum after challenge of mice previously vaccinated or infected with influenza virus. *Acta Virol* 23:253-6.

Semkow, R., and J. Wilczynski. 1979. Detection and tissue localization of components of the immune complex in animals infected and immunized with influenza virus. *Acta Virol* 23:52-8.

Slifka, M.K., and R. Ahmed. 1996. Limiting dilution analysis of virus-specific memory B cells by an ELISPOT assay. *J Immunol Methods* 199:37-46.

Slifka, M.K., and R. Ahmed. 1998. Long-lived plasma cells: a mechanism for maintaining persistent antibody production. *Curr Opin Immunol* 10:252-8.

Slifka, M.K., R. Antia, J.K. Whitmire, and R. Ahmed. 1998. Humoral immunity due to long-lived plasma cells. *Immunity* 8:363-72.

Suzuki, H., Z. Moldoveanu, S. Hall, R. Brown, H.L. Vu, L. Novak, B.A. Julian, M. Tomana, R.J. Wyatt, J.C. Edberg, G.S. Alarcon, R.P. Kimberly, Y. Tomino,

J. Mestecky, and J. Novak. 2008. IgA1-secreting cell lines from patients with IgA nephropathy produce aberrantly glycosylated IgA1. *J Clin Invest* 118:629-39.

Tomana, M., J. Novak, B.A. Julian, K. Matousovic, K. Konecny, and J. Mestecky. 1999. Circulating immune complexes in IgA nephropathy consist of IgA1 with galactose-deficient hinge region and antiglycan antibodies. *J Clin Invest* 104:73-81.

varki a. 2009. Essentials of Glycobiology.

von Horsten, H.H., C. Ogorek, V. Blanchard, C. Demmler, C. Giese, K. Winkler, M. Kaup, M. Berger, I. Jordan, and V. Sandig. Production of non-fucosylated antibodies by co-expression of heterologous GDP-6-deoxy-D-lyxo-4-hexulose reductase. *Glycobiology* 20:1607-18.

Wedepohl, S., M. Kaup, S.B. Riese, M. Berger, J. Dernedde, R. Tauber, and V. Blanchard. N-glycan analysis of recombinant L-Selectin reveals sulfated GalNAc and GalNAc-GalNAc motifs. *J Proteome Res* 9:3403-11.

Woodroffe, A.J., A.A. Gormly, P.E. McKenzie, A.M. Wootton, A.J. Thompson, A.E. Seymour, and A.R. Clarkson. 1980. Immunologic studies in IgA nephropathy. *Kidney Int* 18:366-74.

Xu, L.X., Y. Yan, J.J. Zhang, Y. Zhang, and M.H. Zhao. 2005. The glycans deficiencies of macromolecular IgA1 is a contributory factor of variable pathological phenotypes of IgA nephropathy. *Clin Exp Immunol* 142:569-75.

Zeng, J., H.M. Joo, B. Rajini, J.P. Wrammert, M.Y. Sangster, and T.M. Onami. 2009. The generation of influenza-specific humoral responses is impaired in ST6Gal I-deficient mice. *J Immunol* 182:4721-7.

Appendix

Figure 3. 1. Increased IgA levels in influenza immune ST6Gal I$^{-/-}$ mice.

C57BL/6 wildtype or ST6Gal I$^{-/-}$ mice remained uninfected or were infected with $10^{6.8}$ EID_{50} of influenza A/HKx31 i.n. and serum, urine, or kidney samples were collected. ELISA was performed on samples to measure total or influenza-specific Ig, or albumin levels. (A) Serum levels were measured of total IgG and IgA from naïve, uninfected mice (*left*), or total IgG, total IgA, and influenza-specific IgG and IgA from mice at day 175 post-infection (*right*). (B) Mice were serially bled on indicated days and virus-specific IgG and IgA were measured longitudinally. (C) Albumin levels were measured in urine from mice at day 400 post-infection. (D) Kidneys from mice at day 400 post-infection were formalin fixed, paraffin-embedded, and thin sections were stained with H&E. Magnification 600X. Bar graphs show data from n = 4-10 mice, with black bars showing WT mice and white bars showing ST6Gal I$^{-/-}$ mice (* indicates $p<0.05$ and ** indicates $p<0.01$)

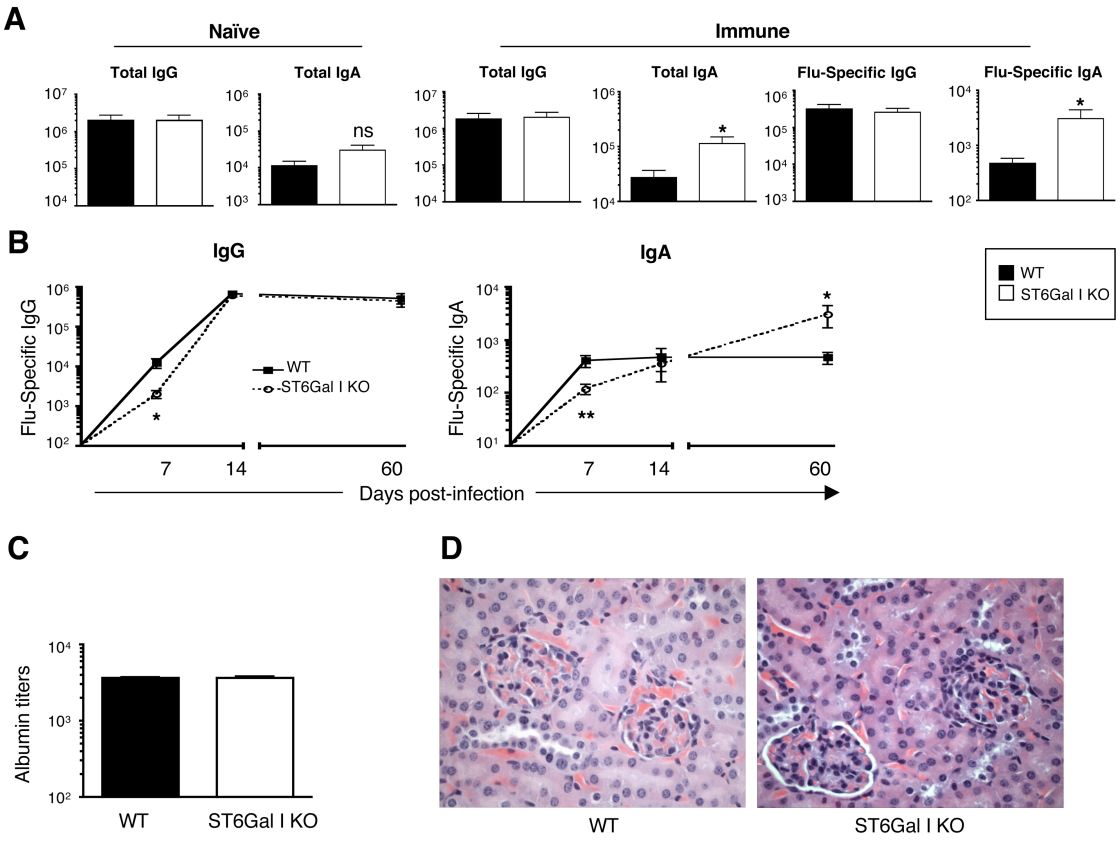
A
Naïve
Immune
Total IgG
Total IgA
Total IgG
Total IgA
Flu-Specific IgG
Flu-Specific IgA
ns
*
*
*
B
IgG
IgA
WT
ST6Gal I KO
Flu-Specific IgG
Flu-Specific IgA
WT
ST6Gal I KO
*
**
*
7
14
60
7
14
60
Days post-infection
C
D
Albumin titers
WT
ST6Gal I KO
WT
ST6Gal I KO

Table 3. 1 Measurement of hematuria and proteinuria by urinalysis test strips.

Mouse Type	No. of Mice	Hematuria	Proteinuria
WT Uninfected	3	-	+/-
KO Uninfected	3	-	-
WT Immune	10	-	-
KO Immune	10	-	-

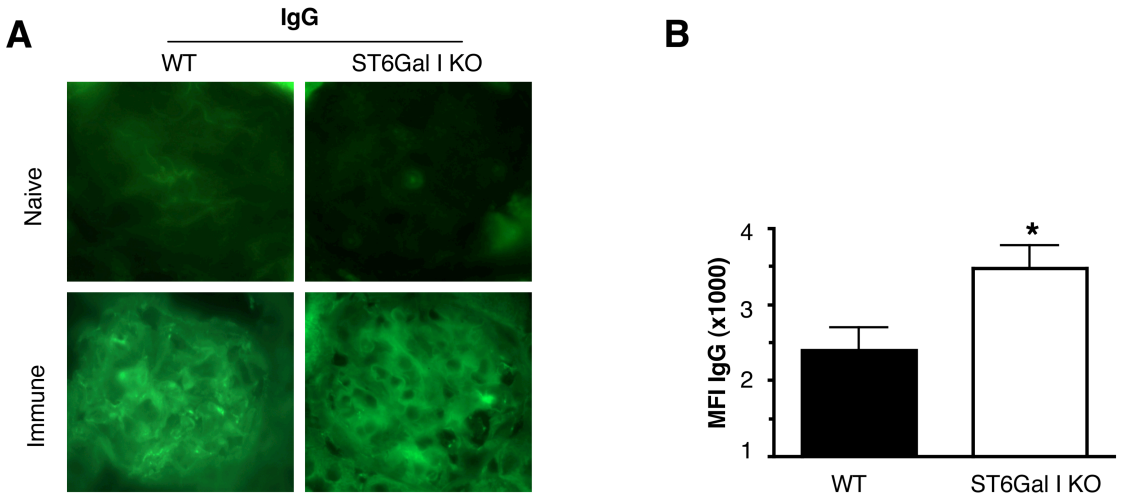

Figure 3. 2. ST6Gal I$^{-/-}$ mice show greater IgG deposition in glomeruli following influenza infection.

WT or ST6Gal I$^{-/-}$ mice remained uninfected or were infected with $10^{6.8}$ EID_{50} of influenza A/HKx31 i.n. and on day 400 kidneys were harvested and frozen for immuno-histology. (A) Representative staining of IgG in kidney glomeruli from naïve WT or ST6Gal I$^{-/-}$ mice (*top*) compared to WT or ST6Gal I$^{-/-}$ at day 400 post-infection (*bottom*). (B) Mean fluorescence intensity of IgG deposition was measured in influenza immune mice. Bar graphs show data from n = 6 samples from two independent experiments, with black bars denoting WT and white bars denoting ST6Gal I$^{-/-}$ mice (* indicates $p<0.05$).

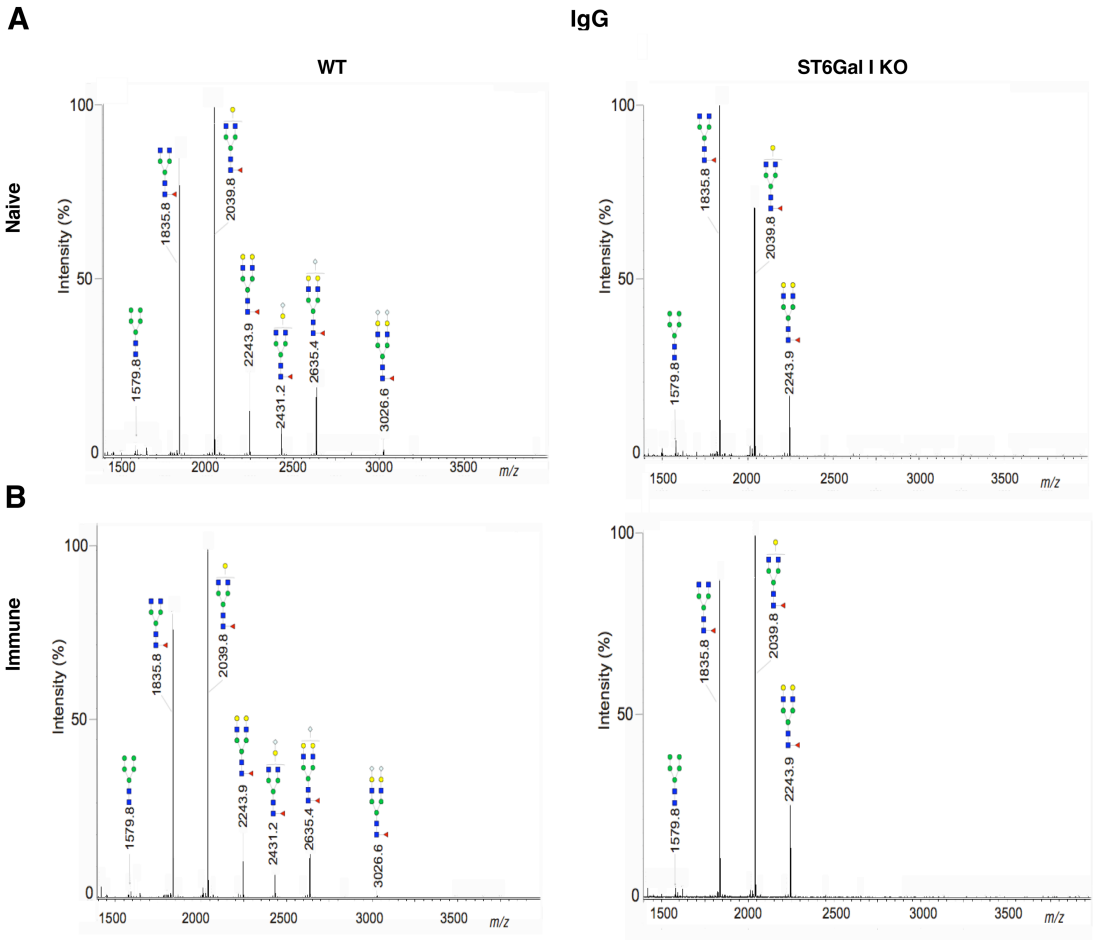

Figure 3. 3. ST6Gal I expression is required for sialylation of N-glycans on IgG.

MALDI-TOF spectra of permethylated N-glycan pools were measured in the positive-ion mode. All molecular ions are present in sodiated form [M + Na]+. (A) IgG from naive mice, or (B) IgG from mice on day 100 post-infection with influenza comparing WT (*left*) or ST6Gal $I^{-/-}$ (*right*). Green circle, Man; yellow circle, Gal; yellow square, GalNAc; blue square, GlcNAc; red triangle, Fuc; white diamond, Neu5Gc. Structures outside the bracket have not been unequivocally assigned.

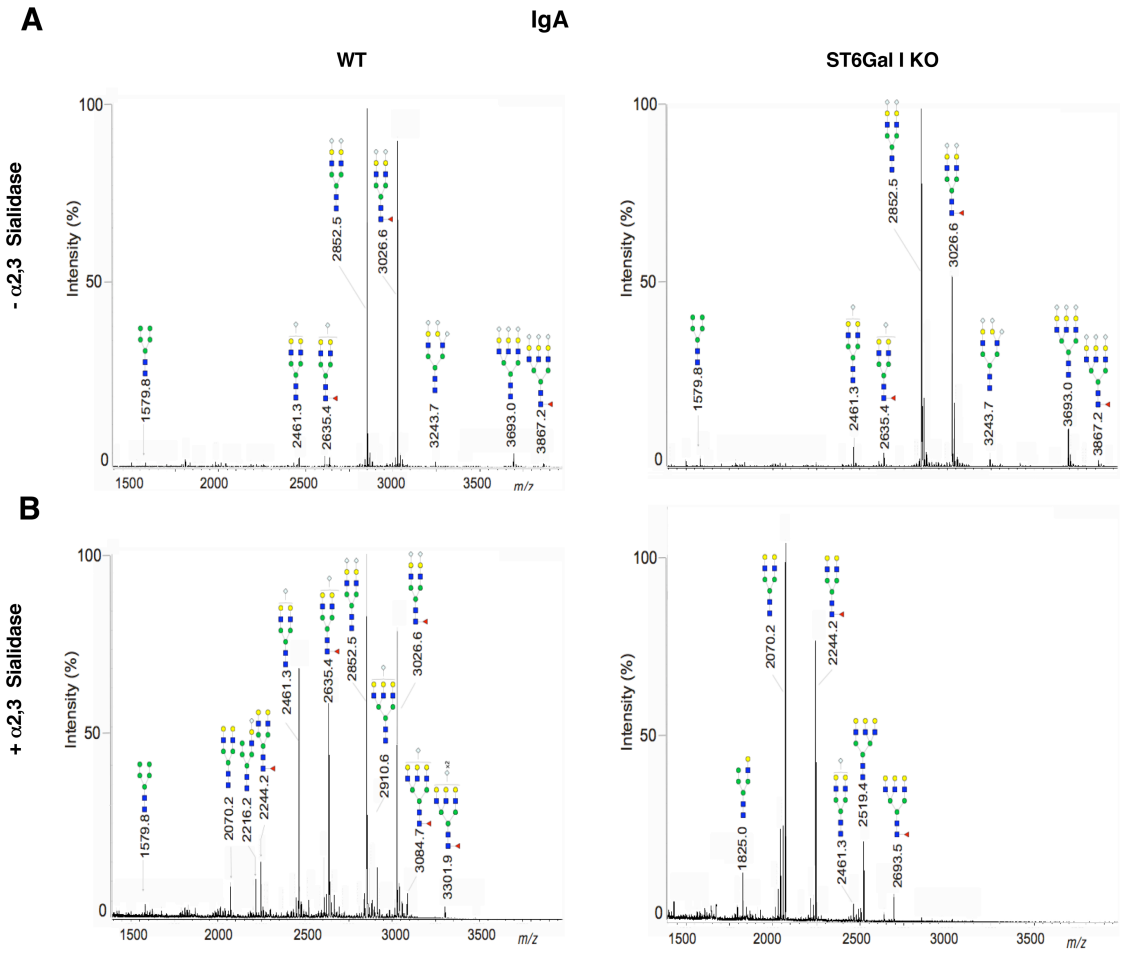

Figure 3. 4. Loss of ST6Gal I expression leads to aberrant IgA glycosylation.

MALDI-TOF spectra of permethylated N-glycan pools were measured in the positive-ion mode. All molecular ions are present in sodiated form [M + Na]+. (A) IgA and (B) IgA digested with sialidase S prior to permethylation from influenza immune WT (*left*) or ST6Gal $I^{-/-}$ (*right*) mice. Green circle, Man; yellow circle, Gal; yellow square, GalNAc; blue square, GlcNAc; red triangle, Fuc; white diamond, Neu5Gc. Structures outside the bracket have not been unequivocally assigned.

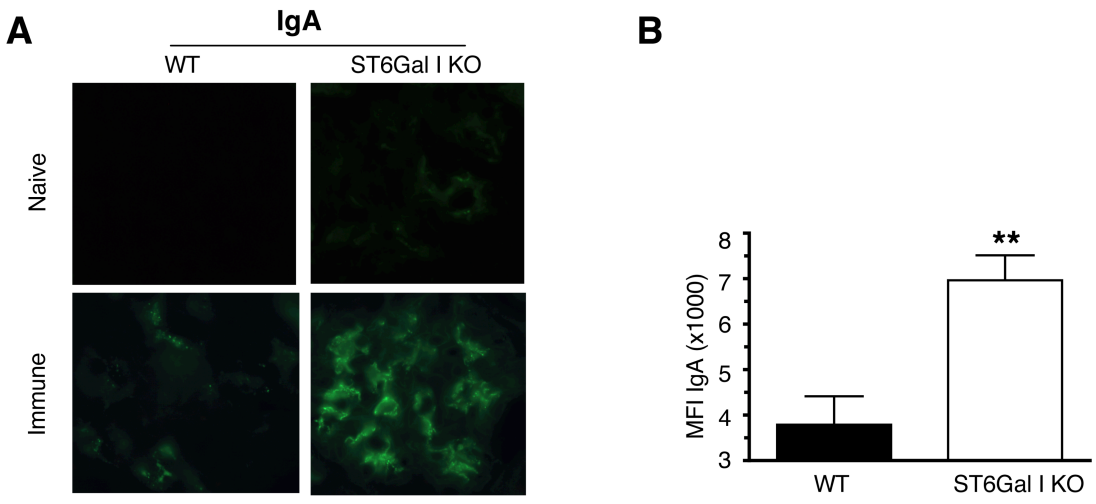

Figure 3. 5. Loss of ST6Gal I expression, concomitant with influenza viral infection, result in mesangial IgA deposition.

WT or ST6Gal $I^{-/-}$ mice remained uninfected or were infected with $10^{6.8}$ EID_{50} of influenza A/HKx31 i.n. and on day 400 kidneys were harvested and frozen for immuno-histology. (A) Representative staining of IgA in kidney glomeruli from naïve WT or ST6Gal $I^{-/-}$ mice (*top*) compared to WT or ST6Gal $I^{-/-}$ at day 400 post-infection (*bottom*). (B) Mean fluorescence intensity of IgA deposition was measured in influenza immune mice. Bar graphs show data from n = 6 samples from two independent experiments, with black bars denoting WT and white bars denoting ST6Gal $I^{-/-}$ mice (** indicates $p<0.01$).CHAPTER II ST6Gal I promotes rapid IL-2Rα surface expression, increasing early proliferation of terminal effector CD8 T cell.

CHAPTER IV

ST6GAL I PROMOTES RAPID IL-2Rα SURFACE EXPRESSION, INCREASING EARLY PROLIFERATION OF TERMINAL EFFECTOR CD8 T CELLS

Abstract

ST6Gal I is a glycosyltransferase highly expressed by lymphocytes and cancer cells that catalyzes the addition of α2,6 sialic acid to galactose (Siaα2-6Gal) on N-linked glycoproteins. We discovered that ST6Gal I shows dramatic changes in gene expression during memory CD8 T cell differentiation that corresponds with lectin binding, but the significance of this regulated carbohydrate modification remained elusive. To identify the role of these regulated glyco-phenotypic changes, we infected ST6Gal $I^{-/-}$ mice and show that viral-specific T and B cell expansion was impaired. Moreover, defective viral-specific CD8 T cell expansion was due to early intrinsic defects in proliferation of terminal effector cells, whereas memory precursor development was enhanced. We provide direct evidence that loss of ST6Gal I expression by CD8 T cells resulted in delayed surface expression of IL-2Rα *in vivo* due to impaired IL-2/IL-2R signaling. These results suggest that CD8 T cells regulate ST6Gal I expression to promote proliferation induced by cytokine-dependent signaling.

Introduction

Over the past several decades it has been appreciated that lymphocytes show dramatic changes in lectin binding during development and differentiation (Galvan et al., 1998b; Harrington et al., 2000; London et al., 1978; London and Horton, 1980; Onami et al., 2002; Rose et al., 1980; Rose et al., 1981). Changes in lectin binding properties were exploited before the wide availability of monoclonal antibodies, allowing for the routine purification of cell subsets. For example, peanut agglutinin (PNA) which recognizes (Galβ1-3GalNAc) on O-linked glycans was used to distinguish developing CD4+CD8+ thymocytes from SP mature T cells, as well as germinal center B cells from naïve, resting B cells (London et al., 1978; London and Horton, 1980; Rose et al., 1980). More recently, effector and memory T cell populations were shown to bind PNA highly, while naïve T cells showed much weaker binding by this lectin (Galvan et al., 1998b; Onami et al., 2002). Additionally, naïve, effector, and memory T cell populations show changes in CD43 glycoform expression which can be visualized by changes in binding with the glycosylation-dependent monoclonal antibody, 1B11 (Harrington et al., 2000; Onami et al., 2002). Although little is known about the significance of altered glycosylation in T cell activation and function, several studies have demonstrated that changes in the gene expression of specific glycosyltransferases are responsible for glyco-phenotypic changes observed in T cell populations (Comelli et al., 2006; Priatel et al., 2000). These studies suggest that precise regulation of enzyme expression occurs during T cell development, activation, and differentiation, and is often responsible for observed glyco-phenotypic changes. However, the functional significance of these glyco-phenotypic changes has remained poorly understood.

Alterations in glycosylation have been defined in several immune-mediated diseases, immuno-deficiencies, and cancer. Among the best-studied examples include the recruitment of leukocyte populations to lymphoid organs and sites of

infection, which is critically dependent on fucosylated, sialylated glyco-conjugates such as the sialyl Lewis X (sLe^x) structure (Harp and Onami, 2010; Lowe, 2003). A leukocyte adhesion deficiency disease, LADII (also known as congenital disorder of glycosylation IIc of CDG-IIc) is caused by mutations in a GDP-fucose transporter (SLC35C1), resulting in hypo-fucosylation of glycoproteins, and consequent impairment in leukocyte interaction with vascular endothelium (Luhn et al., 2001). In cancer, one of the hallmark features of malignant cells is altered sialylation, and specific glycan structures are commonly used as markers of tumor progression (Varki, 2008). ST6Gal I, a glycosyltransferase that catalyzes the addition of α2,6 sialic acid to galactose (Siaα2-6Gal) on N-linked glycoproteins, is up-regulated by oncogenic ras, and shows high expression in several tumors including cervical, colorectal, breast, and hepatocellular tumors (Dall'Olio et al., 2004; Hedlund et al., 2008; Vazquez-Martin et al., 2005; Wang et al., 2002). Several studies have suggested that ST6Gal I expression regulates tumor cell differentiation, motility, and migration (Christie et al., 2008; Hedlund et al., 2008; Qian et al., 2009; Seales et al., 2005).

To gain insight into the glyco-phenotypic changes that occur following T cell activation *in vivo*, we undertook a comprehensive examination of glycosyltransferase gene expression during memory CD8 T cell differentiation using the NIGMS Consortium for Glycomics Glyco-gene chip. We identified changes in glyco-specific gene expression, including changes in the expression of the sialyltransferase ST6Gal I, which showed a striking decrease during the naïve to effector cell transition. In contrast to the results observed in T cells, B cells do not show dramatic reduction in ST6Gal I expression following B cell activation (Comelli et al., 2006; Zeng et al., 2009). We confirmed that changes in ST6Gal I expression in CD8 T cells were accompanied by concomitant changes in cell surface glycosylation, using the lectin *Sambucus nigra* agglutinin (SNA) that recognizes the Siaα2-6Gal linkage created by ST6Gal I on N-linked glycans. Surprisingly, SNA defined heterogeneity in memory CD8 T cells, with SNA^{high}

and SNA^{low} memory CD8 T cell populations present in all tissues following viral resolution. Extensive comparison of SNA^{high} and SNA^{low} memory CD8 T cells with regard to other markers of effector or memory T cells failed to identify any other marker that uniquely distinguished these populations. However, these two populations differed with respect to extent of proliferation and kinetics of viral clearance, suggesting functional heterogeneity within the memory CD8 T cell compartment.

To further investigate the importance of ST6Gal I regulation during memory CD8 T cell differentiation, we undertook a detailed analysis of LCMV-specific responses in ST6Gal I deficient mice. These studies identified early impairments in viral-specific T and B cell responses. Strikingly, we observed that expansion of short-lived effector cell (SLEC) or terminal effector populations were significantly impaired, while ST6Gal $I^{-/-}$ T cells preferentially developed into memory precursor effector (MPEC) populations. We generated transgenic P14xST6Gal $I^{-/-}$ mice, to obtain CD8 T cells specific for the GP33-41 peptide of the LCMV glycoprotein, to probe cell intrinsic defects. We discovered that CD8 T cell loss of ST6Gal I expression resulted in defective early proliferation, and this defective proliferation was not due to defective T cell recruitment, but rather altered kinetics of IL-2Rα up-regulation and surface expression in the initial 24hrs following antigen exposure. We further show that this was due to impaired IL-2/IL-2Rα signaling. Our results provide the first direct evidence that regulation of a glycosyltransferase responsible for post-translational carbohydrate modification of several T cell glycoproteins, influences early T cell proliferation by fine-tuning cytokine dependent signaling, and this in turn influenced effector/memory T cell programming.

Materials and Methods

Mice and immunizations

All animals were handled in strict accordance with good animal practice as defined by the University of Tennessee IACUC committee, and the committee approved all animal work. ST6Gal I-deficient mice were originally generated by J. Marth (University of California, San Diego) and obtained from the Consortium for Functional Glycomics and bred in-house, backcrossed to C57BL/6 x10 generations (Hennet et al., 1998). Transgenic P14 Thy1.1 mice were kindly provided by Dr. Rafi Ahmed (Emory Vaccine Center, GA) and bred in-house. C57BL/6 mice were purchased from The Jackson Laboratory (Bar Harbor, ME). Mice were maintained under specific pathogen-free conditions at the University of Tennessee in accordance with university IACUC guidelines. Mice were infected with 2×10^5 PFU LCMV-Armstrong intra-peritoneal (i.p.) or intravenous (i.v.) as indicated. For memory re-challenge experiments, mice were re-challenged i.v. with 5×10^7 PFU Vaccinia virus expressing GP33-41 (Onami et al., 2002).

Adoptive transfer

All antibodies were purchased from BD-Pharmingen (La Jolla, CA). SNA-FITC was purchased from Sigma Chemicals (St. Louis, MO). DbGP33-41 MHC tetramers were prepared as previously described (Murali-Krishna et al., 1998) or provided by the NIH Tetramer Facility (Atlanta, GA). P14xThy1.1 chimeric mice were generated as previously described (Suvas et al., 2007). Briefly, 0.5-1x106 total Thy1.1 P14 transgenic spleen cells were adoptively transferred into intact C57BL/6 mice followed by infection with 2x105 PFU of LCMV-Armstrong i.p.

For single transfer experiments, ST6Gal-I$^{+/-}$ x P14 Tg$^+$ Thy 1.1-1.2$^+$ (Tg WT) and ST6Gal-I$^{-/-}$ x P14 Tg$^+$ Thy 1.1-1.2$^+$ (Tg KO) mice were sacrificed, spleens were

collected, and processed to yield a single cell suspension. $1x10^6$ Tg WT or Tg KO cells in 0.5 ml PBS were injected into naïve C57BL/6 Thy1.2$^+$ recipient mice by tail vein (i.v.) injection. Recipient mice were infected with $2x10^5$ pfu/ml LCMV Armstrong i.p. or i.v. the next day. Mice were sacrificed at day 8 post- infection and spleens were collected, processed, and single cell suspensions were stained with fluorochrome conjugated anti-Thy1.1, anti-Thy1.2, anti-CD8 antibodies, SNA, and D^{b}GP33-41 MHC-I tetramer for analysis by flow cytometry. All samples were run on a FACSCalibur (BD Biosciences) and analyzed using FlowJo software (Tree Star). Total number of donor cells in recipient mice was calculated from the percent of Thy1.1-1.2$^+$DbGP33-41$^+$CD8$^+$ cells in total splenocytes. Unpaired *t* tests were performed to determine statistical significance, with *** denoting $p<0.001$, ** denoting $p<0.01$, and * denoting $p<0.05$.

For competition co-transfers, ST6Gal I$^{+/-}$ x P14 Tg$^+$ Thy 1.2$^+$ (Tg WT) and ST6Gal I$^{-/-}$ x P14 Tg$^+$ Thy 1.1-1.2$^+$ (Tg KO) mice were sacrificed, spleens were collected, and processed to yield a single cell suspension. A 1:1 mixture of Tg WT and Tg KO cells in a total of $1x10^6$ cells in 0.5 ml PBS per mouse were transferred into recipient C57BL/6 Thy1.1$^+$ mice i.v. Recipient mice were infected with $2x10^5$ pfu/ml LCMV Armstrong i.p. 24 hours following adoptive transfer. Mice were sacrificed at day 8 post-infection, spleens were collected, processed, and single cell suspensions were stained and analyzed as above.

For memory functional experiments, SNA^{high}, SNA^{low}, or total Thy1.1$^+$ CD8$^+$ T cells were FACS sorted using a FACS Advantage (BD La Jolla, CA) from immune (day 100) P14xThy1.1 chimeric mice, and $2x10^4$ sorted memory T cells were adoptively transferred into C57BL/6 mice, followed by challenge with $2x10^6$ LCMV clone 13 i.v. Mice were serially bled and serum and PBMC were analyzed from individual mice as indicated.

DNA Microarray Hybridization

Total RNA was isolated from FACS sorted Ag-specific CD8 T cells in TRIZOL (Gibco/Invitrogen, Rockville, MD) according to manufacturer's protocol. The cDNA was synthesized using Superscript Choice cDNA Synthesis Kit (Gibco/Invitrogen, Rockville, MD) and an oligo(dT) primer containing a T7 promoter. The MEGAscript T7 kit (Ambion, Austin, TX) was used to amplify cRNA from the cDNA. The cRNA was reverse transcribed with fluorescently labeled nucleotides and hybridized to the Glyco-gene chip at the Scripps Research Clinics Microarray Core as part of the CFG (La Jolla, CA).

In vivo CFSE proliferation assay

ST6Gal-I$^{+/-}$ x P14 Tg^{+} Thy 1.1 and ST6Gal-I$^{-/-}$ x P14 Tg^{+} Thy 1.1 mice were sacrificed, spleens were collected, and processed to yield single cell suspensions of 10^7 cells/ml in RPMI media. CD8 T cells were isolated by negative purification using a CD8 T cell isolation kit (Miltenyi Biotec, Germany) following manufacturer's instructions. Briefly, $2x10^7$ splenocytes were incubated with a cocktail of magnetic biotin-conjugated antibodies against non-CD8 T cells, washed, and passed through a MACS LS column placed on a MACS magnetic separator to deplete the magnetically labeled cells, followed by three rinses with MACS buffer. Untouched CD8 T cells were collected, washed, and counted. These purified CD8 T cells were re-suspended at $1x10^7$ cells/ml in PBS and incubated with 5μM final concentration of CFSE in PBS for 3 minutes at room temperature, mixed, and incubated for 4 more minutes. Fetal calf serum (Hyclone, Logan, UT) was added at a final 10% concentration, mixed, and incubated for 3 minutes, followed by addition of complete RPMI. CFSE labeled-CD8 T cells from Tg WT or Tg KO mice were re-suspended in PBS, and $5x10^5$ cells in 0.5 ml PBS were injected i.v. into naïve Thy1.2^{+} C57BL/6 recipient mice, followed by infection with $2x10^5$ PFU LCMV Armstrong i.p. the next day. Recipient mice were sacrificed at day 3 post-infection and splenocytes were

stained with anti-CD8 and anti-Thy1.1 antibodies, and CFSE intensity was measured by flow cytometry.

In vitro assays

Activation and proliferation: Spleen cells were isolated from ST6Gal-I$^{+/-}$ x P14 Tg^{+} Thy 1.1 and ST6Gal-I$^{-/-}$ x P14 Tg^{+} Thy 1.1 mice. 2x10^{5} spleen cells were incubated with 0.01ug/ml GP33-41 peptide in 96-well plates, in triplicate. Cells were harvested as indicated, fixed, and stained as previously described (Kalia et al., 2010).

Vaccinia plaque assay: Plaque assays were performed on homogenized ovaries using M2-10B4 cells, as previously described (Lutarewych et al., 1997).

Results

Dramatic changes in expression of the glycosyltransferase ST6Gal I during memory T cell differentiation

To examine glycosyltransferase gene expression during memory T cell differentiation, we used P14.Thy1.1 TCR transgenic CD8 T cells, specific for the GP33-41 peptide of the LCMV envelope glycoprotein and interrogated gene expression using the NIGMS Consortium for Glycomics (CFG) Glyco-chip that contains probe sets to ~1800 murine and human glycosylation-related genes. Naïve CD8 T cells were obtained directly from uninfected transgenic mice, while Ag-specific effector and memory populations were generated following adoptive transfer and infection of C57BL/6 Thy1.2 mice as previously described (Kaech et al., 2002). Isolation of CD8^{+}Thy1.1^{+} cells at various times post-infection yielded pure populations of T cells with the same TCR specificity undergoing progressive differentiation into memory cells. Gene expression profiles were analyzed and

the results are available online (http://www.functionalglycomics.org/). Of ~50 glycosylation-specific genes that showed changes in gene expression, several were glycosyltransferases. One glycosyltransferase, ST6Gal I, showed a greater than 20-fold reduction in expression comparing day 8 effector cells to naïve cells (Figure 4.1A). However, this expression increased during the transition from day 8 effector cells to day 100 memory cells, with memory cells showing an intermediate expression compared to naïve and effector cells (Figure 4.1B).

To analyze CD8 T cell surface expression of (Siaα2-6Gal) modifications, we used the elderberry bush derived lectin, *Sambucus nigra* agglutinin or SNA. FACs analysis revealed that changes in St6gal1 gene expression were accompanied by concomitant glyco-phenotypic changes in lectin binding (Figure 4.1B). Naïve CD8 T cells were uniformly SNA^{high}, while day 8 effector CD8 T cells were uniformly SNA^{low}. Interestingly, memory CD8 T cells were heterogeneous, with the population showing both SNA^{high} and SNA^{low} populations (Figure 4.1B).

We have previously demonstrated that unlike CD8 T cells, SNA binding remained uniformly high on naïve resting B cells, plasma cells (PC), and germinal center (GC) B cells following viral infection (Zeng et al., 2009). Our data supported previously published work analyzing terminal sialylation of N-linked glycans of B cells activated *in vitro* using MALDI-TOF mass spectrometry (Comelli et al., 2006). To query whether CD4 T cells also undergo glyco-phenotypic changes during activation and differentiation *in vivo* similar to CD8 T cells, we examined SNA binding of CD4 T cell populations following viral infection. As expected, naïve ($CD44^{low}$) CD4 T cells were also uniformly SNA^{high} similar to naïve CD8 T cells and resting B cells (Figure 4.1C). However, we discovered that at day 8 following LCMV infection, CD4 T cell populations diverged, showing unique glyco-phenotypic changes compared to other immune cell populations. Similar to GC B cells and plasma cells, $CXCR5^{+}$ T follicular helper cells at day 8 were SNA^{high} (Figure 4.1C). In contrast, the Ag-specific CD4 T cell population at day 8

was heterogeneous with both SNA^{high} and SNA^{low} GP61-80 specific CD4 T cells (Figure 4.1C). Memory Ag-specific CD4 T cells were mostly SNA^{high}, in contrast to CD8 memory T cells, which were heterogenous with mostly SNA^{low} (~70%), and a sub-population of SNA^{high} memory CD8 T cells. Overall, CD8, CD4, and B cell populations show unique patterns of SNA lectin binding following cell activation *in vivo*. Our observations of unique SNA-binding changes among Ag-specific CD4 T cell populations support and extend recent work showing that different T helper populations show differences in ST6Gal I expression and SNA binding (Toscano et al., 2007).

We further explored the heterogeneous nature of the memory CD8 T cell population by examining expression of other cell markers that have been shown to change during memory differentiation such as CD62L and 1B11, but found no correlative binding (unpublished data). We were unable to identify any other marker that uniquely identified these two subpopulations. To determine whether there were any functional differences between these two memory T cell subsets, we sorted memory CD8 T cell populations into SNA^{high} or SNA^{low} populations, adoptively transferred them into recipient mice, and infected these mice with LCMV clone 13 (Figure 4.1D). Serum and PBMCs were collected from each group, and viral titers and Ag-specific T cells were measured. While all groups of mice that received memory T cell populations cleared virus by day 15, mice that received SNA^{high} memory CD8 T cell populations showed faster kinetics of viral clearance and increased early proliferation compared to mice that received SNA^{low} memory populations (Figure 4.1E, 1F). These data suggested that ST6Gal I expression by CD8 T cells may promote faster viral-specific responses.

Impaired viral-specific responses in ST6Gal I-deficient mice

Since SNA^{high} memory CD8 T cells showed evidence of more rapid viral specific responses, we investigated viral specific T cell responses in ST6Gal $I^{-/-}$ mice.

ST6Gal I$^{-/-}$ mice were generated several years ago and show mostly normal T and B cell development, but display impaired T-dependent and T-independent humoral responses (Hennet et al., 1998; Zeng et al., 2009). Defective B cell responses in these mice can be rescued by genetic ablation of the Siaα2-6Gal specific mammalian lectin CD22, a negative regulator of BCR signaling (Collins et al., 2006; Grewal et al., 2006).

ST6Gal I$^{-/-}$ and C57BL/6 WT mice were infected with 2x10^5 pfu LCMV-Armstrong (Figure 4.2). We measured significant impairments in the generation of LCMV-specific CD8 T cell responses, LCMV-specific CD4 T cell responses, and LCMV-specific humoral responses in ST6Gal I$^{-/-}$ mice at day 8 (Figure 4.2A). When we examined Ag-specific CD8 T cells on day 8, we noted that several memory effector precursor (MPEC) markers were more highly expressed on CD8 T cells of ST6Gal I$^{-/-}$ mice, including CD127 (IL-7Rα) (Figure 4.2B). When we compared terminal effector or short-lived effector cell (SLEC) populations (KLRG1^{high}CD127^{low}), we noted that this population was significantly reduced in ST6Gal I$^{-/-}$ mice, whereas MPEC numbers were similar (Figure 4.2C). When we calculated the ratio of these populations at day 8, we found that 5-10% of the total day 8 CD8 T cells were memory precursors in WT mice, while in ST6Gal I$^{-/-}$ mice 40-45% of total day 8 CD8 T cells were memory precursors (Figure 4.2C). Consistent with the higher ratio of memory precursors, measurement of Ag-specific CD8 and CD4 T cell populations at memory revealed that memory T cell generation was not impaired in ST6Gal I$^{-/-}$ mice, despite reduced T cell expansion at day 8 (Figure 4.2D). Examination of functional memory by analysis of re-call responses following infection of immune WT and ST6Gal I$^{-/-}$ mice with recombinant Vaccinia expressing GP33 (VV-GP33) showed that ST6Gal I$^{-/-}$ mice generated similar numbers at day 3 of re-call and showed similar viral control (Figure 4.2E). Taken together, the loss of ST6Gal I significantly impaired early viral-specific T cell responses, however a greater proportion of the CD8 T cell response was programmed to become functional memory T cells.

T-bet regulates St6gal1 expression

Our discovery that terminal effector or SLEC expansion was reduced in ST6Gal I $^{-/-}$ mice (Figure 4.2C) prodded us to examine gene expression in effector subsets since our earlier studies analyzing total day 8 effectors potentially obscured differences in recently identified SLEC and MPEC subset populations (Joshi et al., 2007) (Figure 4.1). Comparison of KLRG1^{high}IL-7R^{low} (SLEC) to KLRG1^{low}IL-7R^{high} (MPEC) CD8 T cells at day 6-8 revealed that MPECs have higher expression of *St6gal1* (Figure 4.3A). However, this difference in expression may be due to greater down-regulation of *St6gal1* in SLEC. Since several transcriptional regulators have recently been identified as differentially expressed in effector subsets, and high levels of certain transcriptional regulators (eg. T-bet, Blimp-1) promote effector CD8 T cell terminal differentiation (Rutishauser and Kaech, 2010), we queried whether loss of T-bet expression influenced *St6gal1* expression.

T-bet expression increases dramatically upon activation of naive T cells, with higher expression in SLECs compared to MPECs (Kalia et al., 2010; Pipkin et al., 2010; Rutishauser and Kaech, 2010). Examination of T-bet$^{-/-}$ SLECs compared to MPECs revealed similar expression of *St6gal1* (Figure 4.3B left panel). Thus, *T-bet* expression was required for differential expression of *St6gal1* in SLEC versus MPEC populations. Further, comparing *St6gal1* expression in WT MPECs versus T-bet$^{-/-}$ MPECs, T-bet$^{-/-}$ memory precursors expressed ~12-fold higher *St6gal1*, while T-bet$^{-/-}$ SLEC expressed ~80-fold higher *St6gal1* compared to WT SLEC (Figure 4.3B middle and right panel). These data provided evidence that *T-bet* expression regulates the expression *St6gal1*, where loss of T-bet expression results in increased St6gal1 expression in effector subsets. However, we do not yet know if this repression by *T-bet* is direct or indirect, for example if *T-bet* transcriptionally repressed *St6gal1* expression.

Interestingly, day 8 T_{FH} cells remained SNA^{high} (Figure 4.1C) and this population of T cells has been shown to express *Bcl-6*, the mutually antagonistic transcriptional repressor of *Blimp-1* and *T-bet* (Johnston et al., 2009; Rutishauser and Kaech, 2010). ST6Gal $I^{-/-}$ mice showed more disorganized T cell zones in splenic B cell follicles at day 8 post-infection, with variably dispersed CD4 T cells (Figure 4.4).

Impaired CD8 T cell expansion is cell intrinsic

Since we observed reduced expansion of CD8 T cells in ST6Gal $I^{-/-}$ mice (Figure 2A), but also reductions in other viral-specific lymphocyte populations, such as CD4 T cells and B cells which influence CD8 T cell expansion (Crawford et al., 2006), we were unsure whether defective CD8 T cell expansion in these mice was cell autonomous. To understand if reduced expansion of CD8 T cells lacking ST6Gal I was due to cell intrinsic defects, we generated transgenic P14xST6Gal $I^{-/-}$ mice (Figure 4.5A). CD8 T cells from these transgenic mice were adoptively transferred into recipient C57BL/6 Thy1.2 mice and Ag-specific responses were evaluated. As shown in Figure 4.5B, we observed significantly reduced expansion at day 8 of Ag-specific CD8 T cells that lacked ST6Gal I, with a larger fraction of the endogenous/host response contributing to the DbGP33-41 CD8 specific response. To further examine this, we performed a competitive *in vivo* assay and adoptively transferred equal numbers of P14xST6Gal $I^{+/-}$ and P14xST6Gal $I^{-/-}$ CD8 T cells into the same C57BL/6.PL (Thy1.1) recipient mice (Figure 4.5C). As before, Ag-specific CD8 T cells that expressed ST6Gal I showed greater expansion at day 8, with significantly higher frequencies compared to CD8 T cells that did not express ST6Gal I. These data provided evidence that ST6Gal I expression by CD8 T cells was required for optimal CD8 T cell expansion *in vivo*.

These observations of reduced numbers of Ag-specific CD8 T cells at day 8 did not distinguish whether the reduced numbers of ST6Gal I$^{-/-}$ CD8 T cells were due to reduced proliferation or increased apoptosis *in vivo*. To determine whether reduced expansion was due to decreased proliferation, P14xST6Gal I$^{+/-}$ and P14xST6Gal I$^{-/-}$ CD8 T cells were purified and CFSE labeled. These labeled cells were then adoptively transferred into C57BL/6 recipient mice, and CFSE dilution was measured at day 3 post-infection with LCMV. As shown in Figure 4.5D, CD8 T cells that lacked expression of ST6Gal I, showed diminished proliferation, with a greater number of undivided CD8 T cells. Taken together, these data show that loss of ST6Gal I expression by CD8 T cells resulted in reduced expansion due to impaired CD8 T cell proliferation.

Similar recruitment and T cell activation, but delayed IL-2Rα expression of ST6Gal I$^{-/-}$ CD8 T cells

Since our data showed that ST6Gal I deficient CD8 T cells trailed in division of ST6Gal I expressing CD8 T cells following antigen exposure, we examined proliferation in more detail. We hypothesized that the reduced proliferation could be due to a delay in recruitment of ST6Gal I$^{-/-}$ CD8 T cells into the viral specific response. Loss of expression of ST6Gal I by CD8 T cells results in a reduction of sialylated biantennary N-glycans, and may lead to differential recognition of T cells by antigen-presenting cells expressing glycan binding proteins (GBPs) that recognize sialylated N-glycans (Comelli et al., 2006). Examples of GBPs that bind sialic acids include CD22 (aka siglec-2) and CD169 (aka siglec-1, sialoadhesin, or MOMA-1), which are expressed by B cells and marginal zone macrophages, respectively; both CD22+ B cells and CD169+ macrophages have been suggested to play a role in T cell activation (Collins et al., 2004; Junt et al., 2007; Oehen et al., 2002; Oetke et al., 2006; van den Berg et al., 1992). Since several studies have suggested that ST6Gal I expression by tumor cells influences cell motility and migration, we hypothesized that loss of ST6Gal I

expression was inhibiting interaction with CD169+ expressing marginal zone macrophages or other siglec-expressing APCs *in vivo*, leading to reduced recruitment of ST6Gal I$^{-/-}$ CD8 T cells into the immune response (Junt et al., 2007; Kumamoto et al., 2004; Qian et al., 2009). The magnitude of an adaptive immune response is regulated by the number of cells that are recruited from the naïve repertoire, and the burst size of participating clones (van Heijst et al., 2009). If recruitment of naïve CD8 T cells was impaired by the loss of ST6Gal I, this would be reflected in a reduced percentage of transferred T cells becoming initially activated.

We examined early T cell activation *in vivo*. Here we adoptively transferred P14xST6Gal I$^{+/-}$ versus P14xST6Gal I$^{-/-}$ CD8 T cells into WT recipient mice, monitored CD8 T cell expansion and surface expression during the first hours and days of viral infection, and focused on early activation markers CD69 and CD25. CD69 expression comes up rapidly on T cells following TCR stimulation, while expression of CD25, the α chain of the high affinity IL-2R, is regulated both by TCR signaling and IL-2/IL-2R signaling via STAT5 (Malek TR, 2008). We included analysis of the IL-2R because of its pivotal role in T cell proliferation, its recently recognized role in memory T cell programming, and evidence that this receptor is a substrate for ST6Gal I (Leonard et al., 1983; Malek et al., 1995). As shown in Figure 4.6A, by day 5 Ag-specific CD8 T cells expressing ST6Gal I have increased ~700-fold, and consistent with earlier data, Ag-specific CD8 T cells lacking expression of ST6Gal I show significantly less expansion. However, when we examined T cell activation and recruitment into the immune response, we observed that in the first 12 hours, activation of the transferred CD8 T cells occurred similarly, with identical kinetics for CD69 and CD25 (Figure 4.6B, C left panels). By 24 hours post-infection, CD69 expression is high on all transferred CD8 T cells regardless of expression of ST6Gal I (Figure 4.6B). Similar results were seen analyzing CD44 and CD62L (unpublished data). This data provided

strong evidence that recruitment and activation of ST6Gal I$^{-/-}$ Ag-specific CD8 T cells was not impaired. However, examination of CD25 expression revealed that surface expression of the IL-2Rα chain was delayed from 12-24 hrs in Ag-specific CD8 T cells that did not express ST6Gal I (Figure 4.6C, right panel). Thus, these data suggested that ST6Gal I expression by naïve CD8 T cells promoted rapid and prolonged IL-2Rα expression, which would contribute to early and more extensive proliferation of terminal effectors (Kalia et al., 2010).

IL-2/IL-2R signaling and surface expression is impaired in ST6Gal I$^{-/-}$ CD8 T cells

CD25 (IL-2Rα) expression is regulated by signals through both the TCR and the IL-2R, so defects in either TCR signaling, IL-2R signaling, or both, may contribute to impaired surface expression of this receptor chain. We observed no differences in TCR stimulation *in vivo* comparing ST6Gal I-expressing and ST6Gal I-deficient Ag-specific CD8 T cells during the first 24 hours of viral infection (Figure 4.6B). CD25 expression was similar in the initial 12 hours of viral infection, but was different in the ensuing 12-24 hours post-infection (Figure 4.6C). Previous reports have demonstrated that IL-2 splenic concentrations peak within the first day of LCMV infection (Kalia et al., 2010). Based on these data, we formulated a new hypothesis where we considered TCR signaling resulted in normal CD25 expression by ST6Gal I$^{-/-}$ CD8 T cells, however IL-2/IL-2R signaling was impaired, resulting in diminished CD25 expression.

To test this, we examined *in vitro* proliferation of P14xST6Gal I$^{+/-}$ versus P14xST6Gal I$^{-/-}$ CD8 T cells following GP33-41 peptide stimulation (Figure 4.7A). Cell clusters were smaller in P14xST6Gal I$^{-/-}$ CD8 T and we confirmed our observation of reduced proliferation of these cells (Figure 4.7A). Peptide stimulated Ag-specific CD8 T cells made similar amounts of IL-2, TNFa, and IFNg, similar to results we found *in vivo* (unpublished data). Cell viability dropped

significantly during the first day of *in vitro* culture of both WT and ST6Gal $I^{-/-}$ CD8 T cells, and ST6Gal $I^{-/-}$ CD8 T cells showing significantly reduced viability (Figure 4.7B).

We then examined early activation, comparing expression of CD25 and phosphorylated STAT5 (pSTAT5). We stimulated P14xST6Gal $I^{+/-}$ or P14xST6Gal $I^{-/-}$ CD8 T with GP33-41 peptide and IL-2, or IL-2 only. Addition of IL-2 to the culture conditions significantly increased viability of both WT and ST6Gal $I^{-/-}$ CD8 T cells and was dose-dependent (unpublished data). As shown in Figure 7C, in the presence of GP33-41 peptide, both P14xST6Gal $I^{+/-}$ and P14xST6Gal $I^{-/-}$ CD8 T showed similarly high percentages of $CD25^{high}$ cells, although total MFI was reduced for ST6Gal $I^{-/-}$ CD8 T cells. ST6Gal $I^{-/-}$ CD8 T cells showed no difference in pSTAT5 following peptide stimulation (Figure 4.7D). CD8 T cells cultured with IL-2 only showed lower expression of CD25 compared to peptide stimulated cells (Figure 4.7C). However, analysis of ST6Gal $I^{-/-}$ CD8 T cells revealed that these cells had fewer $CD25^{high}$ cells and lower pSTAT5 compared to ST6Gal $I^{+/-}$ CD8 T cells (Figure 4.7C-D). These data provided evidence that IL-2/IL-2R signaling was impaired in ST6Gal $I^{-/-}$ CD8 T cells, inhibiting IL-2Rα expression.

Taken together, our data suggests that CD8 T cells regulate ST6Gal I to promote expression of IL-2Rα following IL-2/IL-2R signaling, leading to more rapid expression of the high affinity IL-2 receptor on Ag-specific CD8 T cells. This earlier and prolonged expression of IL-2Rα by naïve CD8 T cells appears to favor proliferation and differentiation of short-lived effectors. Our data provides the first evidence that a specific carbohydrate modification, the addition of α2,6-linked N-glycans, appears to fine-tune responses through the IL-2R, thus amplifying early T cell expansion and influencing cell fate differentiation.

Discussion

Essentially all mammalian cells are covered with a dense, complex array of oligosaccharides or sugars termed the glycocalyx, through which the cell interacts with its environment (Varki, 2008). Many cell surface glycoprotein receptors have significant numbers of N-glycan sites, and recent work has shown that both the complexity and numbers of N-glycans can regulate cell proliferation and differentiation (Lau et al., 2007). Sialic acids are typically found on the outermost end of glycan chains, and given their wide distribution, can modulate a variety of normal and pathological processes (Varki, 2008). N-linked sialylation in particular, has been suggested to play a significant role in tumor biology, modulating growth and differentiation of carcinomas (Hedlund et al., 2008).

Following T cell activation *in vivo*, T cells undergo an exponential growth phase, characterized by gene expression changes and glyco-phenotypic changes (Kaech et al., 2002; Murali-Krishna et al., 1998; Onami et al., 2002). These cells differentiate into effector cells, and a subset become memory T cells (Joshi et al., 2007). We discovered using a microarray analysis that ST6Gal I, sialyltransferase expressed in the Golgi that is responsible for α2,6-sialylation on N-glycans, was differentially expressed during memory CD8 T cell differentiation and showed concomitant changes in surface SNA lectin binding (Figure 4.1). Moreover, we found that T cells expressing *St6gal1* showed more proliferative capacity, while those lacking *St6gal1* expression divided less and showed slower growth (Figures 4.2 and 4.5). *T-bet* repressed expression of *St6gal1*, and lower expression of *St6gal1* was observed in terminally differentiated effector populations, or SLECs (Figure 4.3). Interestingly, tumors that lacked expression of *St6gal1* also showed more terminal differentiation (Hedlund et al., 2008). In contrast, memory precursor and memory T cells, which retain their stem cell-like proliferative capacity, have higher expression of *St6gal1* compared to effector T cells (Figure 4.1 and 4.3). Similarly, tumors expressing *St6gal1* are less

differentiated and increased *St6gal1* expression correlated with poor prognosis (Hedlund et al., 2008).

IL-2 is tightly regulated due to its potent stimulatory properties, and is typically produced by recently activated T cells, acting in an autocrine or paracrine fashion (Letourneau et al., 2010). CD25 has recently been suggested to play an unanticipated role in the regulation of IL-2 homeostasis (Letourneau et al., 2010). Most IL-2 production *in vivo* occurs in secondary lymphoid organs and evidence suggests it is likely consumed there by proliferating CD25/IL-2Rα^+ T cells (Letourneau et al., 2010). Prolonged CD25/IL-2Rα expression on virus-specific CD8 T cells has been shown to favor the differentiation of terminal effectors (Kalia et al., 2010; Pipkin et al., 2010). CD25^{high} CD8 T cells show more extensive early proliferation *in vivo*, while CD8 T cells with lower expression of CD25 are relatively less sensitive to IL-2, and give rise to long-lived memory cells (Kalia et al., 2010). In ST6Gal I$^{-/-}$ mice, we observed that expansion of SLECs was compromised, while memory precursor development was enhanced (Figure 4.2). CD25/IL-2Ra expression was delayed on ST6Gal I$^{-/-}$ CD8 T cells and we present evidence that the delay in surface expression of the high affinity IL-2Rα on activated ST6Gal I$^{-/-}$ CD8 T cells was likely attributable to defective IL-2/IL-2R induced expression of IL-2Ra (Figure 4.6 and 4.7). Thus, early proliferation was reduced. However, a greater proportion of the ST6Gal I$^{-/-}$ CD8 T cell effector population was memory precursors (Figure 4.2). Thus, despite lower overall CD8 T cell expansion, function and number of memory T cells was comparable in ST6Gal I$^{-/-}$ mice. Thus *St6gal1* expression is not required for memory T cell differentiation, but is required for optimal proliferation of terminally differentiated effectors or SLECs.

St6gal1 expression is significantly down-regulated following activation of CD8 T cell populations compared to naïve CD8 T cells, and we speculate based on our data that for naïve CD8 T cells, the function of high *St6gal1* expression is to

amplify signals through the IL-2 receptor, promoting greater proliferation. In contrast, activated CD8 T cells may limit this amplification of IL-2 signals by reducing expression of this sialyltransferase and consequently altering N-linked sialylation of ST6Gal I glycoprotein substrates. The α and β chains of IL-2R have been shown to be N-glycosylated and sialylated, and changes in glycosylation may change competition for this cytokine receptor in its heterodimeric ($\beta\gamma$) or heterotrimeric ($\alpha\beta\gamma$) forms (Asao et al., 1990; Leonard et al., 1983; Opdenakker et al., 1995). Glycosylation of cytokines or cytokine receptors influences specific biological activities, with several studies asserting that glycosylation attenuates cytokine activity (Opdenakker et al., 1995). Since recent work suggests that sustained IL-2R signaling drives terminal effector differentiation, the reduction in *St6gal1* expression may limit these signals, switching to the promotion of functional long-lived memory differentiation. These memory precursors may undergo less proliferation compared to their shorter-lived counterparts.

REFERENCES

Asao, H., T. Takeshita, M. Nakamura, K. Nagata, and K. Sugamura. 1990. The evidence for the IL-2 receptor beta chain processing from p70 to p75. *Int Immunol* 2:469-72.

Christie, D.R., F.M. Shaikh, J.A.t. Lucas, J.A. Lucas, 3rd, and S.L. Bellis. 2008. ST6Gal-I expression in ovarian cancer cells promotes an invasive phenotype by altering integrin glycosylation and function. *J Ovarian Res* 1:3.

Collins, B.E., O. Blixt, A.R. DeSieno, N. Bovin, J.D. Marth, and J.C. Paulson. 2004. Masking of CD22 by cis ligands does not prevent redistribution of CD22 to sites of cell contact. *Proc Natl Acad Sci U S A* 101:6104-9.

Collins, B.E., B.A. Smith, P. Bengtson, and J.C. Paulson. 2006. Ablation of CD22 in ligand-deficient mice restores B cell receptor signaling. *Nat Immunol* 7:199-206.

Comelli, E.M., M. Sutton-Smith, Q. Yan, M. Amado, M. Panico, T. Gilmartin, T. Whisenant, C.M. Lanigan, S.R. Head, D. Goldberg, H.R. Morris, A. Dell, and J.C. Paulson. 2006. Activation of murine CD4+ and CD8+ T lymphocytes leads to dramatic remodeling of N-linked glycans. *J Immunol* 177:2431-40.

Crawford, A., M. Macleod, T. Schumacher, L. Corlett, and D. Gray. 2006. Primary T cell expansion and differentiation in vivo requires antigen presentation by B cells. *J Immunol* 176:3498-506.

Dall'Olio, F., M. Chiricolo, A. D'Errico, E. Gruppioni, A. Altimari, M. Fiorentino, and W.F. Grigioni. 2004. Expression of beta-galactoside alpha2,6 sialyltransferase and of alpha2,6-sialylated glycoconjugates in normal human liver, hepatocarcinoma, and cirrhosis. *Glycobiology* 14:39-49.

Galvan, M., K. Murali-Krishna, L.L. Ming, L. Baum, and R. Ahmed. 1998. Alterations in cell surface carbohydrates on T cells from virally infected mice can distinguish effector/memory CD8+ T cells from naive cells. *J Immunol* 161:641-8.

Grewal, P.K., M. Boton, K. Ramirez, B.E. Collins, A. Saito, R.S. Green, K. Ohtsubo, D. Chui, and J.D. Marth. 2006. ST6Gal-I restrains CD22-dependent antigen receptor endocytosis and Shp-1 recruitment in normal and pathogenic immune signaling. *Mol Cell Biol* 26:4970-81.

Harp, J.R., and T.M. Onami. 2010. Naive T cells re-distribute to the lungs of selectin ligand deficient mice. *PLoS One* 5:e10973.

Harrington, L.E., M. Galvan, L.G. Baum, J.D. Altman, and R. Ahmed. 2000. Differentiating between memory and effector CD8 T cells by altered expression of cell surface O-glycans. *J Exp Med* 191:1241-6.

Harrington, L.E., R. Most Rv, J.L. Whitton, and R. Ahmed. 2002. Recombinant vaccinia virus-induced T-cell immunity: quantitation of the response to the virus vector and the foreign epitope. *J Virol* 76:3329-37.

Hedlund, M., E. Ng, A. Varki, and N.M. Varki. 2008. alpha 2-6-Linked sialic acids on N-glycans modulate carcinoma differentiation in vivo. *Cancer Res* 68:388-94.

Hennet, T., D. Chui, J.C. Paulson, and J.D. Marth. 1998. Immune regulation by the ST6Gal sialyltransferase. *Proc Natl Acad Sci U S A* 95:4504-9.

Johnston, R.J., A.C. Poholek, D. DiToro, I. Yusuf, D. Eto, B. Barnett, A.L. Dent, J. Craft, and S. Crotty. 2009. Bcl6 and Blimp-1 are reciprocal and antagonistic regulators of T follicular helper cell differentiation. *Science* 325:1006-10.

Joshi, N.S., W. Cui, A. Chandele, H.K. Lee, D.R. Urso, J. Hagman, L. Gapin, and S.M. Kaech. 2007. Inflammation directs memory precursor and short-lived effector CD8(+) T cell fates via the graded expression of T-bet transcription factor. *Immunity* 27:281-95.

Junt, T., E.A. Moseman, M. Iannacone, S. Massberg, P.A. Lang, M. Boes, K. Fink, S.E. Henrickson, D.M. Shayakhmetov, N.C. Di Paolo, N. van Rooijen, T.R. Mempel, S.P. Whelan, and U.H. von Andrian. 2007. Subcapsular sinus macrophages in lymph nodes clear lymph-borne viruses and present them to antiviral B cells. *Nature* 450:110-4.

Kaech, S.M., S. Hemby, E. Kersh, and R. Ahmed. 2002. Molecular and functional profiling of memory CD8 T cell differentiation. *Cell* 111:837-51.

Kaech, S.M., and E.J. Wherry. 2007. Heterogeneity and cell-fate decisions in effector and memory CD8+ T cell differentiation during viral infection. *Immunity* 27:393-405.

Kalia, V., S. Sarkar, S. Subramaniam, W.N. Haining, K.A. Smith, and R. Ahmed. 2010. Prolonged interleukin-2Ralpha expression on virus-specific CD8+ T cells favors terminal-effector differentiation in vivo. *Immunity* 32:91-103.

Kumamoto, Y., N. Higashi, K. Denda-Nagai, M. Tsuiji, K. Sato, P.R. Crocker, and T. Irimura. 2004. Identification of sialoadhesin as a dominant lymph node counter-receptor for mouse macrophage galactose-type C-type lectin 1. *J Biol Chem* 279:49274-80.

Lau, K.S., E.A. Partridge, A. Grigorian, C.I. Silvescu, V.N. Reinhold, M. Demetriou, and J.W. Dennis. 2007. Complex N-glycan number and degree of branching cooperate to regulate cell proliferation and differentiation. *Cell* 129:123-34.

Leonard, W.J., J.M. Depper, R.J. Robb, T.A. Waldmann, and W.C. Greene. 1983. Characterization of the human receptor for T-cell growth factor. *Proc Natl Acad Sci U S A* 80:6957-61.

Letourneau, S., E.M. van Leeuwen, C. Krieg, C. Martin, G. Pantaleo, J. Sprent, C.D. Surh, and O. Boyman. 2010. IL-2/anti-IL-2 antibody complexes show strong biological activity by avoiding interaction with IL-2 receptor alpha subunit CD25. *Proc Natl Acad Sci U S A* 107:2171-6.

London, J., S. Berrih, and J.F. Bach. 1978. Peanut agglutinin. I. A new tool for studying T lymphocyte subpopulations. *J Immunol* 121:438-43.

London, J., and M.A. Horton. 1980. Peanut agglutinin. V. Thymocyte subpopulations in the mouse studied with peanut agglutinin and Ly-6.2 antiserum. *J Immunol* 124:1803-7.

Lowe, J.B. 2003. Glycan-dependent leukocyte adhesion and recruitment in inflammation. *Curr Opin Cell Biol* 15:531-8.

Luhn, K., M.K. Wild, M. Eckhardt, R. Gerardy-Schahn, and D. Vestweber. 2001. The gene defective in leukocyte adhesion deficiency II encodes a putative GDP-fucose transporter. *Nat Genet* 28:69-72.

Lutarewych, M.A., M.R. Quirk, B.A. Kringstad, W. Li, C.M. Verfaillie, and M.C. Jordan. 1997. Propagation and titration of murine cytomegalovirus in a continuous bone marrow-derived stromal cell line (M2-10B4). *J Virol Methods* 68:193-8.

Malek, T.R. 2008. The biology of interleukin-2. *Annu Rev Immunol* 26:453-79.

Malek, T.R., R.K. Furse, M.L. Fleming, A.J. Fadell, and Y.W. He. 1995. Biochemical identity and characterization of the mouse interleukin-2 receptor beta and gamma c subunits. *J Interferon Cytokine Res* 15:447-54.

Murali-Krishna, K., J.D. Altman, M. Suresh, D.J. Sourdive, A.J. Zajac, J.D. Miller, J. Slansky, and R. Ahmed. 1998. Counting antigen-specific CD8 T cells: a reevaluation of bystander activation during viral infection. *Immunity* 8:177-87.

Oehen, S., B. Odermatt, U. Karrer, H. Hengartner, R. Zinkernagel, and C. Lopez-Macias. 2002. Marginal zone macrophages and immune responses against viruses. *J Immunol* 169:1453-8.

Oetke, C., G. Kraal, and P.R. Crocker. 2006. The antigen recognized by MOMA-I is sialoadhesin. *Immunol Lett* 106:96-8.

Onami, T.M., L.E. Harrington, M.A. Williams, M. Galvan, C.P. Larsen, T.C. Pearson, N. Manjunath, L.G. Baum, B.D. Pearce, and R. Ahmed. 2002. Dynamic regulation of T cell immunity by CD43. *J Immunol* 168:6022-31.

Opdenakker, G., P.M. Rudd, M. Wormald, R.A. Dwek, and J. Van Damme. 1995. Cells regulate the activities of cytokines by glycosylation. *Faseb J* 9:453-7.

Pipkin, M.E., J.A. Sacks, F. Cruz-Guilloty, M.G. Lichtenheld, M.J. Bevan, and A. Rao. 2010. Interleukin-2 and inflammation induce distinct transcriptional programs that promote the differentiation of effector cytolytic T cells. *Immunity* 32:79-90.

Priatel, J.J., D. Chui, N. Hiraoka, C.J. Simmons, K.B. Richardson, D.M. Page, M. Fukuda, N.M. Varki, and J.D. Marth. 2000. The ST3Gal-I sialyltransferase controls CD8+ T lymphocyte homeostasis by modulating O-glycan biosynthesis. *Immunity* 12:273-83.

Qian, J., C.H. Zhu, S. Tang, A.J. Shen, J. Ai, J. Li, M.Y. Geng, and J. Ding. 2009. alpha2,6-hyposialylation of c-Met abolishes cell motility of ST6Gal-I-knockdown HCT116 cells. *Acta Pharmacol Sin* 30:1039-45.

Rose, M.L., M.S. Birbeck, V.J. Wallis, J.A. Forrester, and A.J. Davies. 1980. Peanut lectin binding properties of germinal centres of mouse lymphoid tissue. *Nature* 284:364-6.

Rose, M.L., J.A. Habeshaw, R. Kennedy, J. Sloane, E. Wiltshaw, and A.J. Davies. 1981. Binding of peanut lectin to germinal-centre cells: a marker for B-cell subsets of follicular lymphoma? *Br J Cancer* 44:68-74.

Rutishauser, R.L., and S.M. Kaech. 2010. Generating diversity: transcriptional regulation of effector and memory CD8 T-cell differentiation. *Immunol Rev* 235:219-33.

Seales, E.C., G.A. Jurado, B.A. Brunson, J.K. Wakefield, A.R. Frost, and S.L. Bellis. 2005. Hypersialylation of beta1 integrins, observed in colon adenocarcinoma, may contribute to cancer progression by up-regulating cell motility. *Cancer Res* 65:4645-52.

Suvas, P.K., H.M. Dech, F. Sambira, J. Zeng, and T.M. Onami. 2007. Systemic and mucosal infection program protective memory CD8 T cells in the vaginal mucosa. *J Immunol* 179:8122-7.

Toscano, M.A., G.A. Bianco, J.M. Ilarregui, D.O. Croci, J. Correale, J.D. Hernandez, N.W. Zwirner, F. Poirier, E.M. Riley, L.G. Baum, and G.A. Rabinovich. 2007. Differential glycosylation of TH1, TH2 and TH-17 effector cells selectively regulates susceptibility to cell death. *Nat Immunol* 8:825-34.

van den Berg, T.K., J.J. Breve, J.G. Damoiseaux, E.A. Dopp, S. Kelm, P.R. Crocker, C.D. Dijkstra, and G. Kraal. 1992. Sialoadhesin on macrophages:

its identification as a lymphocyte adhesion molecule. *J Exp Med* 176:647-55.

van Heijst, J.W., C. Gerlach, E. Swart, D. Sie, C. Nunes-Alves, R.M. Kerkhoven, R. Arens, M. Correia-Neves, K. Schepers, and T.N. Schumacher. 2009. Recruitment of antigen-specific CD8+ T cells in response to infection is markedly efficient. *Science* 325:1265-9.

Varki, A. 2008. Sialic acids in human health and disease. *Trends Mol Med* 14:351-60.

Vazquez-Martin, C., E. Gil-Martin, and A. Fernandez-Briera. 2005. Elevation of ST6Gal I activity in malignant and transitional tissue in human colorectal cancer. *Oncology* 69:436-44.

Wang, P.H., Y.F. Li, C.M. Juang, Y.R. Lee, H.T. Chao, H.T. Ng, Y.C. Tsai, and C.C. Yuan. 2002. Expression of sialyltransferase family members in cervix squamous cell carcinoma correlates with lymph node metastasis. *Gynecol Oncol* 86:45-52.

Zeng, J., H.M. Joo, B. Rajini, J.P. Wrammert, M.Y. Sangster, and T.M. Onami. 2009. The generation of influenza-specific humoral responses is impaired in ST6Gal I-deficient mice. *J Immunol* 182:4721-7.

Appendix

Figure 4. 1. Dramatic changes in expression of the glycosyltransferase ST6Gal I during memory T cell differentiation.

$1x10^6$ Thy1.1$^+$ D^bGP_{33-41} specific transgenic splenocytes were adoptively transferred into C57BL/6 mice and these mice were infected with $2x10^5$ pfu LCMV Armstrong i.p. CD8 T cell populations were then enriched from splenocytes from naïve transgenic mice (day 0) or day 8, day 15, day 22, or day 100 post-infection chimeric mice by depletion with MHC class II and CD4 beads. Thy1.1$^+$ CD8$^+$ T cells were then FACS sorted to greater than 94% purity and mRNA was isolated and linearly amplified and assayed by the Glyco-Gene chip. *A,* Summary of fold change of specific genes expression in CD8 T cell at day 8 compared to those in naïve CD8 T cell. The function of ST6Gal I is to catalyze the addition of α2,6 sialic acids to galactose. SNA lectin binds α2,6Galβ1-4GlcNAc. B, Time-course of ST6Gal I gene expression during CD8 T cell activation *in vivo* shows dramatically reduced expression. Right panel showed the SNA lectin binding of CD8 T cell populations. Splenocytes from uninfected (naïve) Tg P14 mice, or P14 x Thy1.1 chimeras on day 8 or day 150 post-infection with $2x10^5$ pfu LCMV-Armstrong i.p. were stained with DbGP33-41 tetramer, CD8 mAb, and SNA lectin. Gating on antigen-specific CD8 T cells reveals high staining of SNA on naïve CD8 T cells (SNA^{high}), low binding on day 8 effector CD8 T cells (SNA^{low}), and both populations among memory cells, SNA^{high} and SNA^{low}. C, SNA lectin bingding of CD4 T cell populations. Splenocytes from uninfected (naïve) mice, or C57BL/6 mice on day 8 or day 200 post-infection with $2x10^5$ pfu LCMV-Armstrong i.p. were harvested and stimulated with GP61-80 for 4-5 hours, stained with CD44, or CXCR5, or IFNγ, CD4 mAb, and SNA lectin. D, Cartoons showing experimental procedure of recall responses of SNA^{high} versus SNA^{low} binding memory CD8 T cells. Memory Thy1.1$^+$ CD8$^+$ T cells were sorted for SNA^{high} versus SNA^{low} binding (greater than 95% purity, not shown) and equal numbers of SNA^{high}, SNA^{low}, or total antigen-specific CD8 T cells were adoptively transferred into naïve C57BL/6 mice and

mice were infected with $2x10^6$ pfu LCMV clone 13 i.v. Control mice received no cells. On indicated days, mice were bled to obtain serum to assay viremia and PBMCs to assay T cell expansion. On day 5 and day 8, mice that received SNA^{high} memory CD8 T cells showed lower viremia. E, Higher T cell expansion compared to mice receiving SNA^{low} memory CD8 T cells.

A

Fold Change N/E	Common Name	Description
-21.11	**ST6Gal I**	Glycan transferase, α2,6-sialyltransferase
-45.25	L-Selectin	C-Type lectin, leukocyte selectin CD62L
-1.23	Gal T	Glycan transferase, α1,3-galactosyltransferase
+3.48	ST3Gal IV	Glycan transferase, α2,3-sialyltansferase
+6.96	ST3Gal VI	Glycan transferase, α2,3-sialyltansferase
+3.73	CD44	Proteoglycan, extracellular matrix binding protein

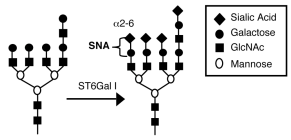

B

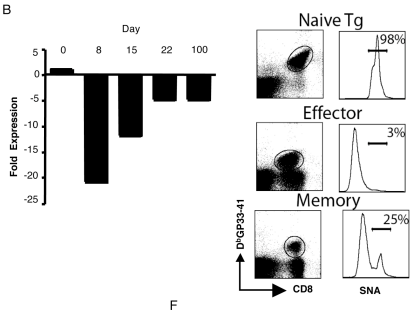

C

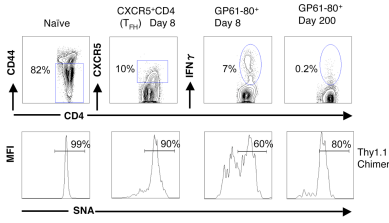

D

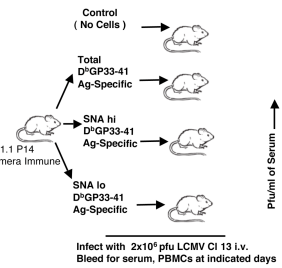

E

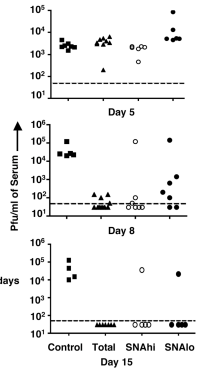

F

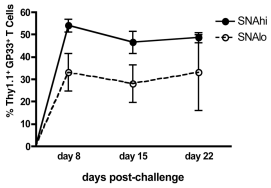

Figure 4. 2. Impaired viral-specific responses in ST6Gal I-deficient mice.
C57BL/6 wildtype or ST6Gal I null mice were infected with $2x10^5$ pfu LCMV Armstrong i.p. Single cell suspensions of the spleen were processed and stained with antibodies as indicated, plasma cells gating on $CD138^+B220^+$cells, germinal center (GC) B cells gating on PNA^{high} Fas^+ cell population of gated $IgD^{low}B220^+$ cells. ELISPOT assay was used to determine the numbers of LCMV-specific IgM and IgG ASCs. On day 8 p.i. A, Total numbers of T and B cells as indicated were enumerated. B, Histogram overlay of indicated antibodies binding of $DbGP_{33-41}CD8^+$ T cells. Blue histogram shows B6, and red histogram shows ST6Gal $I^{-/-}$. Bar graphs show mean fluorescence of indicated antibodies binding in both groups of mice. C. FACS analysis of SLEC and MPEC in same mice. Contour dot plot shows SLEC ($KLRG1^{high}$ $IL7^{low}$) and MPEC ($KLRG1^{low}$ $IL\text{-}7^{high}$) populations. Total numbers of SLEC and MPEC and their ratios were enumerated in bar graphs. D, Kinetics of total numbers of antigen-specific CD8 and CD4 T cells measured by FACS or ICS on indicated days. E, total numbers of antigen-specific CD8 T cell in Memory and recall response. Viral titer in the ovaries on day 3 mice challenged intravenously with 2×10^6 PFU vaccinia expressing the GP33-41 peptide of the LCMV viral protein. Grey bar shows naïve mice; black bars are i.p. B6; and white bars are i.p. ST6Gal $I^{-/-}$. Data from n=6-12 mice.

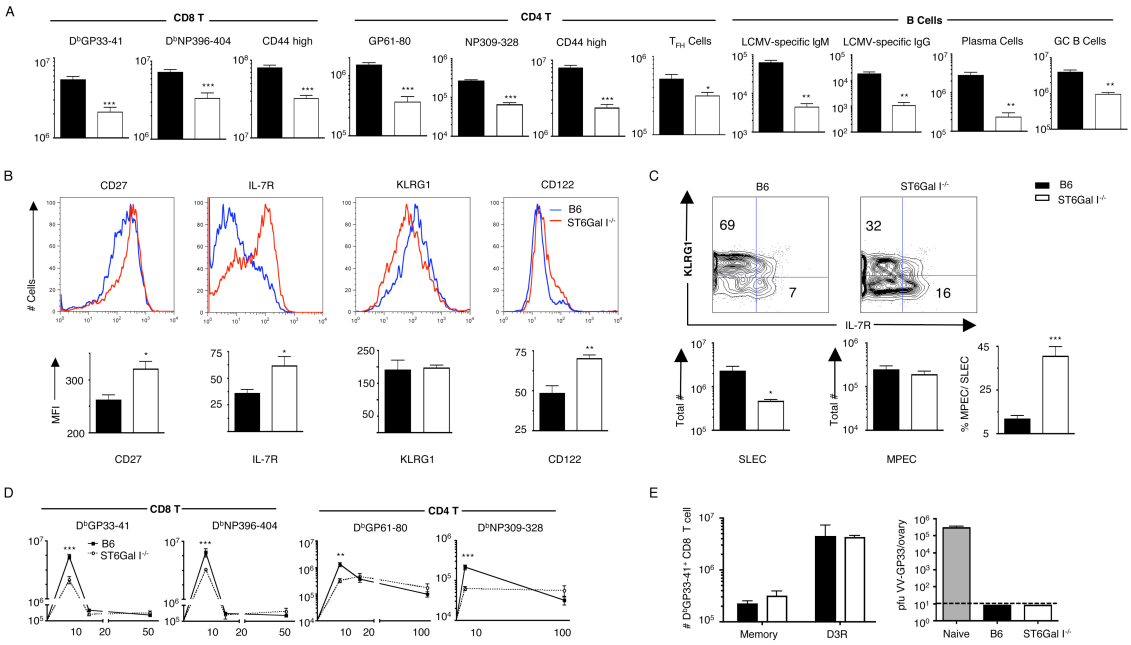
A
CD8 T
CD4 T
B Cells
DbGP33-41
DbNP396-404
CD44 high
GP61-80
NP309-328
CD44 high
TFH Cells
LCMV-specific IgM
LCMV-specific IgG
Plasma Cells
GC B Cells
B
CD27
IL-7R
KLRG1
CD122
B6
ST6Gal I-/-
Cells
MFI
C
B6
ST6Gal I-/-
KLRG1
IL-7R
69
7
32
16
Total #
SLEC
MPEC
% MPEC/ SLEC
D
CD8 T
CD4 T
DbGP33-41
DbNP396-404
DbGP61-80
DbNP309-328
B6
ST6Gal I-/-
E
DbGP33-41+ CD8 T cell
Memory
D3R
pfu VV-GP33/ovary
Naive
B6
ST6Gal I-/-

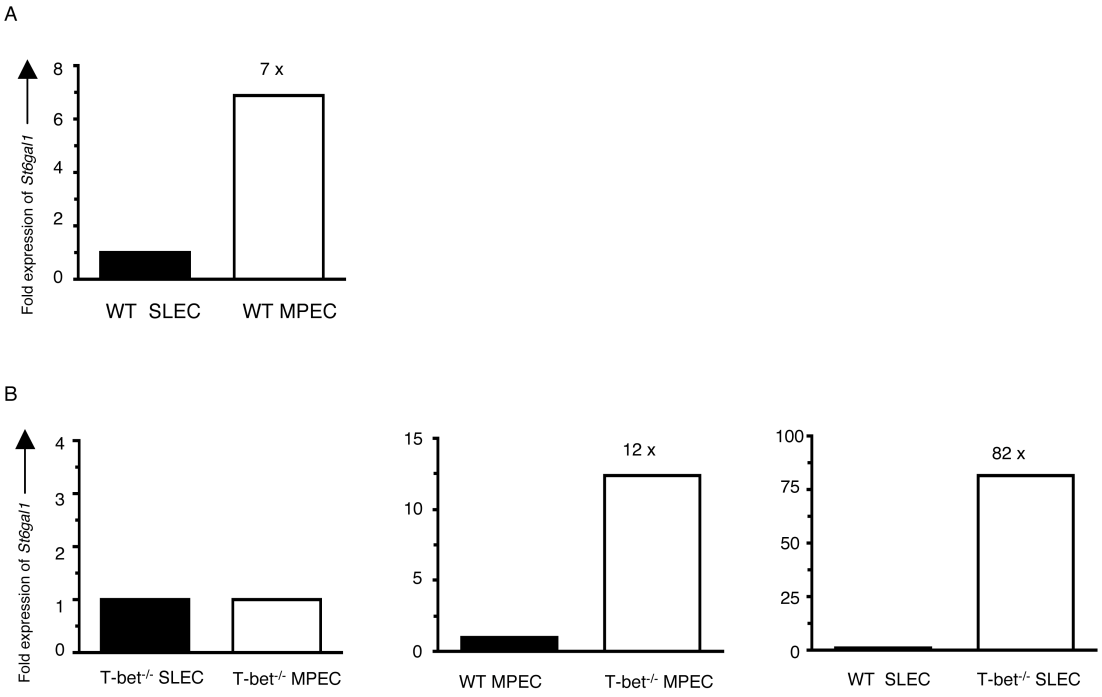

Figure 4. 3. T-bet regulates *St6gal1* expression.

Gene expression analysis was performed on day 6 and 8 p.i. with LCMV Armstrong pooled WT and T-bet null effector cells gating on $CD8^+$ and tetramer D^bGP_{33-41} population by microarray. Fold change of *St6gal1* expression in WT MPEC compared to that in WT SLEC (A). From left to right: T-bet$^{-/-}$ SLEC compared to T-bet$^{-/-}$MPEC, T-bet$^{-/-}$ MPEC to WT MPEC, and T-bet$^{-/-}$ SLEC to WT SLEC (B).

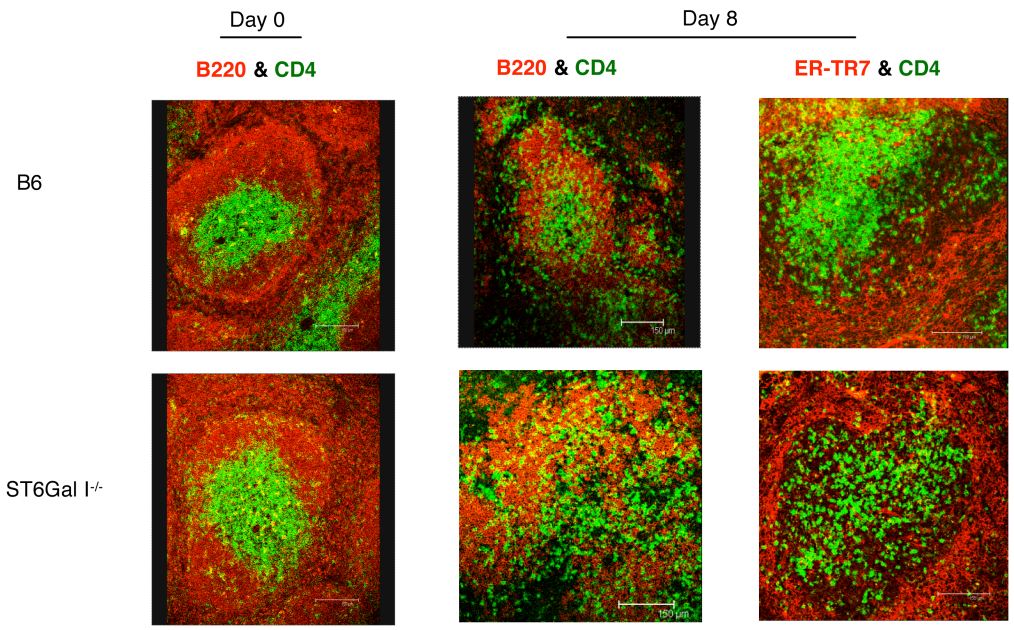

Figure 4. 4. Disrupted B cell follicle in ST6Gal I null mice following LCMV infection.

Mice were infected with LCMV intraperitoneally or remained uninfected, and on day 8 p.i., spleens were isolated and frozen for immunofluorescence staining using B cell follicle marker. B220 in red and CD4 or ER-TR7 in green.

Figure 4. 5. Impaired CD8 T cell expansion is cell intrinsic.

P14 TCR transgenic mice congenic for Thy1.1 were bred to ST6Gal I null mice. *A*, Dot plot of splenocytes from ST6Gal $I^{+/-}$xP14 and ST6Gal $I^{-/-}$xP14 littermates labeled with CD8, DbGP33-41 MHC tetramer, and SNA lectin. $1x10^6$ splenocytes from WT and ST6Gal $I^{-/-}$ TCR transgenic splenocytes were singly-(B) or mixed in a 1:1 ratio and co-transferred (C) into non-transgenic naïve C57BL/6 mice by tail i.v. injection and the recipient mice were infected with LCMV Armstrong the following day. At day 8 p.i., total number of transferred (donor) cells were quantified in the spleens of recipient mice by flow cytometry. Bar graphs show n=7 for WT and n=11 for KO for single transfer (middle panel) and n=5 fo WT and n=5 for KO for co-transfer (lower panel) D, $5x10^5$ WT and ST6Gal $I^{-/-}$ TCR trangenic CD8 T cells were purified and labeled with CFSE and transferred into recipient C57BL/6 non-transgenic mice by tail i.v. injection. The following day, the recipient mice were infected with $2x10^5$ pfu LCMV Armstrong i.p. or left uninfected. On day 3 p.i. CFSE intensity of LCMV antigen-specific CD8 T cells was quantitated by flow cytometry. Bar graphs represent n=5 for WT and n=6 for KO.

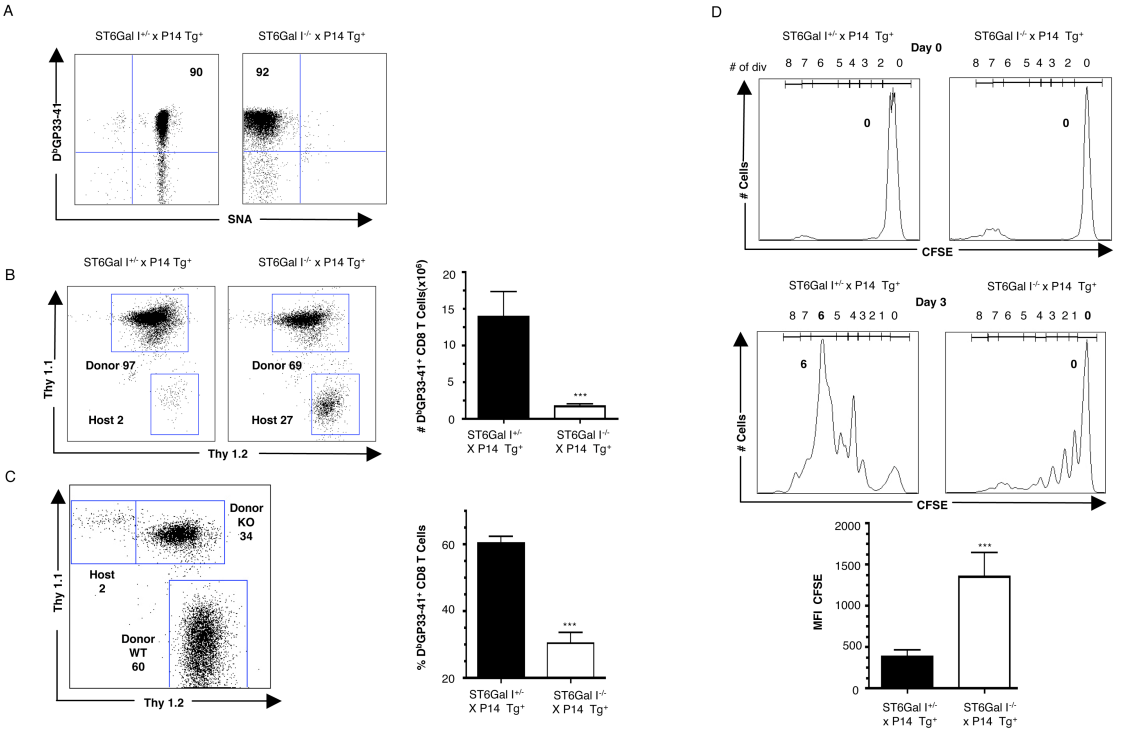
A
ST6Gal I+/- x P14 Tg+
ST6Gal I-/- x P14 Tg+
90
92
DbGP33-41
SNA
B
Donor 97
Host 2
Donor 69
Host 27
Thy 1.1
Thy 1.2
DbGP33-41+ CD8 T Cells(x10⁶)
ST6Gal I+/- X P14 Tg+
ST6Gal I-/- X P14 Tg+
***
C
Donor KO 34
Host 2
Donor WT 60
% DbGP33-41+ CD8 T Cells
D
Day 0
# of div
8 7 6 5 4 3 2 0
Cells
CFSE
Day 3
8 7 6 5 4 3 2 1 0
MFI CFSE

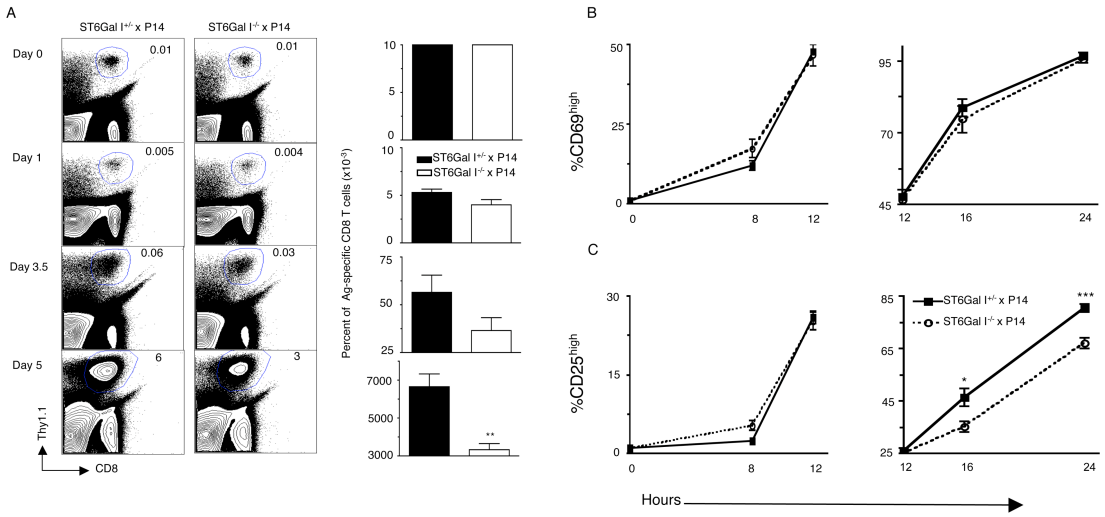

Figure 4. 6. Similar recruitment and T cell activation, but delayed IL-2Rα expression of ST6Gal $I^{-/-}$ CD8 T cells.

$1x10^5$ splenocytes from ST6Gal $I^{+/-}$xP14 wildtype or ST6Gal $I^{-/-}$ xP14 TCR transgenic splenocytes were intravenously transferred into naïve C57BL/6 mice and the recipient mice were intravenously infected with LCMV Armstrong 4 hours later after transfer. Spleen cells were isolated and stained with antibodies on indicated time-points and analyzed by FACS. A, the proportion of donor CD8 Tcells was showed in Contour dot plot and quantified in bar graphs. The linear kinetics of the percent of donor CD8 T cells expressing elevated CD69 (B) and CD25 (C) in spleen of both groups of mice was measured by FACS analysis. Data from n=3-6 mice.

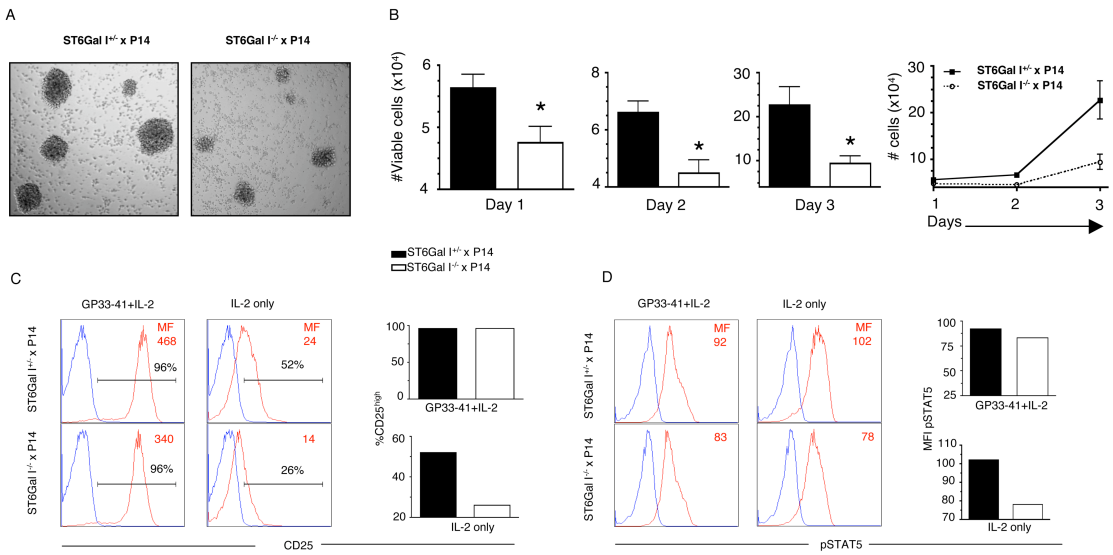

Figure 4. 7. IL-2/IL-2R signaling and surface expression is impaired in ST6Gal I$^{-/-}$ CD8 T cells.

2 x 10^5 splenocytes from ST6Gal I$^{+/-}$xP14 wildtype or ST6Gal I$^{-/-}$ xP14 TCR transgenic mice were transferred to 96-well plate and incubated with GP33-41 (0.01μg/ml) peptide at 37 ^{o}C. A, Spleen cells clustered after 2 days incubation with peptide. Photos are taken under light microscope at 10x magnification. B, P roliferative response of spleen cells after incubation with GP33-41 at day 1, 2, 3. Viable cells from single or pooled from triplicate wells were counted and measured by FACS for live cell percent. For GP33-41+ IL-2 group, after 4 hours incubation with peptide, cells were transferred to another plate and washed peptide away with 10%RPMI 1640. Recombinant IL-2 was added to the wells at a concentration of 10000 U/ml. Cells incubated for another 20 hours and intracellularly stained with CD8, CD25 (C), and pSTAT5 (D) antibodies. For IL-2 only group, recombinant IL-2 was added from the beginning. Cells incubated for 24 hours, stained with antibodies and analyzed by FACS. Data are representative of two independent experiments.

CHAPTER V
CONCLUSIONS

As one of the most abundant post-translational modifications of peoteins, glycosylation can impact cellular signal transduction and functionality (Ohtsubo and Marth, 2006; Rudd et al., 2001). Glyco-phenotypic changes during immune responses have been described for decades (Galvan et al., 1998a; London and Horton, 1980; Onami et al., 2002) . However, their functional relevance is still unclear. ST6Gal I is a glycosyltransferase that catalyze the addition of sialic acid to galactose via α2,6-linkage to generate the Siaα2,6 structure (Hennet et al., 1998). This enzyme is highly expressed on B and T lymphocytes (Hennet et al., 1998). However, the role of this enzyme in adaptive immunity during a viral infection remains largely unexplored. In this study, we comprehensively interrogate the role of ST6Gal I in viral specific T and B cell responses. We also examined the pathogenic outcome in mice loss of this enzyme.

The generation of Influenza-specific humoral responses is impaired in ST6Gal I-deficient mice

We observed that SNA lectin binding, which indicate ST6Gal I expression or activity, remains at high levels on naïve B cells, plasma blasts, and germinal center B cells following viral infection (Figure 2.1). To understand the functional relevance of ST6Gal I expression in B cell immunity, we infected ST6Gal $I^{-/-}$ mice with influenza virus. We demonstrated that the absence of ST6Gal I results in decreased early influenza specific IgM and IgG levels in the serum, as well as

defective generation of influenza specific antibody secreting cells (Figure 2.2). These impairments are not due to reduced viral load or antigen availability in these mice as influenza virus replicates similarly in the lungs (Figure 2.4). In contrast to impairments in the generation of acute antiviral humoral responses, ST6Gal I$^{-/-}$ mice are able to establish antiviral humoral memory, with high levels of IgG antibodies after day 14 p.i. (Figure 2.2, 2.6).

To determine whether the observed impairment of viral specific humoral responses were B cell intrinsic, we adoptively transferred purified B cells with or without ST6Gal I into B cell deficient mice and infected with influenza virus. The viral specific IgM response was significantly reduced in mice that received ST6Gal I$^{-/-}$ B cells, whereas the viral specific IgG response was comparable compared to mice that received ST6Gal I$^{+/+}$ B cells (Figure 2.7). These results indicate the expression of ST6Gal I by B cells, at least partially, is required for optimal antiviral humoral responses.

ST6Gal I deficiency results in altered sialylation of IgG and IgA, and promotes IgA mesengial deposition following influenza infection

Previously, we found that ST6Gal I$^{-/-}$ mice demonstrated impairments in the generation of early antiviral specific IgM and IgG responses (Figure 2.2), whereas humoral immunity was normally established (Figure 2.6). When we analyzed the influenza specific IgA responses, paradoxically, we discovered that although ST6Gal I$^{-/-}$ mice showed impaired early influenza specific IgA responses, by memory time-points the levels of total IgA, and influenza specific

IgA were elevated in the serum of immune ST6Gal $I^{-/-}$ mice following influenza infection (Figure 3.1).

As increased IgA levels in serum is highly correlated with the occurrence of a human disease, IgA nephropathy (D'Amico, 2004). We then examined whether evidence of glomerulonephritis developed in immune ST6Gal $I^{-/-}$ mice following influenza infection. We found that although immune ST6Gal $I^{-/-}$ mice displayed normal gross pathology of the kidneys (Figure 3.1, Table 3.1), they showed increased IgG and IgA deposition in the kidney glomeruli (Figure 3.2, 3.5), which is a hallmark of IgA nephritis (D'Amico, 2004). We noted that aberrant glycosylation of antibody has been proposed to affect the development of IgA nephritis (Novak et al., 2008). We therefore analyzed the glycosylation of IgG and IgA. We found that ST6Gal $I^{-/-}$ mice showed abnormal glycosylation in the N-glycans of both IgG and IgA, with a complete loss of terminal sialylation of N-glycans in IgG, and reductions in sialylated N-glycans in IgA (Figure 3.3, 3.4). Taken together, these data suggested that ST6Gal I deficiency, together with influenza infection, may initiate IgA nephritis.

ST6Gal I promotes rapid IL-2Rα surface expression, increasing early proliferation of terminal effector CD8 cells

We have demonstrated that SNA lectin binding remained high on B cells during activation and differentiation (Figure 2.1). In contrast, we discovered that ST6Gal I was differentially expressed during CD8 T cell differentiation, associated with changes in SNA binding accordingly (Figure 4.1). To investigate the functional significance of this differential regulation of ST6Gal I, we infected ST6Gal $I^{-/-}$ mice and demonstrated significant impairments in the generation of viral-specific T and B cell responses in ST6Gal $I^{-/-}$ mice (Figure 4.2). To ascertain whether reduced

ST6Gal I$^{-/-}$ CD8 T cell expansion was due to cell intrinsic defects, we adoptively transferred CD8 T cell with or without ST6Gal I into recipient mice and viral-specific responses were measured. We found that ST6Gal I$^{-/-}$ effector CD8 T cell displayed defective expansion and diminished proliferation (Figure 4.2, 4.5), indicating that lack of ST6Gal I by CD8 T cells led to defective expansion due to impaired CD8 T cell proliferation. Moreover, ST6Gal I$^{-/-}$ CD8 T cells skewed towards memory precursor cells, while terminal effector cell proliferation was dampened (Figure 4.2). When we examined the proliferation in more detail, we found that IL-2Rα surface expression was delayed *in vivo* on ST6Gal I$^{-/-}$ CD8 T cells (Figure 4.6). We provide evidence of this delayed IL-2Rα expression is likely due to defective IL-2/IL-2R signaling (Figure 4.7). These studies indicate that the intrinsic expression of ST6Gal I promotes the rapid surface expression of IL-2Rα to elevate early proliferation of terminal effector CD8 T cells during viral infection.

REFERENCES

D'Amico, G. 2004. Natural history of idiopathic IgA nephropathy and factors predictive of disease outcome. *Semin Nephrol* 24:179-196.

Galvan, M., K. Murali-Krishna, L.L. Ming, L. Baum, and R. Ahmed. 1998. Alterations in cell surface carbohydrates on T cells from virally infected mice can distinguish effector/memory CD8+ T cells from naive cells. *J Immunol* 161:641-648.

Hennet, T., D. Chui, J.C. Paulson, and J.D. Marth. 1998. Immune regulation by the ST6Gal sialyltransferase. *Proc Natl Acad Sci U S A* 95:4504-4509.

London, J., and M.A. Horton. 1980. Peanut agglutinin. V. Thymocyte subpopulations in the mouse studied with peanut agglutinin and Ly-6.2 antiserum. *J Immunol* 124:1803-1807.

Novak, J., B.A. Julian, M. Tomana, and J. Mestecky. 2008. IgA glycosylation and IgA immune complexes in the pathogenesis of IgA nephropathy. *Semin Nephrol* 28:78-87.

Ohtsubo, K., and J.D. Marth. 2006. Glycosylation in cellular mechanisms of health and disease. *Cell* 126:855-867.

Onami, T.M., L.E. Harrington, M.A. Williams, M. Galvan, C.P. Larsen, T.C. Pearson, N. Manjunath, L.G. Baum, B.D. Pearce, and R. Ahmed. 2002. Dynamic regulation of T cell immunity by CD43. *J Immunol* 168:6022-6031.

Rudd, P.M., T. Elliott, P. Cresswell, I.A. Wilson, and R.A. Dwek. 2001. Glycosylation and the immune system. *Science* 291:2370-2376.

VITA

Junwei Zeng was born on December 18th, 1977 in Guangdong, China. He graduated from Xinhua High School and attended Foshan University in 1996. He received his B.Agr. in Animal Science in the summer of 2000. He obtained his Master of Science degree in Physiology from China Agricultural University in June 2004. In 2006, he joined the graduate program at the University of Tennessee in Knoxville, TN. He will graduate with a Doctor of Philosophy in Microbiology in the fall of 2011.